AD_____

Award Number: W81XWH-11-1-0573

TITLE: Chemical Genetic Screens for TDP-43 Modifiers and ALS Drug Discovery

PRINCIPAL INVESTIGATOR: Pierre Drapeau

CONTRACTING ORGANIZATION: University of Montreal
Montreal, H3C 3J7
Canada

REPORT DATE: October 2013

TYPE OF REPORT: Annual

PREPARED FOR: U.S. Army Medical Research and Materiel Command
Fort Detrick, Maryland 21702-5012

REPORT DOCUMENTATION PAGE

Form Approved
OMB No. 0704-0188

1. REPORT DATE	**2. REPORT TYPE**	**3. DATES COVERED**
October 2013	Annual	15 Sept. 2012 – 14 Sept. 2013

4. TITLE AND SUBTITLE
Chemical Genetic Screens for TDP-43 Modifiers and ALS Drug Discovery

5a. CONTRACT NUMBER
W81XWH-11-1-0573

5b. GRANT NUMBER
W81XWH-11-1-0573

5c. PROGRAM ELEMENT NUMBER

6. AUTHOR(S)
Pierre Drapeau, Alexandre Parker, Edor Kabashi, Jean-Pierre Julien

E-Mail: p.drapeau@umontreal.ca

5d. PROJECT NUMBER

5e. TASK NUMBER

5f. WORK UNIT NUMBER

7. PERFORMING ORGANIZATION NAME(S) AND ADDRESS(ES)

Universite de Montreal,
2900 Boul. Edouard-Montpetit
Montreal H3T 1J4
Canada

8. PERFORMING ORGANIZATION REPORT NUMBER

9. SPONSORING / MONITORING AGENCY NAME(S) AND ADDRESS(ES)
U.S. Army Medical Research and Materiel Command
Fort Detrick, Maryland 21702-5012

10. SPONSOR/MONITOR'S ACRONYM(S)

11. SPONSOR/MONITOR'S REPORT NUMBER(S)

12. DISTRIBUTION / AVAILABILITY STATEMENT
Approved for Public Release; Distribution Unlimited

13. SUPPLEMENTARY NOTES

14. ABSTRACT

Our objective is to screen libraries of several thousand compounds, including clinically approved drugs, for their ability to suppress the *in vivo* phenotypes observed in worm and fish models expressing mutant human TDP-43 related to ALS and validating hits in a mouse model. Our hypothesis is that chemical modifiers of TDP-43 *in vivo* function will provide new therapeutic approaches to ALS. In year 1, our screen of 3,750 FDA-approved compounds identified 20 active compounds, most of which were neuroleptics with the most potent being pimozide. In year 2, the objective (Aim 3) was to have screened a total of 10k molecules. In addition to the 4k screened in year 1, we screened 2k molecules that are structurally related to the neuroleptics as well as novel molecules. Also, we screened 4k novel derivatives of pimozide and identified several dozen active compounds and reached our objective of a total of 10k molecules screened to date. Testing of pimozide in TDP-43 mice (and in a new collaboration, patients) began (Aim 6).

15. SUBJECT TERMS
TDP-43, C. elegans, zebrafish, mice, motility screens, chemical libraries

16. SECURITY CLASSIFICATION OF:			**17. LIMITATION OF ABSTRACT**	**18. NUMBER OF PAGES**	**19a. NAME OF RESPONSIBLE PERSON**
a. REPORT	**b. ABSTRACT**	**c. THIS PAGE**			USAMRMC
U	U	U	UU	58	**19b. TELEPHONE NUMBER** *(include area code)*

TABLE OF CONTENTS

INTRODUCTION

Our project is to screen libraries of small chemicals, including clinically approved drugs, for their ability to suppress the pathogenic motor phenotypes in three unique *in vivo* genetic models of ALS that we have recently generated. Our new, functionally validated models are worms (*C. elegans*)[1,2], zebrafish (*D. rerio*)[3,4] and mice (*M. musculus*)[5] expressing ALS-related mutations of the human *TARDBP* gene coding for TDP-43, a recently discovered major contributing factor in ALS. We hypothesize that chemical genetic modifiers of TDP-43 *in vivo* function will provide new therapeutic approaches to ALS[6,7].

BODY

We have the following specific aims according to our SOW:

Timeline	Year 1 Q1	Year 1 2	Year 1 3	Year 1 4	Year 2 Q1	Year 2 2	Year 2 3	Year 2 4	Year 3 Q1	Year 3 2	Year 3 3	Year 3 4
Aim 1: Set-up motility assays for worms and fish 1A) Semi-automated measurement of spontaneous activity in TDP-43 worms. 1B) Semi-automated measurement of the motor response in TDP-43 zebrafish.	■	■										
Aim 2: Screen TDP-43 worms and zebrafish for restoration of motility with 3k+ approved compounds			■	■								
Aim 3: Screen TDP-43 worms and zebrafish for restoration of motility with 10k+ compounds					■	■	■	■				
Aim 4: Rescreen TDP-43 worms and zebrafish for specificity and potency of active compounds				■	■	■	■	■	■			
Aim 5: Screen TDP-43 worms and zebrafish for restoration of motility with ±10k other compounds									■	■	■	■
Aim 6: Screen active compounds in TDP-43 mice.					■	■	■	■	■	■	■	■

The screen set-up (Aims 1A,B) will begin immediately and proceed in parallel for worms and fish during the first 6 months (Y1Q1-Q2). This will consist of automating and quantifying the video microscopy screens for motility.

The first chemical screen (approved compounds, Aim 2) will begin immediately afterwards and be completed by the end of year 1 (Y1Q3-Q4).

Once completed, the screen of representative molecules from the larger libraries (Aim 3) will begin and require all of year 2 (Y2Q1-Q4).

As hits are identified during Y1Q3-Y2Q4, the active compounds will be rescreened (Aim 4, Y1Q4-Y3Q1). Those that are confirmed will be tested in our mouse model (Aim 6, Y2).

Finally, all members of the families of confirmed (rescreened) active compounds (Aim 5) will be screened in worms and fish (Y3 Q1-Q4) and tested in mice (Aim 6, Y3).

Accordingly, for year 2 we had the following goals:

Goal 1 (Aim 4) - As hits are identified during Y1Q3-Y2Q4, the active compounds will be rescreened (Y1Q4-Y3Q1).
Goal 2 (Aim 3) - Screen of representative molecules from the larger libraries.
Goal 3 (Aim 6) - Those hits that are confirmed will be tested in our mouse model.

Study design.

Our department operates a platform for integrated robotic plating of libraries of small chemicals. We screen worms and fish expressing mutant human TDP-43 by video microscopy for the effects of these compounds on recovery of motility or survival and re-test hits for dose and time dependence and then test promising confirmed hits in mice.

Previous screens with worms took two weeks to perform as that is the period it takes for them to develop adult-onset phenotypes such as for TDP-43 when grown on a solid substrate. We found a similar result for worms expressing human TDP-43 (see appendix 1[1], Figure 3) from a motoneuron promoter (see appendix 1[1], Figure 1). Further we found that by growing the worms in liquid suspension this accelerated the onset of the phenotype such that by 6 hours it was apparent (see appendix 1[1], Figure 10). This transformed our screening protocol as it permits screening within the same working day and makes it possible for one person to screen several hundred molecules per week.

Our stable transgenic zebrafish line required us to raise several generations before obtaining stable expression and is now ready for use in large scale screening. During the first two years we used our established transient model[4,8] to retest hits from the worm screen (i.e. in series rather than in parallel).

In preliminary tests we had found that methylene blue[9] was effective in protecting against the TDP-43 phenotype in both worms (see appendix 2[2], Figure 1B&2A) and fish (see appendix 2[2], Figure 3) by protecting against cellular stress (see appendix 2[2], Figure 6). This compound was used as a positive control for setting up the larger screens and with structural analogs, was shown to promote the protective ER stress response[12].

In year 1 we screened 3,750 clinically approved compounds in the Biomol Natural Products, Microsource Discovery Spectrum, Prestwick Commercial Products and Sigma Lopac sets at a concentration of 20 μM. We identified 22 compounds (see Table 1), but 8 were excluded as being irrelevant (insecticides, tumour drugs – in blue in table 1).

Goal 1 (Aim 4) - As hits are identified during Y1Q3-Y2Q4, the active compounds will be rescreened (Y1Q4-Y3Q1).

We tested these ER stress compounds on longevity in C elegans (see appendix 3[13]). The 13 neuroleptics were retested and confirmed in worms and zebrafish at concentrations ranging from 2-100 μM. Almost all of the confirmed hits (in black, Table 1) were neuroleptics, the most potent of which was **pimozide**, acting at 0.5 uM in zebrafish. We also found **withaferin A** to be a potent compound in our C elegans assay. We started testing paired combinations for 9 of the neuroleptics (Table 2). All combinations were active at 5 uM though some were deleterious at higher concentrations. Lower concentrations will also be tested.

Goal 2 (Aim 3) - Screen of representative molecules from the larger libraries (Year 2).

Our platform chemists examined the available libraries of nearly 100k novel compounds (Chembridge DriverSet, 60k molecules; Maybridge HitFinder, 16k; SPECS Selection, 16k) for structural homologs of the 13 neuroleptics identified in our first (FDA) screen of 3,750 FDA-approved compounds, including pimozide. They identified several dozen compounds present on plates containing a total of 1806 molecules. In year 2 we screened all 1806 molecules and identified 15 hits (see Table 3). As none of these were predicted structural homologs of the neuroleptics, they represent novel molecules that will require further characterization.

Given that pimozide proved to be the neuroleptic of highest potency in our assays, we learnt that Zalicus Pharmaceuticals Ltd. (Cambridge, MA) had prepared pimozide derivatives for testing in other disease models. With approval from the DoD, we entered into agreement with Zalicus for the testing of 3,658 pimozide derivatives in our ALS models. All 3,658 compounds were screened at 20 μM in worms in year 2. 24 hits were obtained (see Table 4) and are currently being rescreened for dose-response at 0.1-100 μM in our worm and zebrafish models. As part of our agreement with Zalicus, once we have confirmed hits in our ALS models they will release structural information on the compounds of mutual interest.

Together, our screening of nearly four thousand FDA-approved molecules, close to two thousand novel compounds and about four thousand pimozide derivatives has reached the goal of screening 10k molecules by this stage of the project.

Goal 3 (Aim 6) - Those hits that are confirmed will be tested in our mouse model. (Years 2&3)

The Julien lab has generated transgenic mice with moderate and ubiquitous expression of TDP-43 species to mimic the human ALS disease. This was accomplished by generating transgenic mice harbouring an 18 kb genomic fragment coding for human *TARDBP*^{WT}, *TARDBP*^{A315T} or *TARDBP*^{G348C}. In year 1, the Julien lab tested methylene blue, our positive control for the drug screening, in their mutant TDP-43 mice[10] (appendix 4).

Julien's lab reported previously that withaferin A, an inhibitor of NF-kB activation, conferred beneficial effects in transgenic mice overexpressing WT TARDBP, a model of ALS, by reduction of inflammation and amelioration of motor impairment[16] . Recently, he further tested this compound in three other mouse models of ALS, transgenic mice expressing either *TARDBP*^{G348C} mice, SOD1^{G93A} or SOD1^{G37R}. Intraperitoneal injection of *TARDBP*^{G348C} mice with withaferin A (4mg/kg) twice a week starting at 30 weeks of age led to amelioration of motor dysfunction within 10 weeks of treatment (Fig. 1). Moreover, injection of withaferin A starting at P40, extended survival of SOD1^{G93A} and SOD1^{G37R} familial mice model of ALS (Fig. 2). His team examined the effect of withaferin A when intraperitoneally injected into the SOD1^{G93A} mice twice a week from the postnatal day 40 until death at a dose of 4 mg/kg body and into SOD1^{G37R} mice injected twice a week with the same dose starting at 9 months of age. Withaferin A treatment increased survival of SOD1^{G93A} by 8 days from 145 days (n=15) to 153 days (n=16, $P<0.05$) whereas this compound increased survival of SOD1^{G37R} mice by 18 days from 379 days (n=8) in controls to 397 days (n=8) in withaferin-treated mice, $P<0.0001$. Results suggest that the beneficial effect of Withaferin A in mutant SOD1 mice may be due in part to an upregulation of heat shock proteins (Hsp27 and Hsp70) and to reduction in levels of misfolded SOD1 species (Fig. 3). A manuscript describing these results is in preparation.

In the original plan, Julien was supposed to test pimozide in adult *TARDBP*^{G348C} mice in year 2. However, this project was delayed due to the move of Julien's laboratory from CHU Laval to l'Institut universitaire en santé mentale de Québec (IUSMQ) during Spring 2013. The good news is that the *TARDBP*^{G348C} mice have been rederived into a new pathogen-free animal facility at IUSMQ and a cohort of these mice at 8 months of age will become available for this test at the beginning of 2014. The *TARDBP*^{G348C} mice will be subjected to daily intraperitoneal injection of pimozide at 1mg/kg or saline for a period of two months, as described previously[14,15]. The mice will be subjected to learning tests (passive avoidance and Barnes maze) and a rotorod test before and after drug treatment as described[16]. This should reveal if the compound ameliorated the cognitive and motor dysfunction impairment of *TARDBP*^{G348C} mice. In addition, the spinal cord and brain of mice will be be analyzed for the effects of the drugs on pathological features (neuroinflammation, cytoplasmic ubiquitinated TDP-43 aggregates) and biochemical hallmarks (25 kd C-terminal cleavage fragment).

Parallel developments.

Pimozide was initially designed as a dopamine antagonist but is now recognized to act also on calcium channels. In a neurophysiological analysis of mutant TDP zebrafish, we showed that calcium agonists could protect against development of the motor phenotype[11]. We therefore hypothesize that pimozide may be acting in a similar manner to stabilise neuromuscular function and indeed have observed this in preliminary work with zebrafish.

In parallel with the DoD project, we have initiated two (independently-funded) collaborations to help with our progress. In the first, Dr. Richard Robitaille of the Univ. Montreal, an expert on mouse neuromuscular transmission, has been testing the effects of pimozide on a mouse model of SOD1-related ALS. He determined synaptic strength of NMJs in the extensor-digitorum-lungus (EDL) nerve-muscle preparation in *SOD1*^{G37R} mice by measuring paired-pulse facilitation (PPF) and quantal content of each NMJ using a low Ca2+/high Mg2+ Ringer solution. Synaptic transmission was elicited by motor nerve stimulation using a suction electrode filled with extracellular saline and intracellular recordings of endplate potentials (EPPs) were performed using glass microelectrodes. Preliminary data reveal that the quantal content at *SOD1*^{G37R} mice was altered compared to wild type littermates while the frequency of miniature endplate potentials (mEPPs) was not different. Upon bath application of pimozide, the amplitude of the EPP doubled while the amplitude of the mEPP remained unaffected. As a whole and consistent with our data obtained using the zebrafish preparation in a TDP-43 background, these data indicate that the pimozide increased transmitter release at NMJs of a mammalian ALS model in an SOD1 mutation background. We have provided Dr. Robitaille with our *TARDBP*^{G348C} mice so that he may test the effectiveness of pimozide in this model that is more closely related to our simpler screening models.

In addition, we have initiated a clinical collaboration with Dr. Lawrence Korngut, Director of the ALS Clinic at the Univ. Calgary (Canada) and Director of the Canadian Neuromuscular Disease Registry. ALS patients show dysfunctional neuromuscular activity that can be easily assessed using repetitive nerve stimulation that reveals decremental responses of the trapezius. Given that pimozide is FDA-approved, Dr. Korngut has initiated a human pilot study in his clinic in Calgary that could potentially be expanded to his national network in Canada. Discussion is underway to test withaferin A as well.

Table 1. Summary of FDA-approved compounds with hits in C. elegans.
Legend. Each compound was first tested at 20 μM. Those showing restoration of motility in worms were retested in both worms and fish (**in black**), then once validated retested at 2,5, 5, 10, 20, 50 and 100 μM. The most potent was pimozide, active at 0.5 μM in zebrafish.

Source plate	Pick plate	Source well	Name / Action	
CCC0327CP1	P00017066	B010	Mianserine HCl	antidepressant/DA
CCC0327CP1	P00017066	C003	Amoxapine	antidep/tetracyclic/DA reuptake block
CCC0327CP1	P00017066	C004	Cyproheptadine HCl	antihistamine/5HT rec antag
CCC0327CP1	P00017066	G008	Nicergoline	senile dementia/vascular/alpha-1A adrenergic receptor antagonist
CCC0328CP1	P00017067	E008	Kawain	anticonvulsant/anxiolytic/many systems
CCC0329CP1	P00017068	F005	Pimethixene maleate	antihsitamine/anxiety
CCC0329CP1	P00017068	G009	**Pimozide**	antipsychotic/Tourette/D2
CCC0330CP1	P00017069	B011	Flupentixol dihydrochloride cis-(Z)	antipsychotic/schizo/antidep/DA, 5-HT
CCC0330CP1	P00017069	C009	Chlorprothixene hydrochloride	antipsychotic/5HT, DA
CCC0330CP1	P00017069	C011	Clozapine	antipsychotic/5HT, DA
CCC0330CP1	P00017069	F006	Methiothepin maleate	antipsychotic/5HT, DA
CCC0346CP1	P00017085	G008	Chlorprothixene hydrochloride	antipsychotic/5HT, DA
CCC0352CP1	P00017091	E006	(±)-Octoclothepin maleate	neuroleptic/many systems
			withaferin A	inhibitor of NF-kB
		H007	Ivermectin (Insecticide)	Glu (Cl)/GABAR
		F009	Fenbufen	inflammation, prostaglandins
		A003	Flavoxate hydrochloride	anticholinergic/bladder
		F009	Melatonin	diurnal/mito, DNA protection/natural
		F010	Menadione	Vit K/cancer/EGFR
		B011	Avermectin B1 (Insecticide)	insectiside, antihelmintic
		C011	hypericin	antibiotic/kinases /DA B-hydroxylase
		D007	deoxyphorbol	antitumour
		D011	mezerein	antitumour/phorbol
		F003	genistein	antihelmintic/natural

Table 2: Paired testing of hits. The neuroleptics identified in Table 1 were tested in pairs at different concentrations for their combined potency in our C elegans model. Positive hits in green, negative hots in red. Chlo= Chlorprothixene hydrochloride; Amo= Amoxapine; Mians= Mianserine hydrochloride; Pizo= Pizotifen malate; Pimet= Pimethixene maleate; Cloz= Clozapine; Meth= Methiothepin maleate; Nicer= Nicergoline; **Pimoz= Pimozide**; DMSO= Dimethyl sulfoxide.

Compound/concentration (uM) (0.5%-0.125 % DMSO)

Rep	1	2	3	4	5	6	7	8	9	10	11	12
1	*Chlo10	Chlo2.5	Amo5	Pizo10	Pizo2.5	Pimozide5	Pimet10	Pimet2.5	Cloz5	Meth10	Meth2.5	Nicer5
2	Chlo10	Chlo2.5	Amo5	Pizo10	Pizo2.5	Pimozide5	Pimet10	Pimet2.5	Cloz5	Meth10	Meth2.5	Nicer5
3	Chlo10	Chlo2.5	Amo5	Pizo10	Pizo2.5	Pimozide5	Pimet10	Pimet2.5	Cloz5	Meth10	Meth2.5	Nicer5
1	Chlo5	Amo10	Amo2.5	Pizo5	Pimozide10	Pimozide2.5	Pimet5	Cloz10	**Cloz2.5	Meth5	Nicer10	Nicer2.5
2	Chlo5	Amo10	Amo2.5	Pizo5	pimozide0	Pimozide2.5	Pimet5	Cloz10	Cloz2.5	Meth5	Nicer10	Nicer2.5
3	Chlo5	Amo10	Amo2.5	Pizo5	Pimozide10	Pimozide2.5	Pimet5	Cloz10	Cloz2.5	Meth5	Nicer10	Nicer2.5
	Mians10	Mians10	Mians10	Mianss5	Mians5	Mians5	Mians2.5	Mians2.5	Mians2.5			
1	Chlo5+ Nicer5	Chlo5+ Mians5	Amo5+ Pizo5	Amo5+ Pimo5	Amo5+ Pimet5	Amo5+ Cloz5	Amo5+ Meth5	Amo5+ Nicer5	Amo5+ Mians5	Pizo5+ Pimo5	Pizo5+ Pimet5	Pizo5+ Cloz5
2	Chlo5+ Nicer5	Chlo5+ Mians5	Amo5+ Pizo5	Amo5+ Pimo5	Amo5+ Pimet5	Amo5+ Cloz5	Amo5+ Meth5	Amo5+ Nicer5	Amo5+ Mians5	Pizo5+ Pimo5	Pizo5+ Pimet5	Pizo5+ Cloz5
3	Chlo5+ Nicer5	Chlo5+ Mians5	Amo5+ Pizo5	Amo5+ Pimo5	Amo5+ Pimet5	Amo5+ Cloz5	Amo5+ Meth5	Amo5+ Nicer5	Amo5+ Mians5	Pizo5+ Pimo5	Pizo5+ Pimet5	Pizo5+ Cloz5

1	Chlo2.5+ Nicer2.5	Chlo2.5+ Mians2.5	Amo.5+ Pizo2.5	Amo2.5+ Pimo2.5	Amo2.5+ Pimet2.5	Amo2.5+ Cloz2.5	Amo2.5+ Meth2.5	Amo2.5+ Nicer2.5	Amo2.5+ Mians2.5	Pizo2.5+ Pimo2.5	Pizo2.5+ Pimet2.5	Pizo2.5+ Cloz 2.5
2	Chlo2.5+ Nicer2.5	Chlo2.5+ Mians2.5	Amo.5+ Pizo2.5	Amo2.5+ Pimo2.5	Amo2.5+ Pimet2.5	Amo2.5+ Cloz2.5	Amo2.5+ Meth2.5	Amo2.5+ Nicer2.5	Amo2.5+ Mians2.5	Pizo2.5+ Pimo2.5	Pizo2.5+ Pimet2.5	Pizo2.5+ Cloz2.5
3	Chlo2.5+ Nicer2.5	Chlo2.5+ Mians2.5	Amo.5+ Pizo2.5	Amo2.5+ Pimo2.5	Amo2.5+ Pimet2.5	Amo2.5+ Cloz2.5	Amo2.5+ Meth2.5	Amo2.5+ Nicer2.5	Amo2.5+ Mians2.5	Pizo2.5+ Pimo2.5	Pizo5+ Pimet5	Pizo 2.5+ Cloz2.5
1	Pizo5+ Meth5	Pizo5+ Nicer5	Pimoz5+ Pimet5	Pimoz5+ Cloz5	Pimoz5+ Meth5	Pimoz5+ Nicer5	Pimoz5+ Mians5	Pimeth5+ Cloza5	Pimeth5 + meth5	Pimeth5+ Nicer5	Cloz5+ Meth5	Cloz5+ Nicer5
2	Pizo5+ Meth5	Pizo5+ Nicer5	Pimoz5+ Pimet5	Pimoz5+ Cloz5	Pimoz5+ Meth5	Pimoz5+ Nicer5	Pimoz5+ Mians5	Pimeth5+ Cloza5	Pimeth5 + meth5	Pimeth5+ Nicer5	Cloz5+ Meth5	Cloz5+ Nicer5
3	Pizo5+ Meth5	Pizo5+ Nicer5	Pimoz5+ Pimet5	Pimoz5+ Cloz5	Pimoz5+ Meth5	Pimoz5+ Nicer5	Pimoz5+ Mians5	Pimeth5+ Cloza5	Pimeth5 + meth5	Pimeth5+ Nicer5	Cloz5+ Meth5	Cloz5+ Nicer5
1	Pizo2.5+ Meth2.5	Pizo2.5+ Nicer2.5	Pimoz2.5+ Pimet2.5	Pimoz2.5+ Cloz2.5	Pimoz2.5+ Meth2.5	Pimoz2.5+ Nicer2.5	Pimoz2.5+ Mians2.5	Pimeth2.5+ Cloza2.5	Pimeth2.5 + meth2.5	Pimeth2.5+ Nicer2.5	Cloz2.5+ Meth2.5	Cloz2.5+ Nicer2.5
2	Pizo2.5+ Meth2.5	Pizo2.5+ Nicer2.5	Pimoz2.5+ Pimet2.5	Pimoz2.5+ Cloz2.5	Pimoz2.5+ Meth2.5	Pimoz2.5+ Nicer2.5	Pimoz2.5+ Mians2.5	Pimeth2.5+ Cloza2.5	Pimeth2.5 + meth2.5	Pimeth2.5+ Nicer2.5	Cloz2.5+ Meth2.5	Cloz2.5+ Nicer2.5
3	Pizo2.5+ Meth2.5	Pizo2.5+ Nicer2.5	Pimoz2.5+ Pimet2.5	Pimoz2.5+ Cloz2.5	Pimoz2.5+ Meth2.5	Pimoz2.5+ Nicer2.5	Pimoz2.5+ Mians2.5	Pimeth2.5+ Cloza2.5	Pimeth2.5 + meth2.5	Pimeth2.5+ Nicer2.5	Cloz2.5+ Meth2.5	Cloz2.5+ Nicer2.5
1	Pizo5+ Meth5	Pizo5+ Nicer5	Pimoz5+ Pimet5	Pimoz5+ Cloz5	Pimoz5+ Meth5	Pimoz5+ Nicer5	Pimoz5+ Mians5	Pimeth5+ Cloza5	Pimeth5 + meth5	Pimeth5+ Nicer5	Cloz5+ Meth5	Cloz5+ Nicer5
2	Pizo5+ Meth5	Pizo5+ Nicer5	Pimoz5+ Pimet5	Pimoz5+ Cloz5	Pimoz5+ Meth5	Pimoz5+ Nicer5	Pimoz5+ Mians5	Pimeth5+ Cloza5	Pimeth5 + meth5	Pimeth5+ Nicer5	Cloz5+ Meth5	Cloz5+ Nicer5
3	Pizo5+ Meth5	Pizo5+ Nicer5	Pimoz5+ Pimet5	Pimoz5+ Cloz5	Pimoz5+ Meth5	Pimoz5+ Nicer5	Pimoz5+ Mians5	Pimeth5+ Cloza5	Pimeth5 + meth5	Pimeth5+ Nicer5	Cloz5+ Meth5	Cloz5+ Nicer5

1	Pizo2.5+ Meth2.5	Pizo2.5+ Nicer2.5	Pimoz2.5+ Pimet2.5	Pimoz2.5+ Cloz2.5	Pimoz2.5+ Meth2.5	Pimoz2.5+ Nicer2.5	Pimoz2.5+ Mians2.5	Pimeth2.5+ Cloza2.5	Pimeth2.5 + meth2.5	Pimeth2.5+ Nicer2.5	Cloz2.5+ Meth2.5	Cloz2.5+ Nicer2.5
2	Pizo2.5+ Meth2.5	Pizo2.5+ Nicer2.5	Pimoz2.5+ Pimet2.5	Pimoz2.5+ Cloz2.5	Pimoz2.5+ Meth2.5	Pimoz2.5+ Nicer2.5	Pimoz2.5+ Mians2.5	Pimeth2.5+ Cloza2.5	Pimeth2.5 + meth2.5	Pimeth2.5+ Nicer2.5	Cloz2.5+ Meth2.5	Cloz2.5+ Nicer2.5
3	Pizo2.5+ Meth2.5	Pizo2.5+ Nicer2.5	Pimoz2.5+ Pimet2.5	Pimoz2.5+ Cloz2.5	Pimoz2.5+ Meth2.5	Pimoz2.5+ Nicer2.5	Pimoz2.5+ Mians2.5	Pimeth2.5+ Cloza2.5	Pimeth2.5 + meth2.5	Pimeth2.5+ Nicer2.5	Cloz2.5+ Meth2.5	Cloz2.5+ Nicer2.5
1	Chlo5+ Amo5	chlo10+ Pizo10	Chlo10+ Pimo10	Chlo10+ Pimet10	Chlo10+ clozt10	Chlo10+ Meth10	Meth10+ nicer10	Meth10+ mians10	Cloz5+ Mians5	Pizo5+ Mians5	Pimeth5+ Mians5	dmso
2	Chlo5+ Amo5	chlo10+ Pizo10	Chlo10+ Pimo10	Chlo10+ Pimet10	Chlo10+ clozt10	Chlo10+ Meth10	Meth10+ nicer10	Meth10+ mians10	Cloz5+ Mians5	Pizo5+ Mians5	Pimeth5+ Mians5	dmso
3	Chlo5+ Amo5	chlo10+ Pizo10	Chlo10+ Pimo10	Chlo10+ Pimet10	Chlo10+ clozt10	Chlo10+ Meth10	Meth10+ nicer10	Meth10+ mians10	Cloz5+ Mians5	Pizo5+ Mians5	Pimeth5+ Mians5	dmso
1	Chlo2.5+ Amo2.5	Chlo5+ Pizo5	Chlo5+ Pimo5	Chlo5+ Pimet5	Chlo5+ cloz5	Chlo5+ Meth5	Meth5+ Nicer5	Meth5+ Mians5	Cloz2.5+ Mians2.5	Pizo2.5+ Mians2.5	Pimeth2.5+ Mians2.5	dmso
2	Chlo2.5+ Amo2.5	Chlo5+ Pizo5	Chlo5+ Pimo5	Chlo5+ Pimet5	Chlo5+ cloz5	Chlo5+ Meth5	Meth5+ Nicer5	Meth5+ Mians5	Cloz2.5+ Mians2.5	Pizo2.5+ Mians2.5	Pimeth2.5+ Mians2.5	dmso
3	Chlo2.5+ Amo2.5	Chlo5+ Pizo5	Chlo5+ Pimo5	Chlo5+ PImet5	Chlo5+ cloz5	Chlo5+ Meth5	Meth5+ Nicer5	Meth5+ Mians5	Cloz2.5+ Mians2.5	Pizo2.5+ Mians2.5	Pimeth2.5+ Mians2.5	dmso
1	Amo 0.2+ Pime 0.2	Amo 2+ Pime 2	Amo 1+ Pime 1	Amo0.2+ Cloz 0.2	Amo2+ Cloz 2	Amo1+ Cloz 1	Amo+cloz+ Pime+pizo+ Nicer 2					dmso
2	Amo 0.2+ Pime 0.2	Amo 2+ Pime 2	Amo 1+ Pime 1	Amo0.2+ Cloz 0.2	Amo 2+ Cloz 2	Amo1+ Cloz 1	Amo+cloz+ Pime+pizo+ Nicer 2					dmso

Table 3. Novel compounds with hits.
Legend. Structural homologs of the neuroleptics (Table 1) were tested in worms at 20 μM, along with novel compounds present on the same plates.

1. 4-bromo-N-[2,2,2-trichloro-1-(1-piperidinyl)ethyl]benzamide;
2. 4-(4-methoxyphenyl)-1,6-dimethyl-5-nitro-3,4-dihydro-2(1H)-pyrimidinone
3. 2-(2-oxopropyl)phenyl 3-nitrobenzoate
4. 1-(phenylsulfonyl)cyclopropanecarboxylic acid
5. 4-bromobenzaldehyde O-(2-methylbenzoyl)oxime
6. N-(1-propylcyclohexyl)acrylamide
7. 2-hexyl-1-cyclopentanone semicarbazone
8. 3-nitro-N'-(1-phenylbutylidene)benzohydrazide
9. 2-(3,4-dimethoxyphenyl)-N-(2-phenylethyl)-4-quinolinecarboxamide
10. N-(4-chlorobenzyl)-3-(2,6-dichlorophenyl)-5-methyl-4-isoxazolecarboxamide
11. N-[2-chloro-5-(trifluoromethyl)phenyl]-3-(4-methoxyphenyl)propanamide
12. 3-({[4-(4-bromophenyl)-1,3-thiazol-2-yl]amino}carbonyl)bicyclo[2.2.1]heptane-2-carboxylic acid;t
13. 4-(4-fluorophenyl)-3,4,5,6-tetrahydrobenzo[h]quinazoline-2(1H)-thione
14. 7-acetyl-3-(allylsulfanyl)-6-(4-ethoxy-3-methoxyphenyl)-6,7-dihydro[1,2,4]triazino[5,6-d][3,1]benzoxazepine
15. 4-(3-methylphenyl)-1'-phenyl-spiro[4-azatricyclo[5.2.1.0~2,6~]dec[8]ene-10,2'-cyclopropane]-3,5-dione

Table 4. Hits obtained upon testing of pimozide derivatives obtained from Zalicus Inc. at 20 uM in C elegans.

	Plate ID	Well ID	Compound identification	Final concentration (uM)
1	1	H07	NP167589.001-2	20
2	2	A02	NP167595.001-2	20
3	2	H07	NP168807.001-2	20
4	2	H08	NP168808.001-2	20
5	3	G06	NP167210.001-2	20
6	7	H10	NP170109.001-2	20
7	7	E02	NP170041.001-2	20
8	7	F08	NP170068.001-2	20
9	9	G02	NP170323.001-2	20
10	12	A02	NP170650.001-2	20
11	29	A04	NP173057.001-2	20
12	29	F07	NP173211.001-2	20
13	29	F09	NP173214.001-2	20
14	29	F11	NP173216.001-2	20
15	29	C05	NP172123.001-2	20
16	35	H02	NP173758.001-2	20
17	35	H03	NP173759.001-2	20
18	*35*	H06	NP173762.001-2	20
19	35	H09	NP173765.001-2	20
20	36	G05	NP173797.001-2	20
21	36	H02	NP173806.001-2	20
22	35	C09	NP173753.001-2	20
23	35	F06	NP173684.001-2	20
24	36	H03	NP173807.001-2	20

Fig. 1. Withaferin A ameliorated motor defects in TDP-43^{G348C} mice

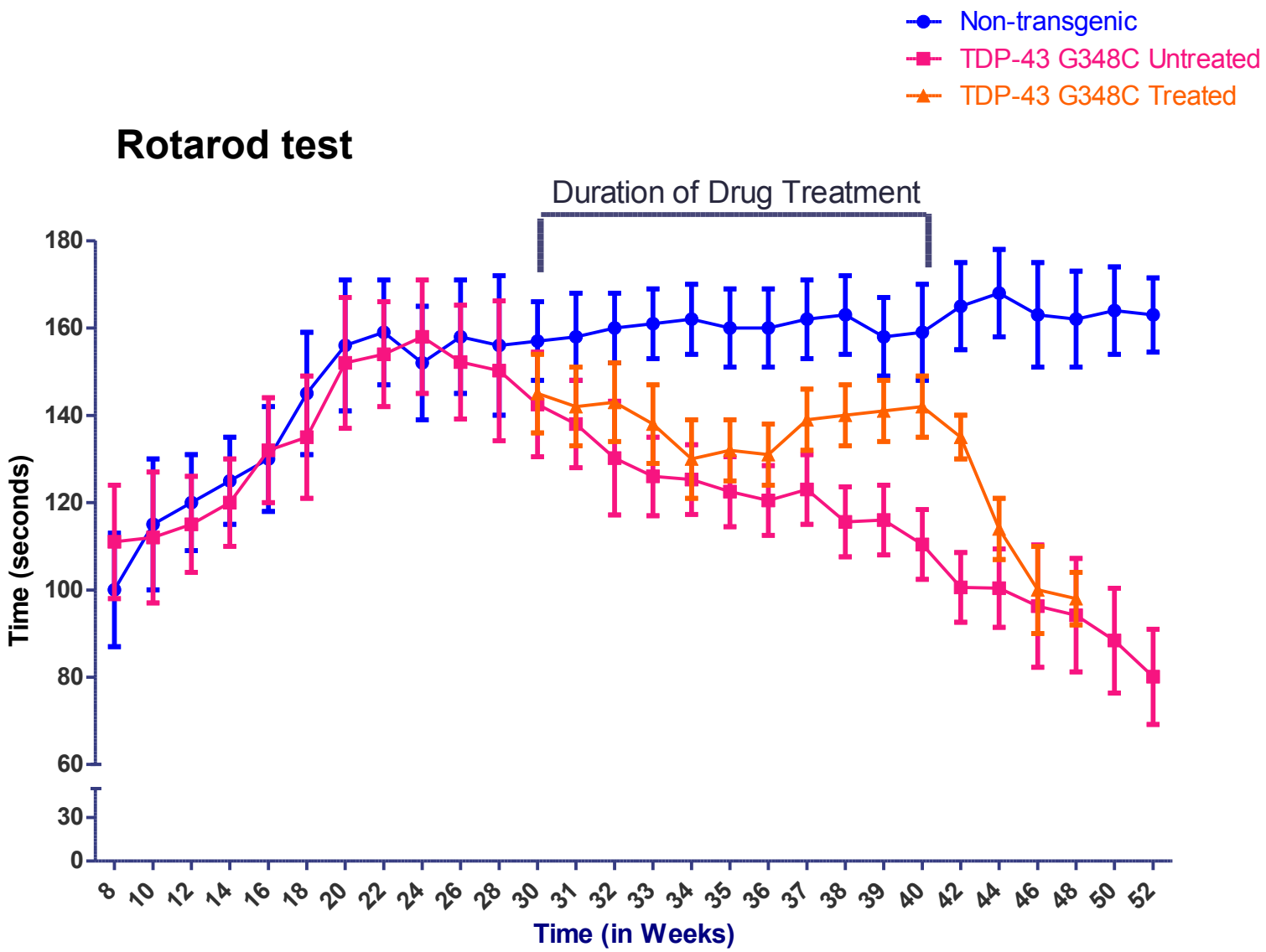

Figure Legends

Figure 2

Withaferin A extended survival of SOD1^{G93A}mice but did not delay the disease onset

To examine whether witahferin A can alleviate the mutant SOD1-induced neurotoxicity in vivo, G93A and G37R mice were intraperitoneally injected with withaferin A (WA,4mg/kg or vehicle (Saline+20%DMSO) twice a week from day 40 until clinical death and then statistically analyzed by Kaplan-Meier method. The disease onset was assessed by monitoring the body weight loss, reflex score and rotarod test once a week.

(A) Kalpan-Meier survival curve shows that vehicle treated SOD1^{G93A} (n=12) transgenic mice had a mean survival of 144 days whereas Withaferin A treated mice (n=12) lived for 153 days. Long rank test shows a statistically significant value of (P=0.0017). (B) Kalpan-Meier survival curve shows that vehicle treated SOD1^{G37R} (n=8) transgenic mice had a mean survival of 379 days whereas Withaferin A treated mice (n=8) lived for 397 days. Long rank test shows a statistically significant value of (P=0.0001).(C) Rotarod coordination: The time on rotarod was determined for SOD1^{G93A} mice injected with withaferin A and with vehicle (n=6 for all).There was no difference in the rotarod score between treated and nontreated group. Similarly WA injection didnot improve the reflex score and body weight reduction in the mice.(E, F). Each point indicates average ± SEM.

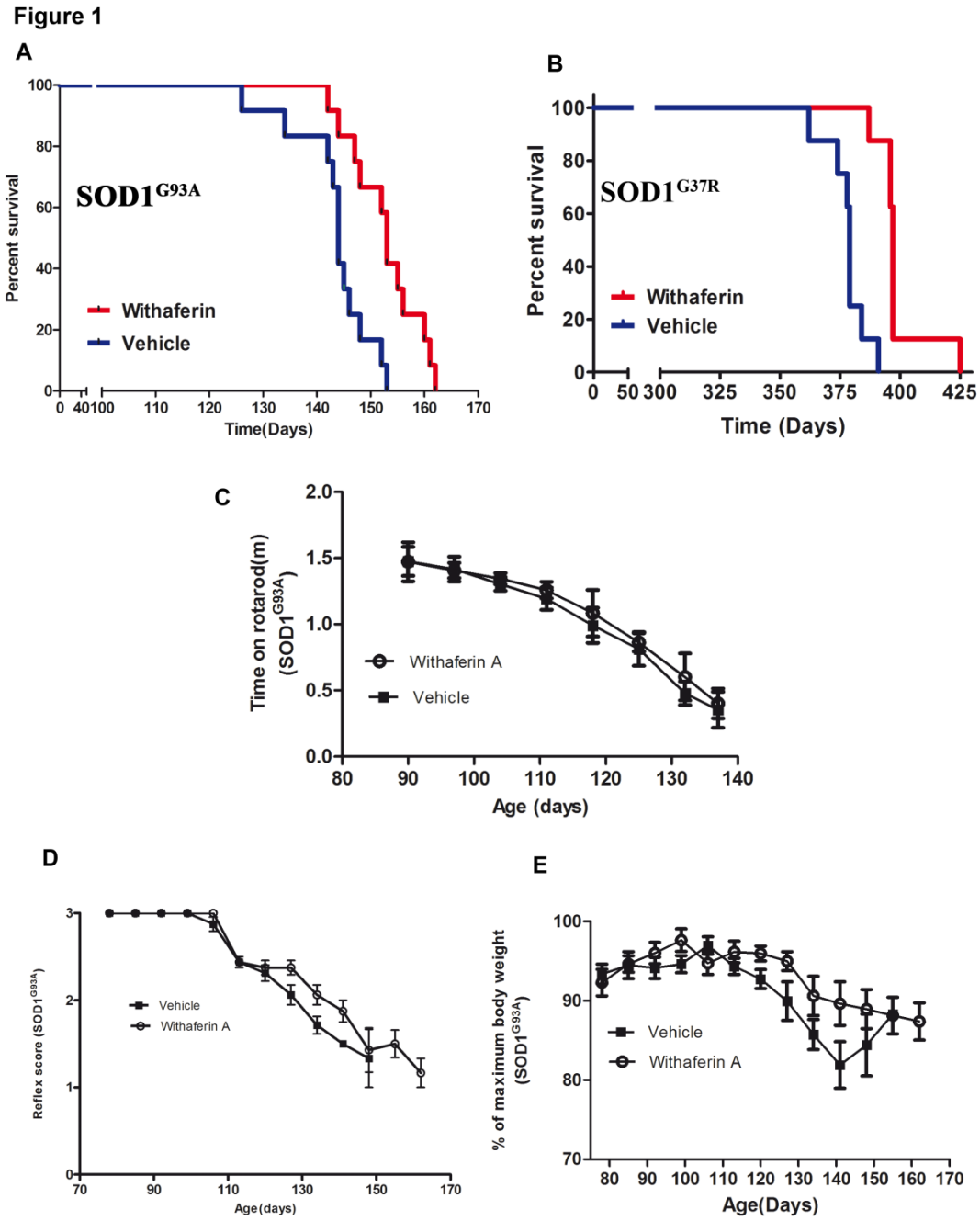

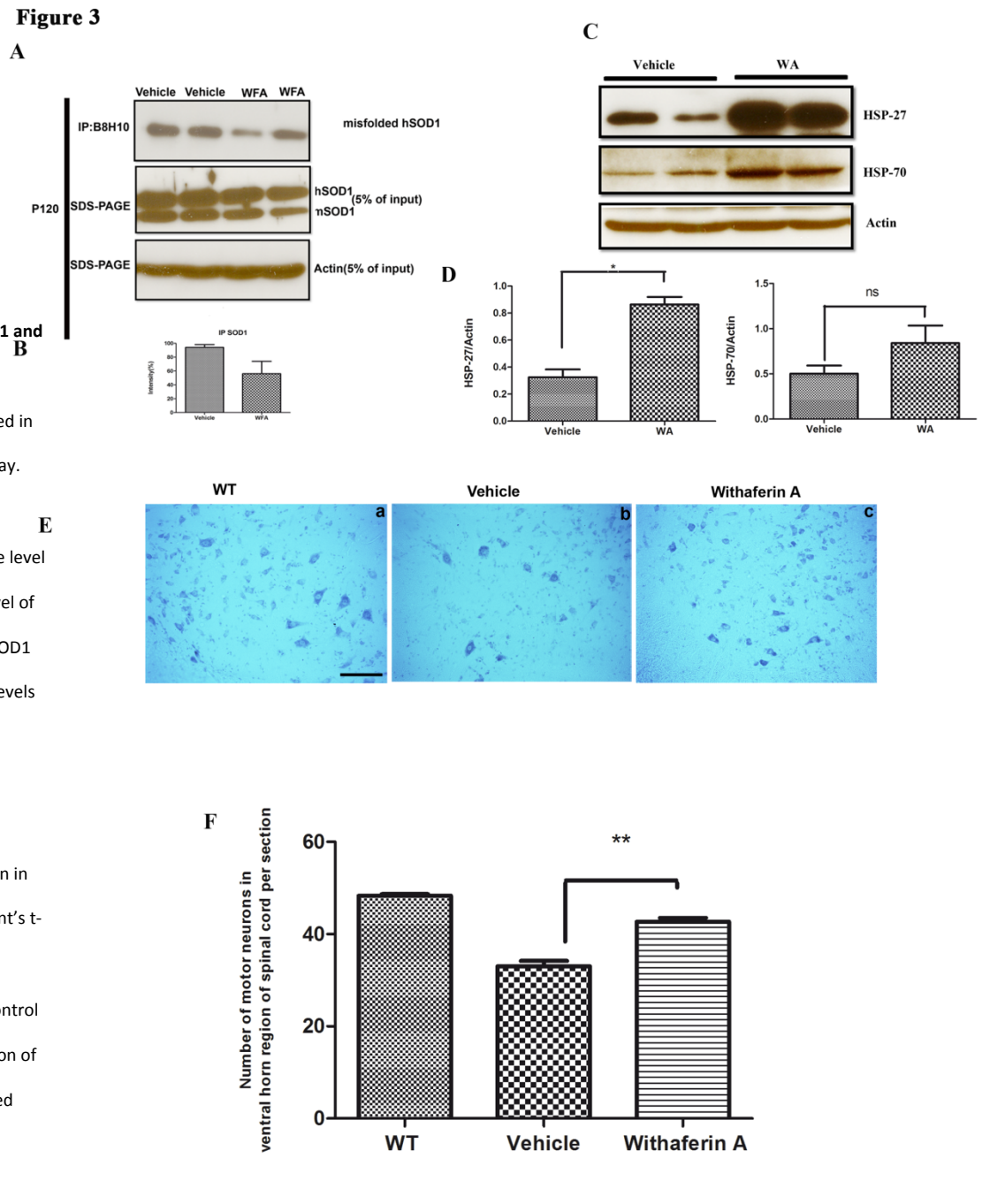

Figure 3

WA induced upregulation of heat shock protein , reduced the level of misfolded SOD1 and attenuated loss of motor neurons

(A) The protein levels of Hsp27 and Hsp70 in the spinal cord lysates were compared in the vehicle and WA-injected mice on day 120 as examined by immunoblot assay. Representative western blots for HSP-27, HSP-70 are shown .(B) Quantitative densitometric analysis of western blot showed a significant upregulation in the level of HSP-27 in the WA treated mice (p=0.0216). There was an increase in the level of HSP-70 also but was not significant(p=0.253) (C) Reduced level of misfolded SOD1 in spinal cord of mice. Intraperitoneal injection of WA led to reduction in the levels of misfolded SOD1 species as detected by B8H10 antibody (p=0.0293). Equal amount of proteins was used as shown on western blots after sodium dodecyl sulfate-polyacrylamide gel electrophoresis (SDS-PAGE) with an actin antibody. Commercial SOD100 polyclonal. antibody shows equal amount of SOD1 protein in all samples. Data represents the mean±SEM. p value were derived from student's t-test. All images are from P120 mice.

(D) Cross sections of cresyl violet stained hemi-lumbar spinal cord in WT, control $SOD1^{G93A}$ andWA treated $SOD1^{G93A}$ mice at P120 are shown.(E) Quantification of number of motor neurons showed that WA treated $SOD1^{G93A}$ mice contained more motor neurons (42.67 ± 0.8819 N=3,) compared with vehicle treated $SOD1^{G93A}$ mice (33.00 ± 1.155 N=3) (P=0.0027). Data are mean± SEM.

KEY RESEARCH ACCOMPLISHMENTS in Year Two

- Validation of 13 neuroleptics in TDP-43 worms and zebrafish.
- Identification and validation of pimozide as the most potent compound.
- Screening of 1,806 new molecules, including some structurally-related to neuroleptics, with identification of 15 novel hits.
- Screening of 3,658 derivatives of pimozide and identification of X hits, for a total of nearly 10k molecules, as expected at this stage of the project.
- Withaferin A testing in *TARDBP*^{G348C} mice, SOD1^{G93A} mice and SOD1^{G37R} mice revealed protective effects.
- Derivation and generation of *TARDBP*^{G348C} mouse cohort in a pathogen-free mouse facility. Pimozide testing in 8 months old mice will start soon.
- New (parallel) collaborations on pimozide and neuromuscular function in mice and ALS patients.

REPORTABLE OUTCOMES

Manuscripts (appendix 3).

Tauffenberger A, Julien C, Parker JA. Evaluation of longevity enhancing compounds against transactive response DNA-binding protein-43 neuronal toxicity. Neurobiology of Aging. 2013 Sep;34(9):2175-82. doi: 10.1016/j.neurobiolaging.2013.03.014. Epub 2013 Apr 13.

Abstracts.

Vaccaro A, Kabashi E, Patten K, Aggad D, Drapeau P, Parker JA, Drug Discovery for ALS, ALS Association USA, 2012, Washington, DC, USA.

Vaccaro A, Kabashi E, Patten K, Aggad D, Drapeau P, Parker JA. Chemical genetic screens for in vivo TDP-43 modifiers and ALS drug discovery. 22nd International symposium on ALS/MND, 2011. Sydney, Australia

Vaccaro A, Tauffenberger A, Parker JA. Development of *C. elegans* models for ALS. 22nd International symposium on ALS/MND, 2011. Sydney, Australia

Vaccaro A, Tauffenberger A, Parker JA. C. elegans models for ALS. International *C. elegans* Meeting 2011, University of California at Los Angeles, Los Angeles, California.

Patten SA, Vaccaro A, Kabashi E, Parker JA, Drapeau P. Pharmacological reduction of ER stress protects against TDP-43 neuronal toxicity in vivo. Society for Neuroscience, New Orleans, LO (2012)

Vaccaro A, Patten SA, Ciura S, Maios C, Therrien M, Drapeau P, Kabashi E, Parker JA. Methylene blue protects against TDP-43 and FUS neuronal toxicity in C. elegans and D. rerio. Pathology and Cellular Biology Department, University of Montreal, QC (2012)

P. Drapeau and A. Parker Chemical genetic screens of TARDBP and FUS modifiers in *C. elegans* and zebrafish. Alzheimer's Disease meeting, Cancun, Mexico (2012)

P. Drapeau and A. Parker Chemical genetic screens of TARDBP and FUS modifiers in *C. elegans* and zebrafish. Keystone Conference 'New Frontiers in Neurodegenerative Disease Research', Santa Fe NM (2013)

Patten SA, Vaccaro A, Aggad D, Maios C, Kabashi E, Parker JA, Drapeau P. Chemical genetic screens of TARDBP modifiers in C. elegans and zebrafish. 8th European Zebrafish meeting, Barcelona, Spain (2013)

Patten SA,Vaccaro A, Aggad D, Kabashi E, Parker JA, Drapeau P. Chemical genetic screens of TARDBP modifiers in C. elegans and zebrafish.. Canada Association for Neuroscience, Toronto, ON (2013)

Patten SA,Vaccaro A, Aggad D, Drapeau P, Kabashi E, Parker JA, Drapeau P. Chemical genetic screens of TARDBP modifiers in C. elegans and zebrafish.. ALS Canada, Toronto, ON (2013)

Patel P, Swarup V, Phaneuf D, Kriz J, Julien J-P. Neuroprotective effects of Withaferin A in three mouse models of amyotrophic lateral sclerosis. The XI European meeting on Glial cell function, Berlin, Germany (2013).

Presentations.

P. Drapeau
- 52nd Annual Meeting of the Canadian Association of Neuropathologists, Mt-Tremblant, Qc, Canada
- Alzheimer's Disease meeting, Cancun, Mexico (2012)
- Keystone Conference 'New Frontiers in Neurodegenerative Disease Research', Santa Fe NM.
- Brain and Mind Institute, Univ. Sydney, AUS
- Concord Hospital/ANZAC Research, Institute, Sydney, AUS
- Motoneuron Disease Group, Australian School of Advanced Medicine, Macquarie Univ., Sydney, AUS
- Department of Biological Sciences, Univ. Québec in Montréal (UQAM)

E. Kabashi
- Breakthroughs in Motor Neuron Diseases (2013) Strasbourg France.

JA. Parker
- Worming forward: Amyotrophic lateral sclerosis toxicity mechanisms and drug discovery in C. elegans. Ninth Annual ALS Canada Research Forum, Toronto, May, 2013.
- Worming forward: Amyotrophic lateral sclerosis toxicity mechanisms and drug discovery in C. elegans. McGill Centre for Research in Neuroscience Seminar Series, Montreal, January, 2013.
- Chemical genetic screens for in vivo TDP-43 and FUS modifiers in C. elegans. ALS/MND Meeting, Chicago, December, 2012.
- Amyotrophic Lateral Sclerosis: Two in vivo screening platforms and service offer. BioTransfert, Montreal, May, 2012
- Chemical genetic screens for in vivo TDP-43 and FUS modifiers in C. elegans. ALS Society of Canada's Eighth Annual ALS Research Forum, May, 2012
- High throughput in vivo drug screening in C. elegans. ALS Canada, Bench 2 Bedside, Universite de Montréal (host: D. Figlewicz) January, 2012
- Development of TDP-43 and FUS motor neuron toxicity models in C. elegans. ICM, Paris, France (host: E. Kabashi) January, 2012

JP. Julien
- ECNP Congress Vienna, 13-17 October 2012.
- Symposium of Global Centre of Excellence University of Nagoya, NF-kB as a new therapeutic target. 15-16 November 2012.
- Symposium on ALS, University of Kyoto. NF-kB as a new therapeutic target. 17 November 2012.
- Columbia University, New York. TDP-43 drives NF-kB activation in ALS, 4 December 2012.

● Conference on Neurodegenerative disorders:immunotherapy and biomarkers. Therapeutic nanobodies for ALS. Uppsala, Sweden 23-24 May 2013.
● Annual Meeting of ALS Society in Toronto. Therapeutic nanobodies for ALS. 4-5 May 2013.

Licenses/patents applied for: none.

Development of repositories. None.

Degrees obtained. None.

Animal models.
Development of a new liquid suspension C elegans model for ALS drug screening:
Vaccaro, A. Tauffenberger, D. Aggad, GA Rouleau, P Drapeau and J.A Parker.
Mutant TDP-43 and FUS Cause Age-Dependent Paralysis and Neurodegeneration in C. elegans. *Plos One* **7**, e31321 (2012).

Funding applied for.
● Synaptic targets for therapeutic protection of motor function in a genetic model of ALS. P Drapeau, Canadian Institutes for Health Research $664,370 **obtained for 04/2013-03/2018**.
● Investigating the ER stress response in TDP-43/FUS motor neuron toxicity. JA Parker, Muscular Dystrophy Association (USA), $231,000 **obtained for 08/2012-07/2015.**
● Nanobodies to disrupt TDP-43 interaction. JP Julien, FRSQ-Pfizer $200,000 **obtained for 07/2013-06/2015**
● Nanobodies for ALS treatment. JPJulien, CIHR/ALS Society of Canada. $220,000 **obtained for 09/2013-08/2015**

Employment/research opportunities.
● Edor Kabashi, Group Leader, ICM institute, Paris, France.
● Johanna Gomez Research Assistant, Kabashi lab, ICM, Paris.
● Dina Agad, postdoctoral fellow, France.
● Alexandra Vaccaro, Ph.D student, France

CONCLUSION

Our screen has identified neuroleptics, of which pimozide is the most potent, as well as withaferin A, an NFkB inhibitor, as being protective in worm and zebrafish models, with withaferin A confirmed in several mouse models and pimozide being tested. We have also identified several new molecules as well as pimozide derivatives in our worm screen. We have also tarted testing combinations of coumdounds to test for synergistic effects at low doses. Based on related observations with calcium channels agonists that proved to be neuroprotective in zebrafish, we have hypothesized that pimozide, which acts off-target on calcium channels, may be acting to help maintain neuromuscular function, offering a readily accessible peripheral target.

So what?
Because pimozide and withaferin A are FDA-approved compunds, they are immediately being tested in patients through an outside collaboration in parallel to this project.

REFERENCES

1 Vaccaro, A. *et al.* Mutant TDP-43 and FUS Cause Age-Dependent Paralysis and Neurodegeneration in C. elegans. *Plos One* **7**, e31321 (2012).

2 Vaccaro et al. Methylene Blue Protects against TDP-43 and FUS Neuronal Toxicity in C. elegans and D. rerio. PLoS ONE 7(7): e42117 (2012).

3 Kabashi, E. *et al.* Gain and loss of function of ALS-related mutations of TARDBP (TDP-43) cause motor deficits in vivo. *Hum Mol Genet* **19**, 671-683 (2010).

4 Kabashi, E. *et al.* FUS and TARDBP but Not SOD1 Interact in Genetic Models of Amyotrophic Lateral Sclerosis. *Plos Genetics* **7**, e1002214 (2011).

5 Swarup, V. *et al.* Pathological hallmarks of amyotrophic lateral sclerosis/frontotemporal lobar degeneration in transgenic mice produced with TDP-43 genomic fragments. *Brain* **134**, 2610-2626 (2011).

6 Kabashi, E., Champagne, N., Brustein, E. & Drapeau, P. In the swim of things: recent insights to neurogenetic disorders from zebrafish. *Trends Genet* **26**, 373-381 (2010).

7 Kabashi, E., Brustein, E., Champagne, N. & Drapeau, P. Zebrafish models for the functional genomics of neurogenetic disorders. *Biochim Biophys Acta* **3**, 335-345 (2011).

8 Kabashi, E. *et al.* Gain and loss of function of ALS-related mutations of TARDBP (TDP-43) cause motor deficits in vivo. *Hum Mol Genet* **19**, 3102-3102 (2010).

9 Vaccaro, A. *et al.* Methylene Blue Protects against TDP-43 and FUS Neuronal Toxicity in C. elegans and D. rerio. *Plos One* **7**, e42117 (2012).

10 Audet JN, Soucy G, Julien JP. (2012) Methylene blue administration fails to confer neuroprotection in two amyotrophic lateral sclerosis mouse models. Neuroscience. 209:136-43.

11 Armstrong, GAB and Drapeau, P. (2013) Calcium channel agonists protect against neuromuscular dysfunction in a genetic model of TDP-43 mutation in ALS. J. Neurosci. 33(4):1741–1752.

12. Vaccaro, A; S.A. Patten; D. Aggad; C. Julien; C. Maios; E. Kabashi; P.Drapeau; JA Parker (2013) Pharmacological reduction of ER stress protects against TDP-43 neuronal toxicity in vivo. Neurobiol. Dis. 55:64-75.

13. Tauffenberger A, Julien C, Parker JA. Evaluation of longevity enhancing compounds against transactive response DNA-binding protein-43 neuronal toxicity. Neurobiology of Aging. 2013 (9):2175-82.

14. Dawe GS 2010 Neuroscience 171, 162-172;

15. Navarro JF et al. Prog Neuropsychopharmacol Biol Psychiatry. 2000 Jan;24(1):131-42)

16. Swarup V., Phaneuf D., Dupré N., Petri S., Strong M., Kriz J. and Julien J.-P. (2011) Deregulation of TDP-43 in ALS triggers nuclear factor-κB-mediated pathogenic pathways. J Exp Med, 208(12):2429-2447

OPEN ACCESS Freely available online

PLoS one

Mutant TDP-43 and FUS Cause Age-Dependent Paralysis and Neurodegeneration in *C. elegans*

Alexandra Vaccaro[1,2,3], Arnaud Tauffenberger[1,2,3], Dina Aggad[1,2,3], Guy Rouleau[1,2,4], Pierre Drapeau[2,3], J. Alex Parker[1,2,3]*

1 The Research Centre of the University of Montreal Hospital Centre, Université de Montréal, Montréal, Québec, Canada, **2** Centre of Excellence in Neuromics, Université de Montréal, Montréal, Québec, Canada, **3** Département de Pathologie et Biologie Cellulaire, Université de Montréal, Montréal, Québec, Canada, **4** Département de Médecine, Université de Montréal, Montréal, Québec, Canada

Abstract

Mutations in the DNA/RNA binding proteins TDP-43 and FUS are associated with Amyotrophic Lateral Sclerosis and Frontotemporal Lobar Degeneration. Intracellular accumulations of wild type TDP-43 and FUS are observed in a growing number of late-onset diseases suggesting that TDP-43 and FUS proteinopathies may contribute to multiple neurodegenerative diseases. To better understand the mechanisms of TDP-43 and FUS toxicity we have created transgenic *Caenorhabditis elegans* strains that express full-length, untagged human TDP-43 and FUS in the worm's GABAergic motor neurons. Transgenic worms expressing mutant TDP-43 and FUS display adult-onset, age-dependent loss of motility, progressive paralysis and neuronal degeneration that is distinct from wild type alleles. Additionally, mutant TDP-43 and FUS proteins are highly insoluble while wild type proteins remain soluble suggesting that protein misfolding may contribute to toxicity. Populations of mutant TDP-43 and FUS transgenics grown on solid media become paralyzed over 7 to 12 days. We have developed a liquid culture assay where the paralysis phenotype evolves over several hours. We introduce *C. elegans* transgenics for mutant TDP-43 and FUS motor neuron toxicity that may be used for rapid genetic and pharmacological suppressor screening.

Citation: Vaccaro A, Tauffenberger A, Aggad D, Rouleau G, Drapeau P, et al. (2012) Mutant TDP-43 and FUS Cause Age-Dependent Paralysis and Neurodegeneration in *C. elegans*. PLoS ONE 7(2): e31321. doi:10.1371/journal.pone.0031321

Editor: Leonard Petrucelli, Mayo Clinic, United States of America

Received October 11, 2011; **Accepted** January 5, 2012; **Published** February 21, 2012

Funding: This research was supported by: Montreal University Hospital Foundation (http://fondationduchum.com/fr) to JAP, Natural Sciences and Engineering Research Council Discovery Grant (http://www.nserc-crsng.gc.ca) to JAP, Canadian Institutes of Health Research New Investigator (http://www.cihr-irsc.gc.ca) to JAP, Frick Foundation for ALS Research (http://frick-fondation.ch) to PD and JAP and a Bernice Ramsay Discovery Grant from the ALS Society of Canada (http://www.als.ca/) to JAP. The funders had no role in study design, data collection and analysis, decision to publish, or preparation of the manuscript.

Competing Interests: The authors have declared that no competing interests exist.

* E-mail: ja.parker@umontreal.ca

Introduction

Amyotrophic Lateral Sclerosis (ALS) is a late-onset progressive disease affecting motor neurons ultimately causing fatal paralysis [1,2]. Most cases are sporadic, but ~10% of patients have an inherited familial form of the disease. Dominant mutations in SOD1 (copper/zinc superoxide dismutase 1) account for ~20% of familial ALS cases and ~1% of sporadic cases [1]. The recent discovery of mutations in TAR DNA-binding protein-43 (TDP-43) and Fused in sarcoma (FUS, also named TLS) in both familial ALS and frontotemporal dementia (FTD) has shifted research into disease mechanisms and potential therapeutics [3–9].

TDP-43 and FUS are evolutionarily conserved DNA/RNA binding proteins that shuttle between the nucleus and cytoplasm having multiple roles including DNA transcription and RNA processing [3,9–12]. Mutant TDP-43 and FUS (mTDP-43 and mFUS) are found in cytoplasmic inclusions in the disease state while the accumulation of wild type TDP-43 and FUS (wtTDP-43 and wtFUS) are observed in an increasing number of disorders including Alzheimer's Disease, Parkinson's Disease and the polyglutamine diseases (reviewed in [10]). The pathogenic mechanisms for mutant TDP-43 and FUS age-dependent neuronal toxicity remain unclear. As of now there is no consensus whether mutant TDP-43 and FUS employ a loss-of-function, a gain-of-function, or both in motor neuron cell death.

Since TDP-43 and FUS are evolutionarily conserved we used the nematode *Caenorhabditis elegans* to investigate mutant TDP-43 and FUS age-dependent neurodegeneration. We created transgenic nematodes that express full-length wild type or mutant TDP-43 and FUS in the worm's GABAergic motor neurons. Transgenic TDP-43 and FUS worms recapitulate a salient feature of ALS; they display adult-onset, age-dependent, progressive paralysis and degeneration of motor neurons. Importantly, mTDP-43 and mFUS, but not wtTDP-43 and wtFUS, strains show the presence of insoluble proteins in extracts from whole animals suggesting that protein misfolding may be a primary cause of toxicity. We introduce a genetically tractable platform to investigate motor neuron toxicity caused by mutant TDP-43 and FUS that can be used for suppressor screening.

Results

Transgenic worms expressing full-length human TDP-43 or FUS in motor neurons display age-dependent paralysis

Since ALS is a motor neuron disease we expressed wild type and mutant human TDP-43 and FUS proteins in the worm's 26 GABAergic motor neurons with the vesicular GABA transporter (*unc-47*) promoter (Figures 1A, B) [13]. Multiple transgenic strains carrying extrachromosomal arrays were obtained by microinjection and stable lines with chromosomally-integrated transgenes

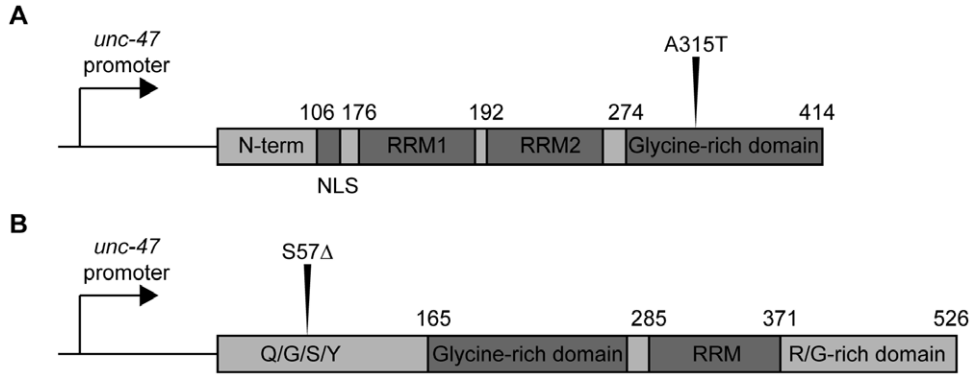

Figure 1. TDP-43 and FUS transgene constructs. (A) Full-length wild type human TDP-43 and the clinical mutation A315T were cloned into a vector for expression in motor neurons by the *unc-47* promoter and injected into *C. elegans*. (B) Full-length wild type human FUS and the clinical mutation S57Δ were cloned into the *unc-47* expression vector and injected into *C. elegans*. RRM (RNA Recognition Motif), Q/G/S/Y (Glutamine-Glycine-Serine-Tyrosine-rich region), R/G (Arginine-Glycine-rich region), NLS (Nuclear localization signal).
doi:10.1371/journal.pone.0031321.g001

were isolated after UV-irradiation [14]. Both wild type TDP-43 and the ALS-associated A315T mutant proteins were expressed in transgenic worms as detected by immunoblotting of worm protein extracts with a human specific TDP-43 antibody (Figure 2A) [4]. Similarly, using a FUS antibody we confirmed the expression of wild type and the ALS-linked S57Δ mutant proteins by western blotting (Figure 2B) [15].

All strains were morphologically normal and showed no adverse phenotypes during development. However, during adulthood the transgenic strains begin to display uncoordinated motility phenotypes that progressed to paralysation. Paralysis was age-dependent and occurred at higher rate for mTDP-43 and mFUS worms compared to wtTDP-43 and wtFUS transgenics (Figures 3 A, B). Typically, after 12–13 days on plates 100% of the mTDP-43 and mFUS worms were paralysed while only 20% of the wtTDP-43 and wtFUS worms were affected. The low rate of paralysis for wtTDP-43 and wtFUS strains is comparable to what is observed in transgenics expressing GFP from the same *unc-47* promoter (Figure 3C). Additionally, the paralysis assay is widely used to study age-dependent degenerative phenotypes and is not observed in wild type non-transgenic worms until they reach advanced age (approximately 20 days) [16–18]. Finally, motility defects and adult onset paralysis have been previously observed in worms with degenerating GABAergic motor neurons suggesting that mTDP-43 and mFUS may negatively affect GABAergic neuronal function and survival [19].

TDP-43 and FUS transgenics have normal lifespans

One of the signs of aging in worms is decreased motility [18,20]. Thus the progressive paralysis phenotypes observed in the TDP-43 and FUS transgenics may be due to overall decreased health from the expression of toxic non-native proteins leading to accelerated mortality, a part of which is a decline in motility. We conducted lifespan analyses and observed that all of the transgenics had lifespans indistinguishable from non-transgenic wild type N2 worms (Figures 4A, B and Table S1). These observations suggest that the paralysis observed in our models is specific to the expression of TDP-43 and FUS in motor neurons and not due to secondary effects from general sickness and reduced lifespan.

TDP-43 and FUS cause neuronal dysfunction

The progressive paralysis phenotypes caused by mTDP-43 and mFUS suggest there may be motor neuron dysfunction and/or

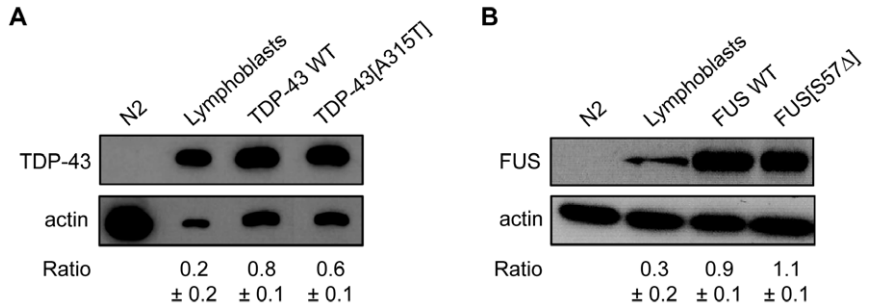

Figure 2. Expression of human TDP-43 and FUS proteins in *C. elegans* transgenics. (A) Total protein levels from non-transgenic worms, human lymphoblast cells and transgenic worms expressing wtTDP-43 or mTDP-43. Staining with a human TDP-43 antibody showed no signal for non-transgenic worms but a signal corresponding to full-length human TDP-43 at ~45 kDa in size was observed in extracts from human cells and the two transgenic TDP-43 worm strains. wtTDP-43 and mTDP-43 strains showed comparable protein expression levels. (B) Total protein levels from non-transgenic worms, human lymphoblast cells and transgenic worms expressing wtFUS or mFUS. Using a human FUS antibody, no signal was detected in non-transgenic worms, but a signal corresponding to full-length human FUS at ~75 kDa in size was observed in extracts from lymphoblast cells and the transgenic FUS worm strains. wtFUS and mFUS worms showed identical levels of protein expression. For all experiments actin staining was used as a loading control and expression ratios ± SEM of TDP-43 or FUS to actin was determined from 3 independent experiments. Representative western blots are shown.
doi:10.1371/journal.pone.0031321.g002

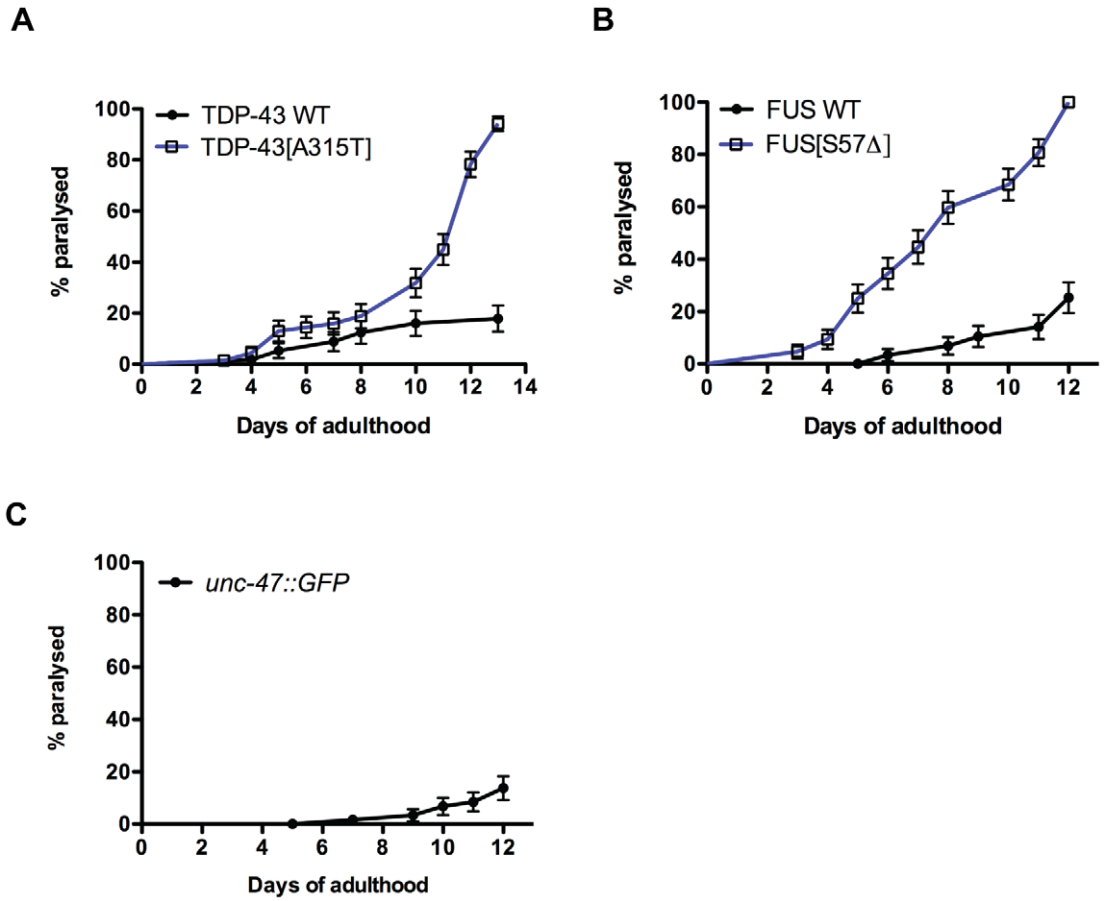

Figure 3. Mutant TDP-43 and FUS cause adult-onset, age-dependent paralysis in *C. elegans*. Transgenics were monitored from the adult stage and scored daily for paralysis. (A) mTDP-43 worms show a rate of progressive paralysis that is greater than transgenics expressing wtTDP-43 ($P<0.001$). (B) Transgenics expressing mFUS become paralysed significantly sooner than wtFUS control transgenics ($P<0.001$). (C) Transgenic worms expressing GFP in motor neurons show low levels of paralysis.
doi:10.1371/journal.pone.0031321.g003

degeneration in these animals. *C. elegans* body wall muscle cells receive excitatory (acetylcholine) and inhibitory (GABA) inputs to coordinate muscle contraction/relaxation and facilitate movement [21,22]. Body wall muscle activity can be measured indirectly with the acetylcholinesterase inhibitor aldicarb [23]. Exposure to aldicarb causes accumulation of acetylcholine at neuromuscular junctions resulting in hyperactive cholinergic synapses, muscle hypercontraction, and acute paralysis [23]. Hypersensitivity to

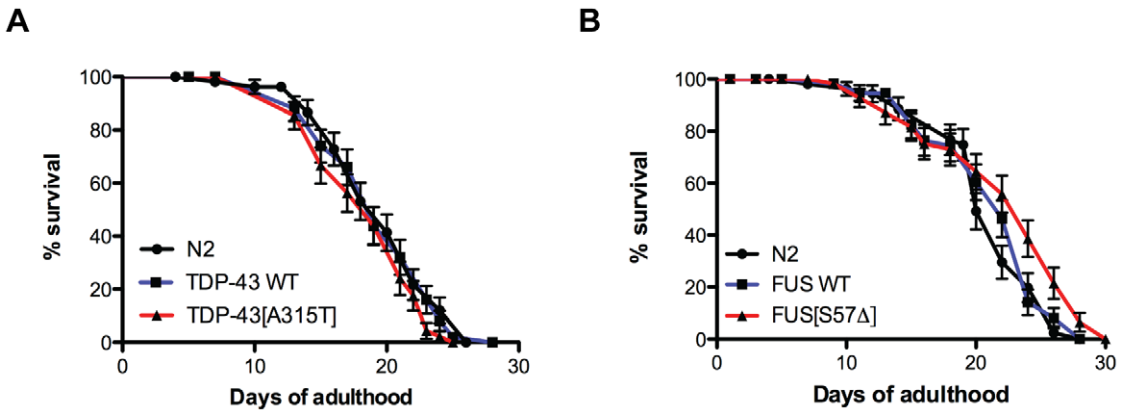

Figure 4. TDP-43 and FUS transgenes do not affect lifespan. Beginning at Day 1 of adulthood we tested the lifespans of wild type non-transgenic N2 worms and transgenics expressing (A) wtTDP-43 and mTDP-43 as well as (B) animals expressing wtFUS and mFUS. Animals expressing TDP-43 or FUS transgenes had lifespans indistinguishable from N2 worms.
doi:10.1371/journal.pone.0031321.g004

aldicarb-induced paralysis has been used to identify genes that increase acetylcholine secretion or decrease inhibitory GABA signalling [24]. For example mutants lacking genes required for GABA transmission like the vesicular GABA transporter *unc-47* are hypersensitive to aldicarb-induced paralysis [25]. To investigate if our TDP-43 and FUS transgenics had abnormal activity at the neuromuscular junction we exposed the animals to aldicarb. We observed that, like *unc-47* mutants, mTDP-43 and mFUS animals were hypersensitive to aldicarb-induced paralysis, while wtTDP-43 and wtFUS transgenics showed a rate paralysis identical to non-transgenic N2 worms (Figures 5A, B). These data suggest that the inhibitory GABA signalling is impaired in mTDP-43 and mFUS transgenics. *unc-47* mutants are classically described as having a "shrinker" phenotype, where in response to touch the worm does not move away but instead the whole body undergoes longitudinal shortening [21], and we observed that the shrinker phenotype was weakly penetrant in adult mTDP-43 and mFUS worms. To determine if impaired GABAergic neurotransmission contributed to the paralysis phenotype we examined two *unc-47* loss-of-function mutants and they both showed age-dependent paralysis, a phenotype not previously reported for *unc-47* (Figure 5C) [21]. Thus, mTDP-43 and mFUS cause neuronal dysfunction in GABA neurons leading to progressive motility defects culminating in paralysis, a phenotype similar to animals deficient in GABAergic signalling.

TDP-43 and FUS cause progressive degeneration of motor neurons

Many neurodegenerative diseases are characterized by neuronal dysfunction prior to degeneration [26]. To investigate if the progressive paralysis phenotypes in our TDP-43 and FUS transgenics were accompanied by neurodegeneration we crossed all of the transgenics with an integrated reporter (*unc-47p::GFP*) that expresses GFP in the same GABAergic motor neurons [13] (Figures 6A, B). Similar to reports from another *C. elegans* TDP-43 toxicity model [27], we observed gaps/breaks in motor neuron processes in TDP-43 and FUS animals compared to animals expressing *unc-47p::GFP* alone (Figures 6 C–F). We extended our analysis by scoring degeneration in living GFP, wtTDP-43, mTDP-43, wtFUS and mFUS transgenics at days 1, 5 and 9 of adulthood. We observed that degeneration was age-dependent and occurred at higher rate for the mTDP-43 and mFUS animals compared to the wtTDP-43 and wtFUS transgenics (Figure 6G). Thus our TDP-43 and FUS transgenics mimic the adult-onset, gradual decline of neuronal function ultimately resulting in age-dependent motor neuron degeneration seen in diseases like ALS.

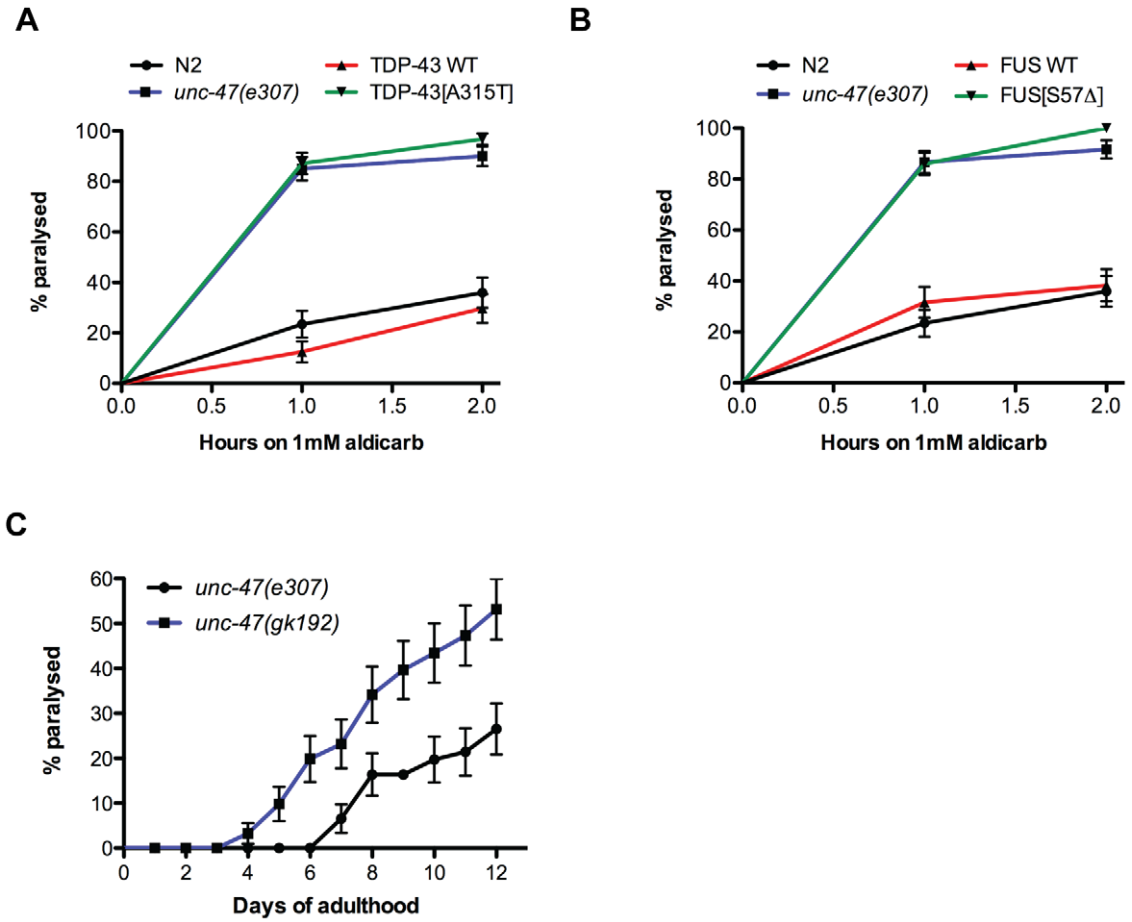

Figure 5. Mutant TDP-43 and FUS impair synaptic transmission. (A) Cholinergic neuronal transmission was measured by determining the onset of paralysis induced by the cholinesterase inhibitor aldicarb. *unc-47(e307)* mutants and mTDP-43 transgenics were hypersensitive to aldicarb-induced paralysis compared to either wtTDP-43 transgenics or N2 worms ($P<0.001$ for *unc-47* or mTDP-43 compared to N2 or wtTDP-43 worms). (B) mFUS transgenics and *unc-47(e307)* mutants were more sensitive to aldicarb induced paralysis compared to either wtFUS transgenics or N2 controls ($P<0.001$). (C) *unc-47* mutants grown on regular worm plates showed age-dependent progressive paralysis.
doi:10.1371/journal.pone.0031321.g005

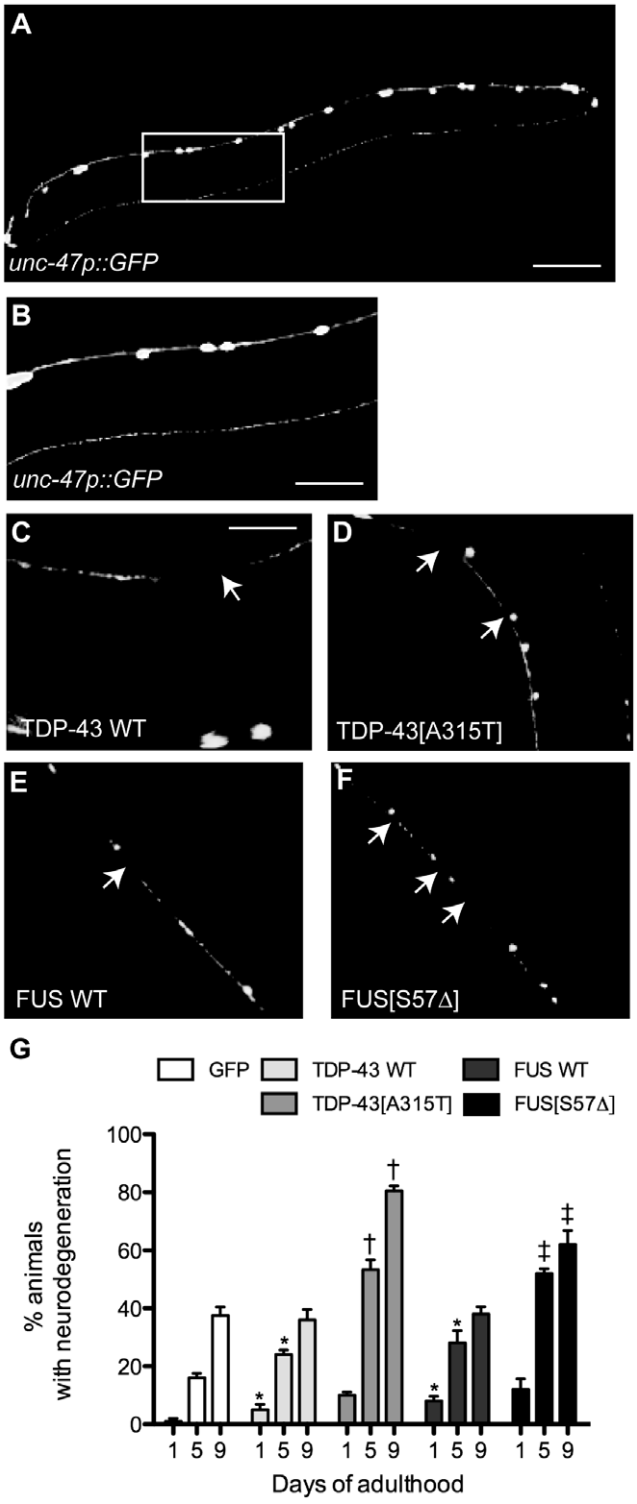

Figure 6. Mutant TDP-43 causes motor neuron degeneration. Shown are representative photos of living, adult *unc-47p::GFP*, *unc-47p::GFP;TDP-43*, and *unc-47p::GFP;FUS* transgenics. (A) Image of an entire *unc-47p::GFP* worm showing the GABAergic motor neurons. Scale bar represents 50 μm. (B) High-magnification of the framed area from (A) showing wild type morphology of motor neurons. Scale bar represents 20 μm. High magnification of motor neurons labelled with *unc-47p::GFP* in (C) wtTDP-43, (D) mTDP-43, (E) wtFUS and (F) mFUS transgenics showing gaps along neuronal processes (arrows). Scale bar represents 10 μm for photos (C) to (F). (G) Quantification of neurodegeneration in transgenic worms at days 1, 5 and 9 of adulthood. * wtTDP-43 and wtFUS have a higher rate of neurodegeneration compared to *unc-47p::GFP* controls at days 1 and 5 of adulthood ($P<0.05$). †mTDP-43 transgenics have a higher rate of neurodegeneration at days 5 and 9 compared to wtTDP-43 transgenics ($P<0.001$). ‡mFUS transgenics show an enhanced rate of neurodegeneration at days 5 and 9 of adulthood in compared to wtFUS transgenics ($P<0.001$).
doi:10.1371/journal.pone.0031321.g006

Mutant TDP-43 and FUS are highly insoluble

Since TDP-43 and FUS are prone to aggregation in several model systems including *C. elegans*, we tested if the same was true for our transgenics [27–33]. To examine if protein misfolding is more pronounced for strains expressing mTDP-43 and mFUS, we used a biochemical assay to detect protein aggregation. Homogenized protein extracts from transgenic worms were separated into supernatant (detergent-soluble) and pellet (detergent-insoluble) fractions [30]. Immunoblotting the TDP-43 transgenics with a human TDP-43 antibody revealed the accumulation of mTDP-43 in the pelleted, insoluble fraction, while wtTDP-43 proteins were predominantly detected in the supernatant, or soluble fractions (Figure 7A). Similar results were obtained for the FUS transgenics where immunoblotting with a human FUS antibody showed that mFUS accumulated in the insoluble pellet fraction while wtFUS proteins remained soluble (Figure 7B). These data suggest that mTDP-43 and mFUS proteins are susceptible to misfolding leading to insolubility and aggregation that may contribute to motor neuron dysfunction and degeneration.

Next focusing on the mTDP-43 and mFUS transgenics we fixed whole *unc-47p::GFP;mTDP-43* and *unc-47p::GFP;mFUS* worms and respectively stained them with human TDP-43 and human FUS antibodies. We detected mTDP-43 and mFUS in both the nuclei and cytoplasm of motor neurons (Figure 8). The cytoplasmic accumulation of mTDP-43 and mFUS in our transgenics is consistent with findings in patients suggesting that these proteins misfold leading to intracellular build-up and aggregation [10].

Finally, we noticed that the fixed mTDP-43 and mFUS showed gaps or breaks along the GFP labelled neuronal processes similar to what was observed in living animals (Figures 6D, F). To confirm that neurodegeneration was not simply due to loss of GFP signals, we stained whole *unc-47p::GFP;mTDP-43* and *unc-47p::GFP;mFUS* worms for GABA [22]. We observed that the gaps along the processes as visualized by a loss of GFP signal likewise corresponded to a loss of GABA staining (Figure 9). Altogether these data suggest that the expression of TDP-43 and FUS lead to degeneration of motor neurons as has been observed for TDP-43 in other worm models [27].

Paralysis phenotypes are enhanced in liquid culture

One goal in developing these transgenics is for use in genetic and pharmacological suppressor screens. TDP-43 and FUS transgenics may have decreased inhibitory GABA signalling ultimately causing muscle hypercontraction leading to paralysis. When grown on solid media the mTDP-43 and mFUS paralysis phenotypes manifest over a period of 5 to 13 days (Figure 3). Worms grown in liquid culture exhibit a stereotypical swimming motion that is considerably more vigorous than worms crawling on solid media [34]. We hypothesized that placing worms in liquid culture would increase activity at the neuromuscular junction and precipitate paralysis phenotypes much earlier than worms grown on solid media.

Using age-synchronized worms we transferred young adult TDP-43 and FUS transgenics to 96-well plates with liquid media and scored their motility every 2 hours. We observed a rapid

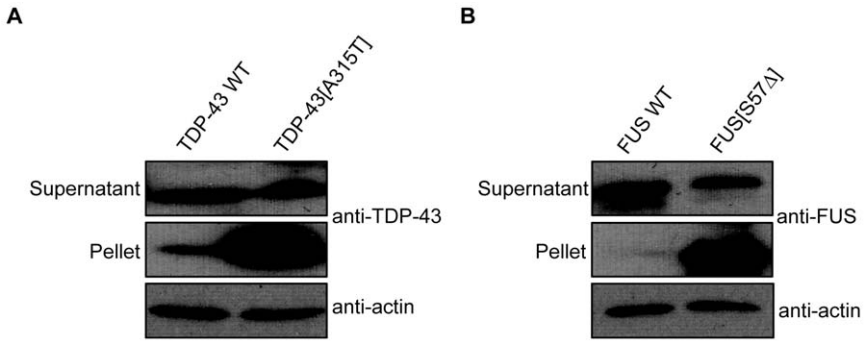

Figure 7. Mutant TDP-43 and FUS are highly insoluble. Shown are representative images from western blotting of the soluble supernatant and insoluble pellet fractions of protein extracts from transgenic TDP-43 and FUS strains. (A) Blotting against TDP-43 shows that a large proportion of the TDP-43 signal resides in the insoluble fraction for mTDP-43 worms, while the signal is largely soluble for the wtTDP-43 samples. (B) Immunoblotting with a human FUS antibody revealed that mFUS proteins primarily resided in the insoluble fractions while wtFUS proteins were exclusively soluble. Immunoblotting for actin was used as the loading control.
doi:10.1371/journal.pone.0031321.g007

onset of paralysis for the mTDP-43 and mFUS lines with approximately 80% of the population becoming immobile after 6 hours progressing to 100% paralysis after 12 hours (Figure 10A, B Videos S1, S2, S3, S4). wtTDP-43 and wtFUS animals also showed increased paralysis but at a much lower rate, with approximately 20% of the animals immobile after 6 hours moving to 80% paralysis after 12 hours (Figure 10, Videos S5, S6, S7, S8). Non-transgenic N2 animals showed a very low rate of paralysis of approximately 15% after 12 hours (Figure 10C, Videos S9, S10). In comparison, approximately 50% of transgenic *unc-47p::GFP* control animals were paralysed after 12 hours, a rate intermediate between non-transgenic N2 worms and transgenic wtTDP-43 and wtFUS animals (Figure 10C, Videos S11, S12). The difference between wild type and mutant transgenic lines is easy to distinguish, particularly at 6 hours, and suggests that this phenotype may be used for rapid genetic and chemical screening.

Discussion

Here we introduce a novel *C. elegans* platform for investigating mechanisms of motor neuron toxicity caused by mTDP-43 and mFUS. To more closely model human disease we chose to express full-length human TDP-43 and FUS without additional tags since the inclusion of tags like GFP can mask or enhance the phenotypes of wild type and mutant proteins [35,36]. Additionally, we reasoned that restricting expression to a smaller set of neurons might produce phenotypes less severe, or later, than observed in other *C. elegans* models [27,29,30,33]. Since ALS is characterized by degeneration of the motor neurons we engineered strains expressing human TDP-43 and FUS in the animal's 26 GABAergic neurons [13,22]. Additionally, ALS patients show cortical hyperexcitability that may be due to reduced inhibitory signalling from the GABAergic system [37,38]. We believe our transgenic mTDP-43 and mFUS worms recapitulate this patho-

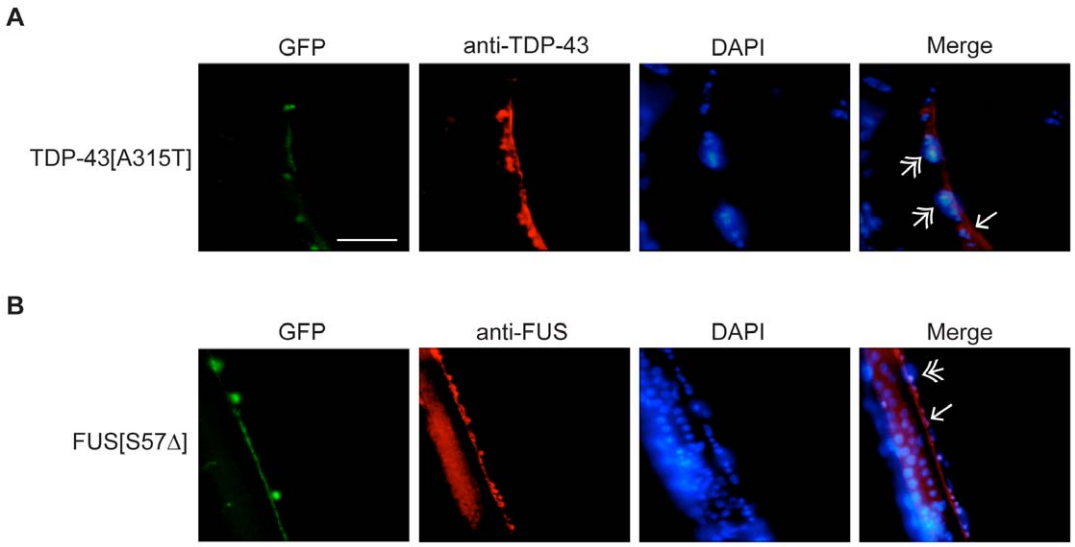

Figure 8. Mutant TDP-43 and FUS aggregate in vivo. (A) Representative image of a fixed *unc-47p::GFP;mTDP-43* worm stained with a human TDP-43 antibody. The green channel shows GFP labelled motor neurons. Antibody staining (red signal) revealed aggregation of TDP-43 signals in motor neurons. Staining of motor neuron nuclei with DAPI (blue signal) revealed that TDP-43 is both cytoplasmic (single arrowhead) and nuclear (double arrowhead). Scale bar represents 10 μm for all photos. (B) Staining of *unc-47p::GFP;mFUS* worms with a human FUS antibody (red signal) and DAPI (blue signal) revealed cytoplasmic (single arrowhead) and nuclear (double arrowhead) accumulations in motor neurons.
doi:10.1371/journal.pone.0031321.g008

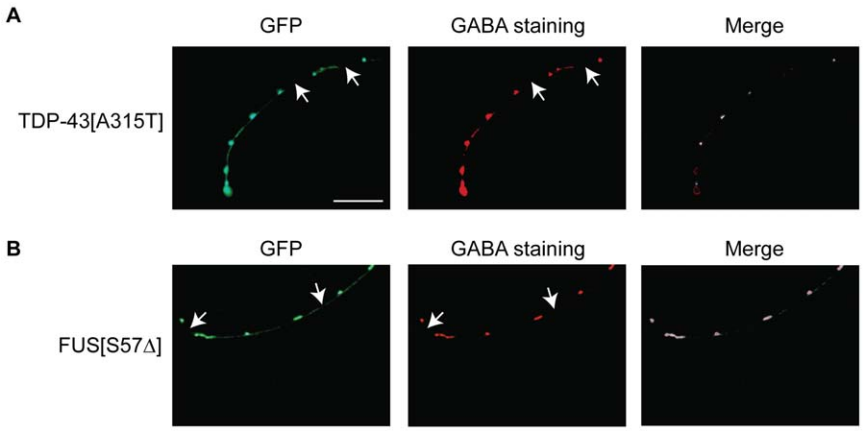

Figure 9. Decreased GABA staining in mutant TDP-43 and FUS worms. (A) Fluorescent micrograph of a fixed *unc-47p::GFP;mTDP-43* worm stained with a GABA antibody revealed neurodegeneration in motor neurons that mirrors the loss of GFP signals. Scale bar represents 10 μm for all photos. (B) Staining of *unc-47p::GFP;mFUS* worms also showed loss of GABA signals similar to the loss of GFP in the motor neurons.
doi:10.1371/journal.pone.0031321.g009

physiological mechanism; they show decreased GABA staining and are hypersensitive to the acetylcholinesterase inhibitor aldicarb, suggesting a reduction of inhibitory GABA input at neuromuscular junctions [24,25]. In our models sensitivity to aldicarb can be detected in day 1 adult worms, while paralysis and motor neuron degeneration can first be detected starting at day 5 of adulthood demonstrating that similar to ALS, neuronal dysfunction occurs prior to neurodegeneration [39].

Importantly, our transgenic TDP-43 and FUS animals only begin to show motility defects once they have reached adulthood a feature absent from other models [27,29,30,33]. Thus our models mirror a prominent clinical feature of ALS, they display adult-

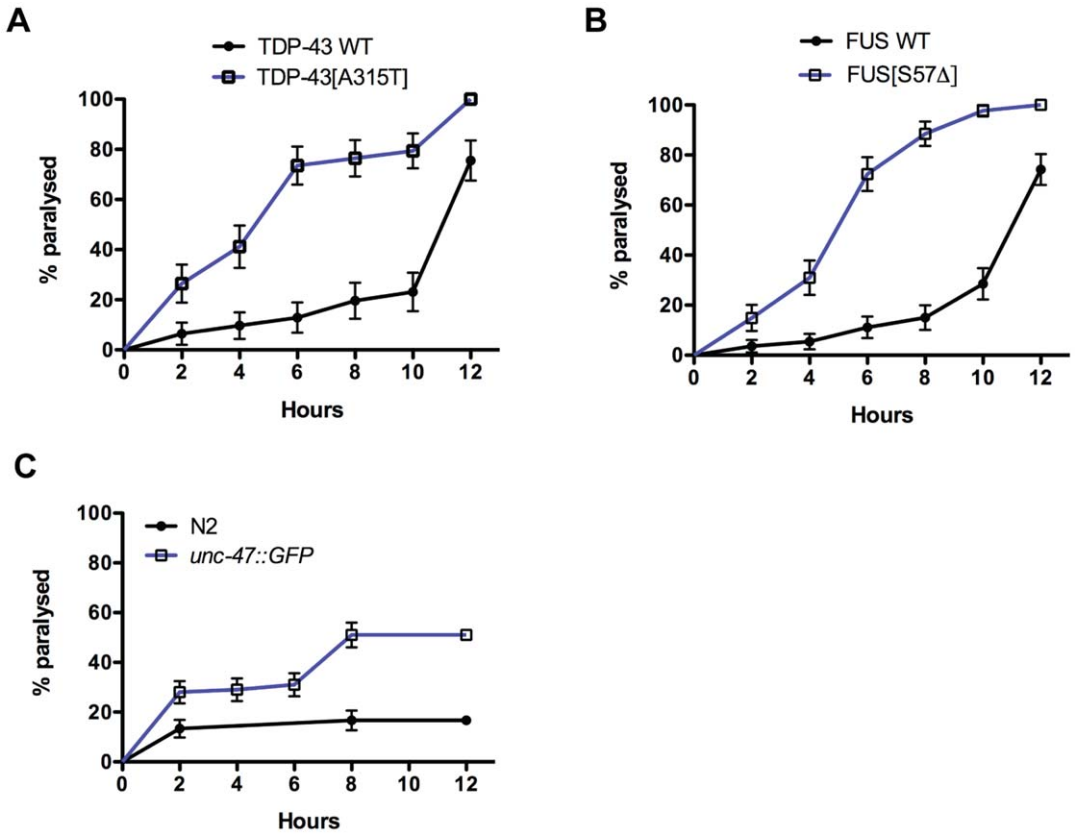

Figure 10. Accelerated paralysis phenotypes for TDP-43 and FUS transgenics in liquid culture. (A) Paralysis phenotypes resolve over a number of hours for wtTDP-43 and mTDP-43 worms grown in liquid culture. mTDP-43 worms have a faster rate of paralysis compared to wtTDP-43 transgenics ($P<0.001$). (B) Transgenic mFUS worms show motility defects and become paralysed at a rate faster than wtFUS controls ($P<0.001$). (C) *unc-47p::GFP* transgenics have an increased rate of paralysis compared to non-transgenic N2 worms ($P<0.001$).
doi:10.1371/journal.pone.0031321.g010

onset, age-dependent, progressive paralysis [40,41]. Additionally, unlike previously described TDP-43 and FUS models based on pan-neuronal expression [27,30,33] our transgenics do not show reduced lifespan suggesting the behavioural phenotypes observed in our transgenics are not influenced by general sickness. Our transgenics do share many features with other neuronal-based models, notably the aggregation and insolubility of mutant TDP-43 and FUS as well as degeneration of motor neurons suggesting there may be common mechanisms of toxicity amongst the models [27,29,30,32,33,42–45]. However, cytoplasmic aggregation of TDP-43 and FUS is a prominent feature of the human pathologies and this is seen in a recently described worm FUS model [33], but is absent from previously reported TDP-43 models [27,29,30]. We detect TDP-43 and FUS in both the nucleus and the cytoplasm of motor neurons from young adult (Day 1) transgenics. The preferential toxicity of mutant TDP-43 and FUS alleles along with their cytoplasmic accumulation suggests our models may recapitulate aspects of neurotoxicity relevant to the disease state.

With no clear mechanism for TDP-43 and FUS neuronal toxicity it is currently not possible to design *in vitro* assays for high-throughput drug screening. Thus the further development and characterization of *in vivo* models for neurodegeneration will guide studies in mammalian systems. We believe our models strike an optimal balance between strong, age-dependent phenotypes and the expression of mutant proteins in relatively few neurons and may be useful for modifier screening. In terms of sensitivity, genetic mechanisms and/or small molecules need only to work on 26 neurons to achieve suppression. In terms of speed, our transgenics offer the possibility of medium-throughput suppressor screening based on the accelerated paralysis phenotype of mTDP-43 and mFUS worms grown in liquid culture. mTDP-43 and mFUS cause neuronal dysfunction in advance of motor neuron degeneration. The path from protein misfolding to neuronal dysfunction and cell death takes many decades in humans and it may be more efficient to target therapies to early pathogenic stages. Thus using simple systems to screen for suppression of neuronal dysfunction may be useful to prevent subsequent neurodegeneration.

A number of models for TDP-43 and FUS toxicity in various systems have been described, but there is still no clear answer whether TDP-43 and FUS neuronal toxicity are due to a loss/gain of function of these proteins individually or together in some common genetic pathway [44–46]. Furthermore it is still unclear if all TDP-43 and FUS mutations share similar pathogenic mechanisms but having similarly constructed models for each may address this question. Now that we have validated the *unc-47* motor neuron approach for modelling toxicity, future work will focus on the development of new transgenics with additional TDP-43 and FUS mutations.

We present here novel transgenics for investigating age-dependent motor neuron toxicity caused by mutant TDP-43 and FUS. We expect these strains will be useful for identifying genetic and chemical suppressors to give insights into disease mechanisms and support the development of new therapies for age-dependent neurodegeneration.

Materials and Methods

Nematode strains

Standard methods of culturing and handling worms were used [47]. Worms were maintained on standard NGM plates streaked with OP50 *E. coli*. Strains used in this study were obtained from the *C. elegans* Genetics Center (University of Minnesota, Minneapolis) and include: N2, *oxIs12[unc-47p::GFP+lin-15]*, *unc-47(e307)*, *unc-47(gk192)* and *unc-119(ed3)*.

Transgenic TDP-43 and FUS worms

Human cDNAs for wild type and mutant TDP-43[A315T], and wild type and mutant FUS-TLS[S57Δ] were obtained from Dr. Guy Rouleau (CRCHUM, Université de Montréal). The cDNAs were amplified by PCR and cloned into the Gateway vector pDONR221 following the manufacturer's protocol (Invitrogen). Multisite Gateway recombination was performed with the pDONR TDP-43 and FUS clones along with clones containing the *unc-47* promoter (kind gift from Dr. Erik Jorgensen, University of Utah), the *unc-54* 3′UTR plasmid pCM5.37 (Dr. Geraldine Seydoux, Johns Hopkins, Addgene plasmid 17253) and the destination vector pCFJ150 to create *unc-47*::TDP-43 and *unc-47*::FUS expression vectors. Transgenic lines were created by microinjection of *unc-119(ed3)* worms, multiple lines were generated and strains behaving similarly were kept for further analysis. Transgenes were integrated by UV irradiation and lines were outcrossed to wild type N2 worms 5 times before use. The main strains used in this study include: *xqIs132[unc-47::TDP-43-WT;unc-119(+)]*, *xqIs133[unc-47::TDP-43[A315T];unc-119(+)]*, *xqIs173[unc-47::FUS-WT;unc-119(+)]*, and *xqIs98[unc-47::FUS[S57-Δ];unc-119(+)]*.

Paralysis assays on plates

For worms expressing TDP-43 or FUS, 20–30 adult day 1 animals were picked to NGM plates and scored daily for movement. Animals were counted as paralyzed if they failed to move upon prodding with a worm pick. Worms were scored as dead if they failed to move their head after being prodded in the nose and showed no pharyngeal pumping. All experiments were conducted at 20°C.

Lifespan assays

Worms were grown on NGM-FUDR plates to prevent progeny from hatching. 20 animals/plate by triplicates were tested at 20°C from adult day 1 until death. Worms were declared dead if they did not respond to tactile or heat stimulus. Survival curves were produced and compared using the Log-rank (Mantel-Cox) test.

Aldicarb test

To evaluate synaptic transmission, worms were grown on NGM and transferred to NGM plates +1 mM aldicarb at adult day 1. Paralysis was scored after 1 and 2 hours on aldicarb plates. Animals were counted as paralyzed if they failed to move upon prodding with a worm pick. All tests were performed at 20°C.

Liquid culture protocol

Synchronized populations of worms were obtained by hypochlorite extraction. Young adult worms were distributed in 96-wells plate (20 µl per well; 20–30 worms per well), containing DMSO or test compounds and incubated for up to 6 h at 20°C on a shaker. The motility test was assessed by stereomicroscopy. Videos of worms were taken with on an Olympus S7x7 stereomicroscope equipped with a Grasshopper GRAS-03K2M camera using Flycap software (Point Grey Research) at a rate of 300 frames per second.

Immunostaining of whole worms

Age synchronized, adult day 1, whole worms were fixed and stained as described in WormBook [48]. Antibodies used include:

rabbit anti-TDP-43 (1:50, Proteintech), rabbit anti-FUS/TLS (1:50, AbCam), and rabbit anti-GABA (1:50, Proteintech).

Fluorescence microscopy

For scoring gaps/breaks from TDP-43 and FUS transgenics, synchronized animals were selected at days 1, 5 and 9 of adulthood for visualization of motor neurons *in vivo*. Animals were immobilized in M9 with 5 *mM* levamisole and mounted on slides with 2% agarose pads. Motor neurons were visualized with a Leica 6000 microscope and a Leica DFC 480 camera. A minimum of 100 animals was scored per treatment over 4–6 trials. The mean and SEM were calculated for each trial and two-tailed t-tests were used for statistical analysis.

Worm lysates

Worms were collected in M9 buffer, washed 3 times with M9 and pellets were placed at −80°C overnight. Pellets were lysed in RIPA buffer (150 mM NaCl, 50 mM Tris pH 7.4, 1% Triton X-100, 0.1% SDS, 1% sodium deoxycholate)+0.1% protease inhibitors (10 mg/ml leupeptin, 10 mg/ml pepstatin A, 10 mg/ml chymostatin LPC; 1/1000). Pellets were passed through a $27_{1/2}$ G syringe 10 times, sonicated and centrifuged at 16000*g*. Supernatants were collected.

Protein quantification

All supernatants were quantified with the BCA Protein Assay Kit (Thermo Scientific) following the manufacturer instructions.

Protein solubility

For TDP-43 and FUS transgenics soluble/insoluble fractions, worms were lysed in Extraction Buffer (1 M Tris-HCl pH 8, 0.5 M EDTA, 1 M NaCl, 10% NP40+protease inhibitors (LPC; 1/1000)). Pellets were passed through a $27_{1/2}$ G syringe 10 times, sonicated and centrifuged at 100000*g* for 5 min. The soluble supernatant was saved and the remaining pellet was resuspended in extraction buffer, sonicated and centrifuged at 100000g for 5 min. The remaining pellet was resuspended into 100 µl of RIPA buffer, sonicated until the pellet was resuspended in solution and saved.

Immunoblots

Worm RIPA samples (175 µg/well) were resuspended directly in 1× Laemmli sample buffer, migrated in 12.5% or 10% polyacrylamide gels, transferred to nitrocellulose membranes (BioRad) and immunoblotted. Antibodies used: rabbit anti-human-TDP-43 (1:200, Proteintech), rabbit anti-human-FUS/TLS (1:200, AbCam), and mouse anti-actin (1:10000, MP Biomedical). Blots were visualized with peroxidase-conjugated secondary antibodies and ECL Western Blotting Substrate (Thermo Scientific). Densitometry was performed with Photoshop (Adobe).

Statistics

For paralysis and stress-resistance tests, survival curves were generated and compared using the Log-rank (Mantel-Cox) test, and 60–100 animals were tested per genotype and repeated at least three times. For image analysis statistical significance was determined by Student's t-test and the results shown as mean ± standard error. Prism 5 (GraphPad Software) was used for all statistical analyses.

Supporting Information

Table S1 Lifespan analysis for all experiments.
(PDF)

Video S1 mTDP-43 worms in liquid culture at time 0.
(MOV)

Video S2 mTDP-43 worms after 6 hours in liquid culture.
(MOV)

Video S3 mFUS worms in liquid culture at time 0.
(MOV)

Video S4 mFUS worms after 6 hours in liquid culture.
(MOV)

Video S5 wtTDP-43 worms in liquid culture at time 0.
(MOV)

Video S6 wtTDP-43 worms after 6 hours in liquid culture.
(MOV)

Video S7 wtFUS worms in liquid culture at time 0.
(MOV)

Video S8 wtFUS worms after 6 hours in liquid culture.
(MOV)

Video S9 N2 worms in liquid culture at time 0.
(MOV)

Video S10 N2 worms after 6 hours in liquid culture.
(MOV)

Video S11 *unc-47p::GFP* worms in liquid culture at time 0.
(MOV)

Video S12 *unc-47p::GFP* worms after 6 hours in liquid culture.
(MOV)

Acknowledgments

We thank S. Peyrard, E. Bourgeois and S. Al Ameri for technical support, H. Catoire for critical reading of the manuscript, and Dr. E. Jorgensen for the *unc-47* plasmid.

Author Contributions

Conceived and designed the experiments: JAP. Performed the experiments: AV AT DA. Analyzed the data: AV JAP. Contributed reagents/materials/analysis tools: GAR PD. Wrote the paper: AV JAP.

References

1. Boillee S, Vande Velde C, Cleveland DW (2006) ALS: a disease of motor neurons and their nonneuronal neighbors. Neuron 52: 39–59.
2. Lomen-Hoerth C (2008) Amyotrophic lateral sclerosis from bench to bedside. Semin Neurol 28: 205–211.
3. Neumann M, Sampathu DM, Kwong LK, Truax AC, Micsenyi MC, et al. (2006) Ubiquitinated TDP-43 in frontotemporal lobar degeneration and amyotrophic lateral sclerosis. Science 314: 130–133.
4. Gitcho MA, Baloh RH, Chakraverty S, Mayo K, Norton JB, et al. (2008) TDP-43 A315T mutation in familial motor neuron disease. Ann Neurol.
5. Kabashi E, Valdmanis PN, Dion P, Spiegelman D, McConkey BJ, et al. (2008) TARDBP mutations in individuals with sporadic and familial amyotrophic lateral sclerosis. Nat Genet.
6. Sreedharan J, Blair IP, Tripathi VB, Hu X, Vance C, et al. (2008) TDP-43 mutations in familial and sporadic amyotrophic lateral sclerosis. Science 319: 1668–1672.
7. Vance C, Rogelj B, Hortobagyi T, De Vos KJ, Nishimura AL, et al. (2009) Mutations in FUS, an RNA processing protein, cause familial amyotrophic lateral sclerosis type 6. Science 323: 1208–1211.

8. Deng HX, Chen W, Hong ST, Boycott KM, Gorrie GH, et al. (2011) Mutations in UBQLN2 cause dominant X-linked juvenile and adult-onset ALS and ALS/dementia. Nature.
9. Mackenzie IR, Rademakers R, Neumann M (2010) TDP-43 and FUS in amyotrophic lateral sclerosis and frontotemporal dementia. Lancet Neurol 9: 995–1007.
10. Lagier-Tourenne C, Polymenidou M, Cleveland DW (2010) TDP-43 and FUS/TLS: emerging roles in RNA processing and neurodegeneration. Hum Mol Genet 19: R46–64.
11. Kim SH, Shanware NP, Bowler MJ, Tibbetts RS (2010) Amyotrophic lateral sclerosis-associated proteins TDP-43 and FUS/TLS function in a common biochemical complex to co-regulate HDAC6 mRNA. J Biol Chem 285: 34097–34105.
12. Ling SC, Albuquerque CP, Han JS, Lagier-Tourenne C, Tokunaga S, et al. (2010) ALS-associated mutations in TDP-43 increase its stability and promote TDP-43 complexes with FUS/TLS. Proc Natl Acad Sci U S A 107: 13318–13323.
13. McIntire SL, Reimer RJ, Schuske K, Edwards RH, Jorgensen EM (1997) Identification and characterization of the vesicular GABA transporter. Nature 389: 870–876.
14. Evans TC (2006) Transformation and microinjection. WormBook. pp 1–15.
15. Belzil VV, Valdmanis PN, Dion PA, Daoud H, Kabashi E, et al. (2009) Mutations in FUS cause FALS and SALS in French and French Canadian populations. Neurology 73: 1176–1179.
16. Cohen E, Bieschke J, Perciavalle RM, Kelly JW, Dillin A (2006) Opposing activities protect against age-onset proteotoxicity. Science 313: 1604–1610.
17. Steinkraus KA, Smith ED, Davis C, Carr D, Pendergrass WR, et al. (2008) Dietary restriction suppresses proteotoxicity and enhances longevity by an hsf-1-dependent mechanism in Caenorhabditis elegans. Aging Cell 7: 394–404.
18. Collins JJ, Huang C, Hughes S, Kornfeld K (2008) The measurement and analysis of age-related changes in Caenorhabditis elegans. WormBook. pp 1–21.
19. Earls LR, Hacker ML, Watson JD, Miller DM, 3rd (2010) Coenzyme Q protects Caenorhabditis elegans GABA neurons from calcium-dependent degeneration. Proc Natl Acad Sci U S A 107: 14460–14465.
20. Herndon LA, Schmeissner PJ, Dudaronek JM, Brown PA, Listner KM, et al. (2002) Stochastic and genetic factors influence tissue-specific decline in ageing C. elegans. Nature 419: 808–814.
21. Jorgensen EM (2005) Gaba. WormBook. pp 1–13.
22. McIntire SL, Jorgensen E, Kaplan J, Horvitz HR (1993) The GABAergic nervous system of Caenorhabditis elegans. Nature 364: 337–341.
23. Mahoney TR, Luo S, Nonet ML (2006) Analysis of synaptic transmission in Caenorhabditis elegans using an aldicarb-sensitivity assay. Nat Protoc 1: 1772–1777.
24. Loria PM, Hodgkin J, Hobert O (2004) A conserved postsynaptic transmembrane protein affecting neuromuscular signaling in Caenorhabditis elegans. J Neurosci 24: 2191–2201.
25. Vashlishan AB, Madison JM, Dybbs M, Bai J, Sieburth D, et al. (2008) An RNAi screen identifies genes that regulate GABA synapses. Neuron 58: 346–361.
26. Saxena S, Caroni P (2011) Selective neuronal vulnerability in neurodegenerative diseases: from stressor thresholds to degeneration. Neuron 71: 35–48.
27. Liachko NF, Guthrie CR, Kraemer BC (2010) Phosphorylation Promotes Neurotoxicity in a Caenorhabditis elegans Model of TDP-43 Proteinopathy. J Neurosci 30: 16208–16219.
28. Johnson BS, McCaffery JM, Lindquist S, Gitler AD (2008) A yeast TDP-43 proteinopathy model: Exploring the molecular determinants of TDP-43 aggregation and cellular toxicity. Proc Natl Acad Sci U S A.
29. Ash PE, Zhang YJ, Roberts CM, Saldi T, Hutter H, et al. (2010) Neurotoxic effects of TDP-43 overexpression in C. elegans. Hum Mol Genet.
30. Zhang T, Mullane PC, Periz G, Wang J (2011) TDP-43 neurotoxicity and protein aggregation modulated by heat shock factor and insulin/IGF-1 signaling. Hum Mol Genet.
31. Swarup V, Phaneuf D, Bareil C, Robertson J, Rouleau GA, et al. (2011) Pathological hallmarks of amyotrophic lateral sclerosis/frontotemporal lobar degeneration in transgenic mice produced with TDP-43 genomic fragments. Brain.
32. Li Y, Ray P, Rao EJ, Shi C, Guo W, et al. (2010) A Drosophila model for TDP-43 proteinopathy. Proc Natl Acad Sci U S A 107: 3169–3174.
33. Murakami T, Yang SP, Xie L, Kawano T, Fu D, et al. (2011) ALS mutations in FUS causes neuronal dysfunction and death in C. elegans by a dominant gain-of-function mechanism. Hum Mol Genet.
34. McDonald PW, Hardie SL, Jessen TN, Carvelli L, Matthies DS, et al. (2007) Vigorous motor activity in Caenorhabditis elegans requires efficient clearance of dopamine mediated by synaptic localization of the dopamine transporter DAT-1. J Neurosci 27: 14216–14227.
35. Catoire H, Pasco MY, Abu-Baker A, Holbert S, Tourette C, et al. (2008) Sirtuin Inhibition Protects from the Polyalanine Muscular Dystrophy Protein PABPN1. Hum Mol Genet.
36. Wang J, Farr GW, Hall DH, Li F, Furtak K, et al. (2009) An ALS-linked mutant SOD1 produces a locomotor defect associated with aggregation and synaptic dysfunction when expressed in neurons of Caenorhabditis elegans. PLoS Genet 5: e1000350.
37. Caramia MD, Palmieri MG, Desiato MT, Iani C, Scalise A, et al. (2000) Pharmacologic reversal of cortical hyperexcitability in patients with ALS. Neurology 54: 58–64.
38. Vucic S, Nicholson GA, Kiernan MC (2008) Cortical hyperexcitability may precede the onset of familial amyotrophic lateral sclerosis. Brain 131: 1540–1550.
39. Kiernan MC, Vucic S, Cheah BC, Turner MR, Eisen A, et al. (2011) Amyotrophic lateral sclerosis. Lancet 377: 942–955.
40. Pasinelli P, Brown RH (2006) Molecular biology of amyotrophic lateral sclerosis: insights from genetics. Nat Rev Neurosci 7: 710–723.
41. Dion PA, Daoud H, Rouleau GA (2009) Genetics of motor neuron disorders: new insights into pathogenic mechanisms. Nat Rev Genet 10: 769–782.
42. Ju S, Tardiff DF, Han H, Divya K, Zhong Q, et al. (2011) A yeast model of FUS/TLS-dependent cytotoxicity. PLoS Biol 9: e1001052.
43. Lanson NA, Jr., Maltare A, King H, Smith R, Kim JH, et al. (2011) A Drosophila model of FUS-related neurodegeneration reveals genetic interaction between FUS and TDP-43. Hum Mol Genet 20: 2510–2523.
44. Kabashi E, Bercier V, Lissouba A, Liao M, Brustein E, et al. (2011) FUS and TARDBP but not SOD1 interact in genetic models of Amyotrophic Lateral Sclerosis. PLoS Genet;in press.
45. Kabashi E, Lin L, Tradewell ML, Dion PA, Bercier V, et al. (2009) Gain and loss of function of ALS-related mutations of TARDBP (TDP-43) cause motor deficits in vivo. Hum Mol Genet 19: 671–683.
46. Wang JW, Brent JR, Tomlinson A, Shneider NA, McCabe BD (2011) The ALS-associated proteins FUS and TDP-43 function together to affect Drosophila locomotion and life span. J Clin Invest.
47. Stiernagle T (2006) Maintenance of C. elegans. WormBook. pp 1–11.
48. Duerr JS (2006) Immunohistochemistry. WormBook. pp 1–61.

OPEN ACCESS Freely available online

PLoS one

Methylene Blue Protects against TDP-43 and FUS Neuronal Toxicity in *C. elegans* and *D. rerio*

Alexandra Vaccaro[1,2,3], Shunmoogum A. Patten[2,3], Sorana Ciura[2,3], Claudia Maios[2], Martine Therrien[1,2,3], Pierre Drapeau[2,3], Edor Kabashi[2*¤], J. Alex Parker[1,2,3*]

1 Université de Montréal Hospital Research Centre, Montréal, Québec, Canada, **2** Département de pathologie et biologie cellulaire and Groupe de recherche sur le système nerveux central, Université de Montréal, Montréal, Canada, **3** Centre of Excellence in Neuromics, Université de Montréal, Montréal, Canada

Abstract

The DNA/RNA-binding proteins TDP-43 and FUS are found in protein aggregates in a growing number of neurodegenerative diseases, including amyotrophic lateral sclerosis (ALS) and related dementia, but little is known about the neurotoxic mechanisms. We have generated *Caenorhabditis elegans* and zebrafish animal models expressing mutant human TDP-43 (A315T or G348C) or FUS (S57Δ or R521H) that reflect certain aspects of ALS including motor neuron degeneration, axonal deficits, and progressive paralysis. To explore the potential of our humanized transgenic *C. elegans* and zebrafish in identifying chemical suppressors of mutant TDP-43 and FUS neuronal toxicity, we tested three compounds with potential neuroprotective properties: lithium chloride, methylene blue and riluzole. We identified methylene blue as a potent suppressor of TDP-43 and FUS toxicity in both our models. Our results indicate that methylene blue can rescue toxic phenotypes associated with mutant TDP-43 and FUS including neuronal dysfunction and oxidative stress.

Citation: Vaccaro A, Patten SA, Ciura S, Maios C, Therrien M, et al. (2012) Methylene Blue Protects against TDP-43 and FUS Neuronal Toxicity in *C. elegans* and *D. rerio*. PLoS ONE 7(7): e42117. doi:10.1371/journal.pone.0042117

Editor: Weidong Le, Baylor College of Medicine, Jiao Tong University School of Medicine, United States of America

Received March 9, 2012; **Accepted** July 2, 2012; **Published** July 27, 2012

Funding: This research was supported by: Montreal University Hospital Foundation (http://fondationduchum.com/fr) to JAP, Canadian Institutes of Health Research New Investigator Award (http://www.cihr-irsc.gc.ca) to JAP, Frick Foundation for ALS Research (http://frick-fondation.ch) to JAP, EK, PD, and a Bernice Ramsay Discovery Grant from the ALS Society of Canada (http://www.als.ca/) to JAP. Genome Québec to EK and PD. The funders had no role in study design, data collection and analysis, decision to publish, or preparation of the manuscript.

Competing Interests: The authors have declared that no competing interests exist.

* E-mail: edor.kabashi@icm-institute.org (EK); or ja.parker@umontreal.ca (JAP)

¤ Current address: Institut du Cerveau et de la Moelle épinière, Centre de Recherche, CHU Pitié-Salpétrière, Paris, France.

Introduction

ALS is a late-onset progressive neurodegenerative disease affecting motor neurons and ultimately resulting in fatal paralysis [1,2]. The majority of cases are sporadic but ~10% of patients have an inherited familial form of the disease. Dominant mutations in SOD1 (copper/zinc superoxide dismutase 1) account for ~20% of familial ALS cases and ~1% of sporadic cases [1]. A recent biochemical approach identified cytosolic aggregates of TDP-43 in ALS and frontotemporal lobar dementia pathological tissue [3]. This breakthrough discovery was quickly followed by the identification of TDP-43 mutations in ALS patients by numerous groups [3–6]. TDP-43 is a multifunctional RNA/DNA binding protein and mutations in the related protein FUS have also been found in ALS patients [7] though the molecular pathology induced by mutant TDP-43 and FUS is not understood. The mislocalization and subsequent aggregation of TDP-43 has been observed in pathological tissue obtained from a number of neurological disorders including frontotemporal lobar dementia, Parkinson's disease, polyglutamine diseases and several myopathies [8]. Similarly, FUS inclusions have been observed in clinically distinct forms of frontotemporal lobar dementia and the polyglutamine diseases [8] suggesting that TDP-43 and FUS may be a common pathogenic factor in neurodegeneration. Furthermore, TDP-43 and FUS interact genetically (though not with SOD1) in zebrafish [9] and *Drosophila* [10] indicating that they may act in a common pathway. In the absence of knowledge concerning the biochemical defects caused by these ALS-related mutations in TDP-43 and FUS, the use of *in vivo* models is currently the most promising approach available to further our understanding of pathogenic mechanisms as well as for therapeutic discovery for ALS.

Indeed a number of chemical and drug screens have been published using *in vivo* models such as *C. elegans* and zebrafish [11–14]. These model organisms offer several advantages over mouse models for cheaper, faster and large-scale initial drug screening and target characterization. For instance, it is possible to rapidly produce large numbers of mutant offspring that can be assayed in liquid culture in multiwell plates and treated with various compounds to determine if disease phenotypes are rescued. Moreover, these organisms have relatively short reproductive cycles, they are easy to manipulate genetically, and their transparency permits visual assessment of developing cells and organs. Also, biochemical pathways are highly conserved between *C. elegans*, zebrafish and humans. We developed novel *in vivo* genetic models of mutant human TDP-43 and FUS in *C. elegans* [15] and zebrafish [9,16,17]. Our models exhibit several aspects of ALS including motor neuron degeneration, axonal deficits and progressive paralysis. The goal of this study was to test the ability of our *in vivo* models to identify neuroprotective compounds and determine their suitability as a platform for pre-clinical drug discovery in ALS. We focused on three compounds with known

neuroprotective properties in an attempt to identify small molecules that might rescue disease phenotypes observed in our models. Here, we show that methylene blue (MB) restores normal motor phenotypes in *C. elegans* and zebrafish ALS models.

Results

Methylene blue rescues mutant TDP-43 and FUS behavioral phenotypes in *C. elegans*

Using *C. elegans* transgenics that express mutant TDP-43 or FUS (TDP-43[A315T] or FUS[S57Δ], referred to herein as mTDP-43 and mFUS respectively) in motor neurons [15] we evaluated the efficacy of these models as drug discovery tools by testing three compounds with known clinically neuroprotective properties: lithium chloride, MB and riluzole [18,19]. The mTDP-43 and mFUS transgenic worms show adult-onset, progressive motility defects leading to paralysis when grown under standard laboratory conditions on solid agar plates over the course of 10 to 12 days [15]. However, worms grown in liquid culture exhibit a swimming behavior that is more vigorous than crawling on plates and accelerates neuronal dysfunction in the TDP-43 and FUS transgenics [15]. As a result, paralysis phenotypes manifest in a matter of hours instead of days. We took advantage of this phenomenon to develop a chemical screening assay to identify compounds that suppress the acute paralysis of mTDP-43 and mFUS transgenic worms grown in liquid culture. With this assay we tested if lithium chloride, MB or riluzole could suppress the paralysis caused by mTDP-43 and mFUS (**Figure 1**). Of the three compounds tested, we observed that MB reduced the rate of paralysis for mTDP-43 and mFUS transgenics with no effect on wild type TDP-43 (wtTDP-43) or wild type FUS (wtFUS) control strains (**Figures 1B, 1E**). Furthermore MB had no significant effect on movement phenotypes for wild type, non-transgenic N2 worms (**Figure S1A**).

To ensure that suppression of paralysis was not an artifact of the liquid culture assay and to confirm that MB retained its rescuing activity in the context of aging we retested it at two doses (6 and 60 μM) for mTDP-43 and mFUS worms grown on plates and observed a reduction in the rates of paralysis for treated animals compared to untreated controls (**Figures 2A, B**). The paralysis phenotype likely results from impaired synaptic transmission at the neuromuscular junction as shown by the hypersensitivity of the mTDP-43 worms to the acetylcholine esterase inhibitor aldicarb. mTDP-43 animals treated with MB showed reduced sensitivity to aldicarb, matching the response from control strains, suggesting that MB restores synaptic function in animals expressing mutant proteins (**Figure 2C**). Transgenic *C. elegans* expressing ALS-related mutations mTDP-43 or mFUS in motor neurons also show age-dependent degeneration most frequently observed as gaps or breaks along neuronal processes [15]. These neurodegenerative phenotypes were significantly reduced by treatment with MB (**Figures 2D, E, F**) and did not change mTDP-43 or mFUS transgene expression (**Figures 2G, H**).

Methylene blue rescues motor phenotypes in mutant TDP-43 and FUS zebrafish

To test if MB had protective effects beyond *C. elegans* we turned to zebrafish. First, as in worms, we observed that MB had no effect on the movement phenotypes of wild type non-transgenic fish (**Figure S1B, C, D, E**). Zebrafish expressing mTDP-43[G348C] or mFUS[R521H] have impaired swimming as assessed by their ability to produce a touch-evoked escape response (TEER) [9,16]. mTDP-43 fish showed a greatly reduced TEER compared to non-transgenic or wtTDP-43 fish (**Figure 3A**). mTDP-43 fish treated with 60 μM MB showed improved swimming response including swim duration, distance swam and maximum swim velocity (**Figures 3A, B, C, D**). Zebrafish expressing mFUS also show greatly reduced swimming activity compared to wild type or wtFUS fish and the swimming phenotype of mFUS fish was greatly improved when treated with 60 μM MB (**Figures 3E, F, G, H**). Besides behavioral defects, immunohistochemical analyses show that transgenic zebrafish expressing mTDP-43 or mFUS also displayed abnormally shortened and branched motor neuron axonal processes as observed by the unbranched axonal length (UAL) quantification [9,16] and this phenotype was rescued by incubation with either 30 or 60 μM MB (**Figures 4A, B**). These results demonstrate that MB can significantly reduce the motor neuron phenotypes elicited by expression of mTDP-43 and mFUS both in *C. elegans* and zebrafish genetic models of disease.

Methylene blue protects against oxidative stress in *C. elegans* and zebrafish

Since we observed that MB rescued paralysis in transgenic models of mTDP-43 or mFUS, we sought to further examine the protective effects of MB in an aging and stress context. First, MB treatment had no effect on the lifespan of wild type N2 worms suggesting that its cellular protection mechanisms are not due to non-specific effects from extended longevity (**Figure 5A, Table S1**). To test for protective effects against environmental stress we tested wild type N2 worms for their ability to withstand lethal exposure to thermal, hyperosmotic or oxidative stresses. We observed that MB offered no protection to worms subjected to elevated temperature or hyperosmotic stress from treatment with NaCl as their survival rate was indistinguishable from untreated control animals (**Figures 5B, C**). Juglone is a natural aromatic compound found in the black walnut tree that induces high levels of oxidative stress within cells [20]. Juglone is highly toxic to wild type N2 worms and causes complete mortality after approximately 4 hours in our assay. We observed that MB provided significant protection against oxidative stress since wild type N2 worms were resistant to juglone in a dose dependent manner (**Figure 5D**). These data suggest that MB is specific in its cell protection capabilities and helps overcome oxidative stress conditions in *C. elegans*.

Since we showed that MB confers protection to wild type N2 worms under oxidative stress in a dose dependent manner we hypothesized that MB may help reduce oxidative damage in mTDP-43 worms. To test this hypothesis we stained our TDP-43 transgenic strain with dihydrofluorescein diacetate (DHF), a compound known to fluoresce when exposed to intracellular peroxides associated with oxidative stress [21]. We observed no DHF signal from wtTDP-43 transgenics but strong fluorescence from mTDP-43 worms (**Figure 6A**). The fluorescence observed in the mTDP-43 transgenics was reduced when treated with 60 μM MB (**Figure 6A**). We observed a similar effect with our FUS transgenics, with no DHF signal from wtFUS animals, but strong fluorescence from mFUS worms that was reduced upon MB treatment (**Figure 6B**). Extending our findings we examined oxidative stress with DHF in mTDP-43 and mFUS fish. Similar to worms, we observed a strong fluorescent signal in mTDP-43 fish compared to non-transgenic or wtTDP-43 fish and that this signal was reduced by treatment with MB (**Figures 6C, D**). MB also reduced the fluorescent signal in mFUS fish stained with DHF (**Figure 6E**). These data suggest that MB reduces the general level of oxidative status generated by the expression of mutant proteins *in vivo*.

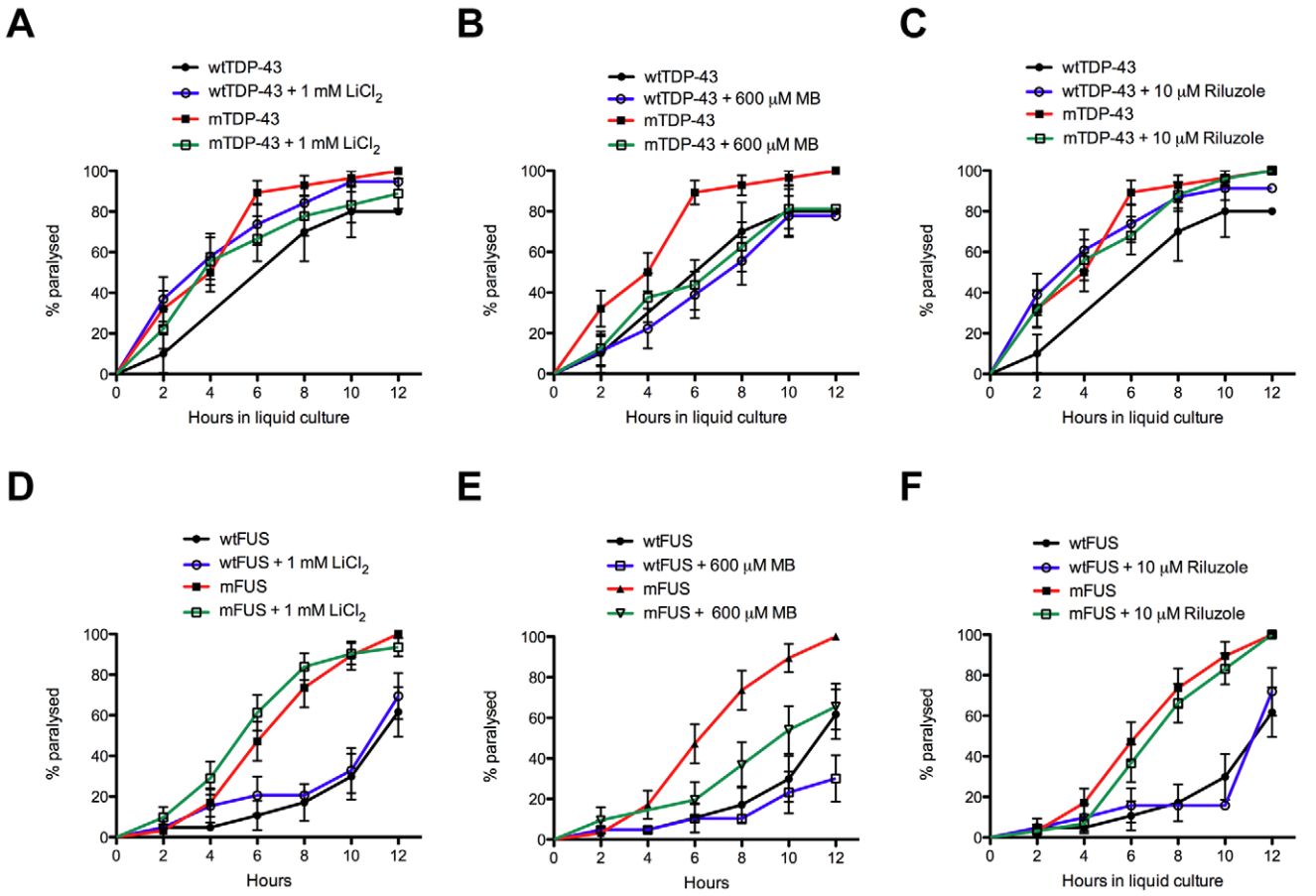

Figure 1. Methylene blue suppresses mTDP-43 and mFUS associated paralysis in *C. elegans*. We screened for suppression of TDP-43 (A–C) and FUS (B–D) induced paralysis in liquid culture by lithium chloride ($LiCl_2$), methylene blue (MB) or riluzole. MB significantly reduced the rate of paralysis in (B) mTDP-43 and (D) mFUS transgenics compared to untreated mutant transgenic worms ($P<0.05$) with no effect on wild type transgenic controls.
doi:10.1371/journal.pone.0042117.g001

Reduced neuroprotection from late administration of methylene blue

In the previous experiments worms and fish were treated with MB from hatching. We tested whether the timing of treatment had an effect on the magnitude of neuroprotection by growing mTDP-43 worms on normal plates and transferring them at day 5 of adulthood to plates supplemented with MB. We observed that late administration of MB reduced paralysis with approximately 55% of treated animals becoming paralysed at day 12 of adulthood compared to a paralysis rate of approximately 80% for untreated animals (**Figure 7**). However the extent of rescue by late MB administration was far less than the approximate 10% paralysis rate observed for mTDP-43 animals grown on MB plates from hatching (**Figure 2A**). These data suggest that early administration of MB is more effective at reducing mTDP-43 toxicity than intervention in older animals.

Discussion

In this study we demonstrated that our *C. elegans* and zebrafish ALS models can be used to identify neuroprotective molecules which represents the first *in vivo* chemical genetic screening platform for ALS. With this platform we discovered that MB is a potent suppressor of mTDP-43 and mFUS motor neuron toxicity *in vivo*. In both worms and fish MB corrected motor deficits and reduced the level of oxidative stress associated with the expression of mutant proteins.

MB is a pleiotropic molecule with a long and varied history of medical use [18] but in the context of neurodegeneration MB has been reported to prevent amyloid-β and tau aggregation *in vitro* [22,23]. A previous study also showed that the treatment of cells with MB inhibited the formation of TDP-43 aggregates [24] suggesting this compound might be appropriate for the treatment of ALS and other dementias. The efficacy of MB as a neuroprotective compound has been examined in Alzheimer's disease and ALS models where in some studies it is protective while in others it has no effect [24–28]. We decided to include this compound in our assay from which we identified MB as a potent suppressor of mTDP-43 and mFUS toxicity in both *C. elegans* and zebrafish. However, our data do not agree with a recent study examining the effects of MB in a TDP-43 mouse model [26]. Mutant TDP-43[G348C] mice treated with MB showed no improvement in motor phenotypes as determined by the rotarod assay. Furthermore no difference in the cytoplasmic localization of TDP-43 was observed in treated mice.

Worms and fish live in aqueous media and a simple explanation for their greater susceptibility may be that they are more permeable to MB. We further hypothesize that the differences in MB efficacy might also be due to variations in timing for delivery of the compound. Specifically, our worms and fish were treated

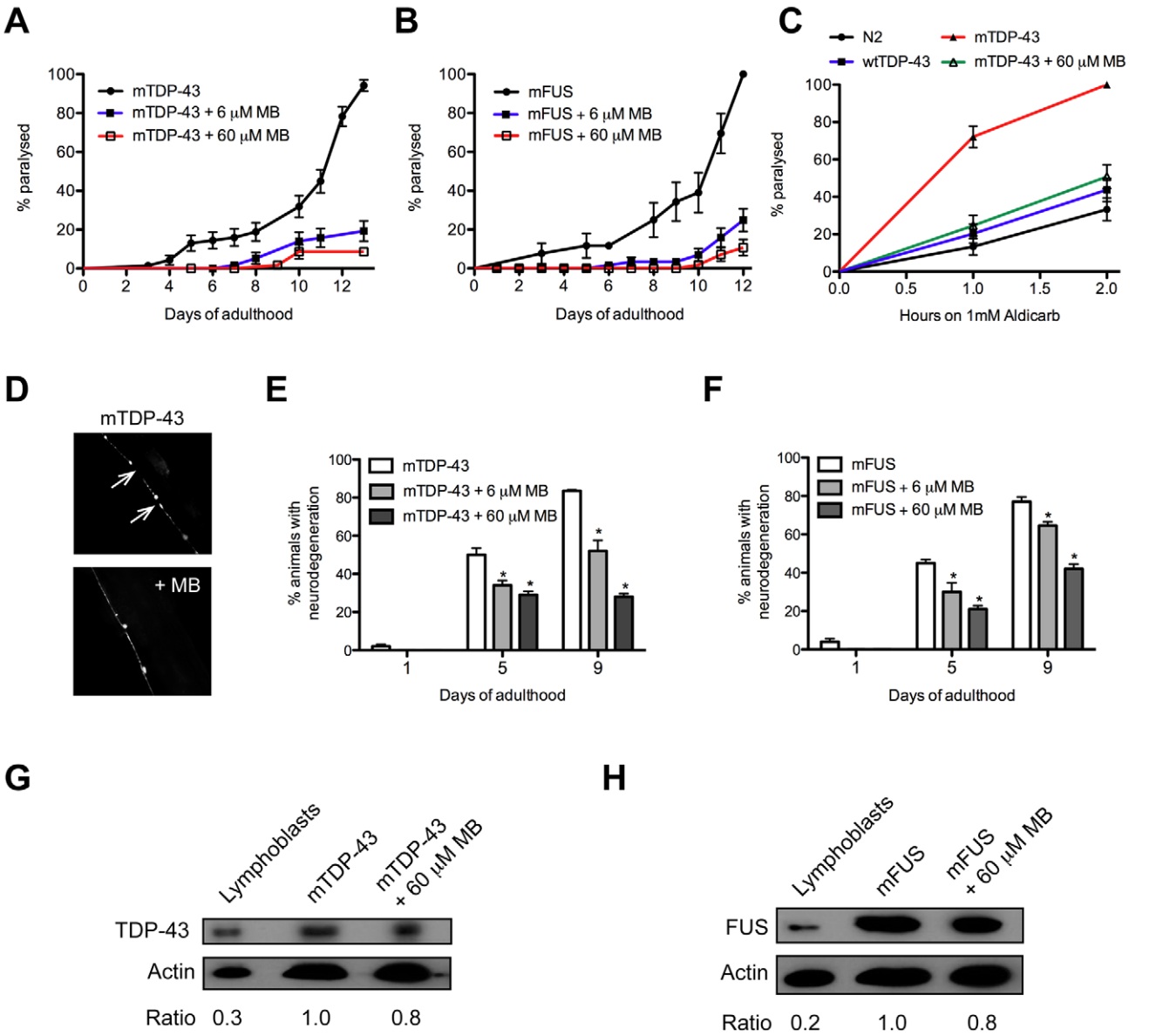

Figure 2. Methylene blue reduces TDP-43 and FUS neuronal toxicity. mTDP-43 and mFUS transgenics were grown on plates and assayed for various phenotypes. (**A**) MB reduced mTDP-43 induced paralysis in worms at two doses compared to untreated controls ($P<0.001$). (**B**) MB at two doses reduced mFUS induced paralysis in worms compared to untreated controls ($P<0.001$). (**C**) Aldicarb induced paralysis for mTDP-43 worms is significantly higher for mTDP-43 worms compared to non-transgenic N2 worms or transgenic wtTDP-43 controls ($P<0.001$). MB reduced aldicarb induced paralysis of mTDP-43 worms back to non-transgenic N2 and wtTDP-43 levels. (**D**) Representative photos of motor neuron degeneration phenotypes observed in mTDP-43 transgenic worms. Similar phenotypes were observed for mFUS transgenics. Degeneration is most frequently seen as gaps (white arrows) along neuronal processes. MB reduced the age-dependent degeneration of motor neurons in (**E**) mTDP-43 and (**F**) mFUS transgenic worms (*$P<0.001$ compared to untreated transgenics). MB did not affect the expression of mutant proteins in (**G**) mTDP-43 or (**H**) mFUS strains as determined by western blotting of protein extracts from transgenic worms grown with or without MB. Immunoblotting of human lymphoblasts was used as a size control.
doi:10.1371/journal.pone.0042117.g002

with MB from hatching whereas the TDP-43 mice were treated at 6 months. To confirm this hypothesis we treated mTDP-43 worms with MB at day 5 of adulthood and observed that late administration of the compound was significantly less effective at reducing paralysis. Thus, perhaps earlier (pre-clinical) treatment with MB may have greater effects in mouse models for ALS. Additionally there may be differences between the models since our worm and fish models capture a clinical aspect of ALS, namely progressive paralysis in animals expressing mTDP-43 that is absent from the TDP-43 mouse model.

Aging is a risk factor common to a number of neurodegenerative disorders including ALS, and oxidative stress is suspected to play a key role in the development of the disease by contributing to aging [29,30]. Indeed, interactions between genetic, environmental, and age-dependent risk factors have been hypothesized to trigger disease onset [31]. Consequently, we investigated the impact of MB treatment focusing on aging and stress response. Our *C. elegans* data are in agreement with the survival data from the mouse studies where we observed no effect on lifespan in MB treated worms even though there was a positive effect on multiple

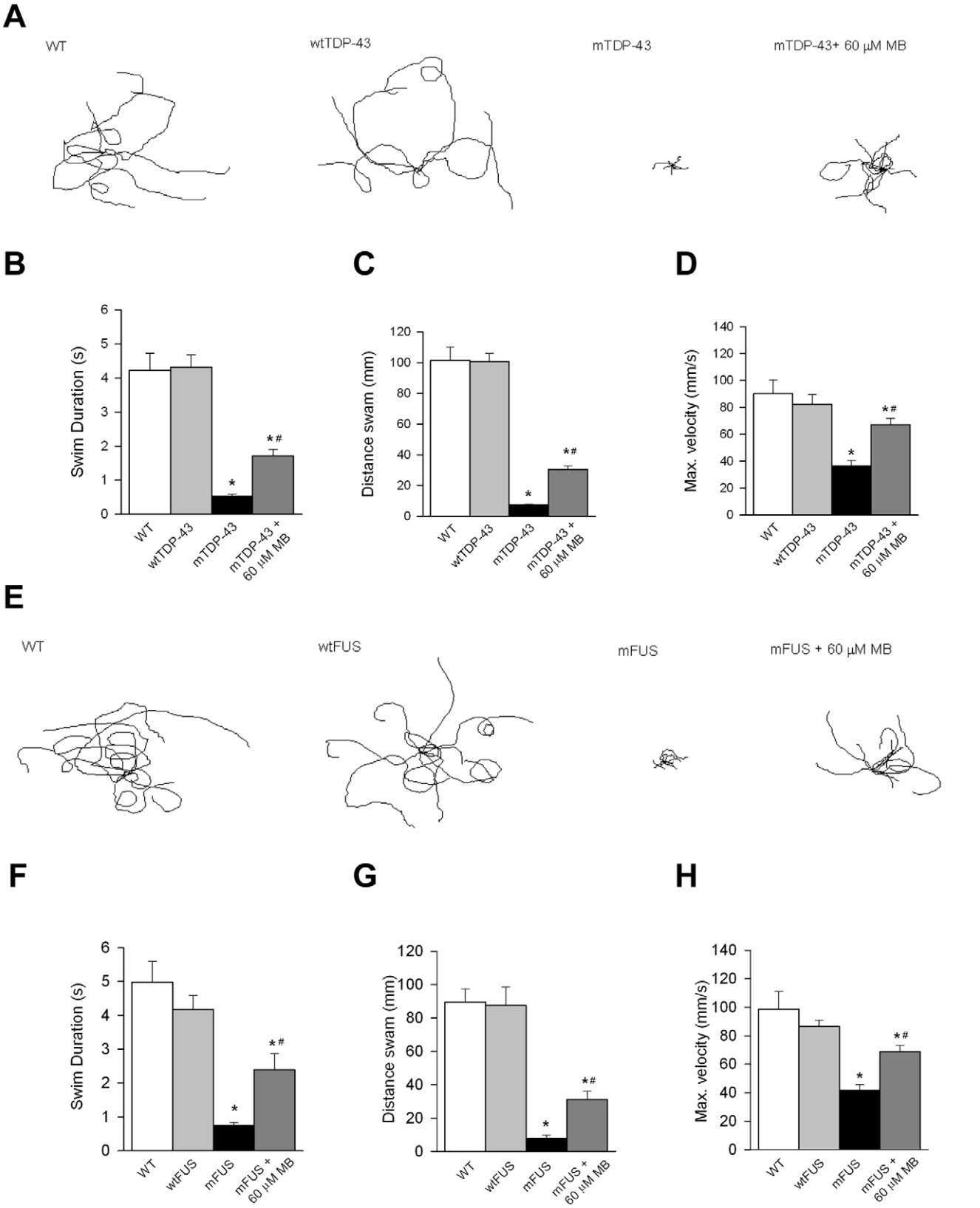

Figure 3. Methylene blue reduces motor deficits in zebrafish expressing mutant TDP-43 or FUS. (**A**) Representative traces of TEER phenotypes in wild type (WT), wtTDP-43, mTDP-43 and mTDP-43+MB. MB improved the swim duration (**B**), distance swam (**C**) and maximum swimming velocity (**D**) of mTDP-43 fish. (**E**) Representative traces of TEER phenotypes in WT, wtFUS, mFUS and mFUS+MB. Application of MB led to a significant improvement in the swim duration (**F**), distance swam (**G**) and maximum swimming velocity (H) of mTDP-43 fish. * denotes significant difference from WT, $P<0.001$; # significantly different from mutant fish $P<0.05$.
doi:10.1371/journal.pone.0042117.g003

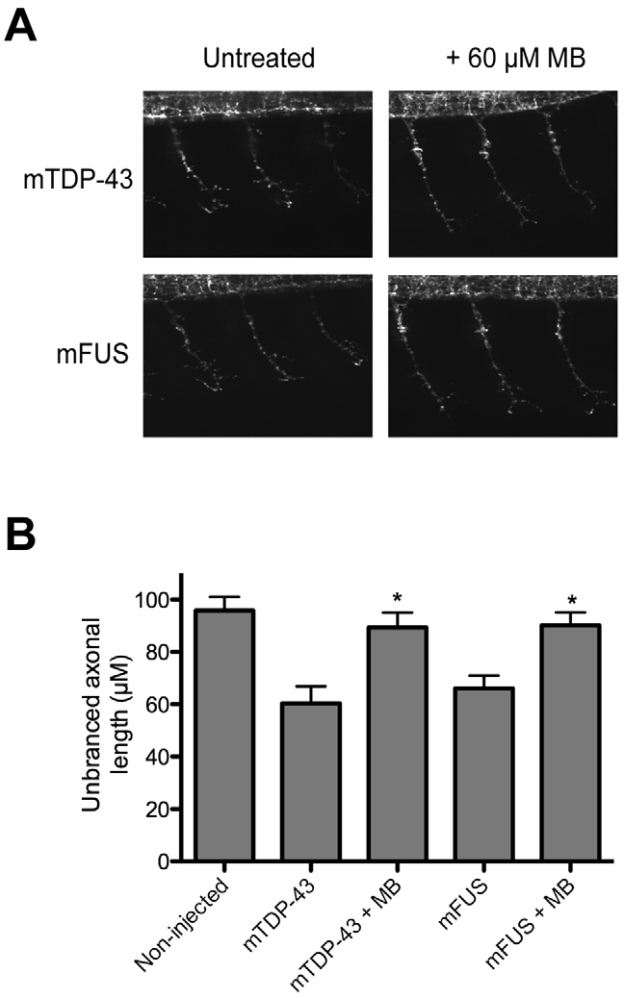

Figure 4. Methylene blue reduces axon defects in zebrafish expressing mutant TDP-43 or FUS. (**A**) Appearance of motor neurons in mTDP-43 and mFUS transgenic zebrafish with and without MB treatment. (**B**) MB reduced the unbranched axon length phenotype of motor neurons in mTDP-43 and mFUS transgenic zebrafish (*P<0.01 compared to untreated transgenics).
doi:10.1371/journal.pone.0042117.g004

phenotypes associated with mTDP-43 or mFUS. Thus, at least in simple systems lifespan effects can be uncoupled from neuroprotection but it remains to be seen if the same is true for mouse models of neurodegeneration.

In our previous work we showed that our TDP-43 and FUS transgenic *C. elegans* models exhibited no difference in lifespan compared to non-transgenic worms [15]. Thus, the paralysis phenotypes observed in our models specifically reflect the consequences of the expression of TDP-43 and FUS in motor neurons and are not due to secondary effects from general sickness and reduced lifespan. Therefore, it may be difficult to detect significant improvement on motor function or reflex phenotypes after MB treatment in mice showing generalized defects instead of treating problems resulting from TDP-43 or FUS proteotoxicity alone.

Finally, the TDP-43 mouse study did not examine the effects of MB on synaptic function or oxidative stress where we see clear effects in the worm and zebrafish models. MB can interact with nitric oxide synthase and also has an antioxidant potential by decreasing the generation of reactive oxygen species [32]. Using *C. elegans* we showed that MB specifically decreased the sensitivity of wild type worms to oxidative stress. We also investigated the impact of MB treatment in the formation of reactive oxygen species in both *C. elegans* and *D. rerio* and have observed a significant reduction in the generation of reactive oxygen species. Consistent with the literature [33], our data suggest that MB counteracts oxidative stress to provide protection against proteotoxicity in both our *in vivo* models. Synaptic function was also restored after treatment with MB in transgenic mTDP-43 worms suggesting that this compound might also have an effect on synaptic transmission.

In summary, we present novel *in vivo* chemical genetic screening assays that may be useful for ALS drug discovery. Using two genetic models for ALS we report here that MB acts through reduction of oxidative stress and also restoration of normal synaptic function in genetic models of ALS. In addition, an important issue here is that in simple systems like *C. elegans*, lifespan effects can be uncoupled from neuroprotection. The next step will be to unravel MB's exact target and mechanism of action to develop compounds with more specific activities and also to capitalize on the strength of our assays to screen additional compounds as potential therapeutics in ALS.

Materials and Methods

C. elegans experiments

***C. elegans* strains.** Strains used in this study include: N2, *gas-1(fc21), let-60(ga89), oxIs12[unc-47p::GFP;lin-15(+)], xqIs98[unc-47::FUS[S57Δ];unc-119(+)], xqIs132[unc-47::TDP-43-WT;unc-119(+)], xqIs133[unc-47::TDP-43[A315T];unc-119(+)]* and *xqIs173[unc-47::FUS-WT;unc-119(+)]*.

***C. elegans* liquid culture assay.** Young adult TDP-43 or FUS transgenic worms were distributed in 96-wells plate (20 μl per well; 20–30 worms per well), containing DMSO or test compounds and incubated for up to 12 hours at 20°C on a shaker. Compounds and final concentrations tested were 1 mM lithium chloride, 600 μM methylene blue, and 10 μM riluzole. The motility test was assessed by microscopy every 2 hours. Compounds were purchased from Sigma-Aldrich (St-Louis, MO).

***C. elegans* drug testing on plates.** Worms were grown on standard NGM plates with or without compounds. For worms expressing mFUS or mTDP-43, animals were counted as paralyzed if they failed to move upon prodding with a worm pick. Worms were scored as dead if they were immotile, showed no pharyngeal pumping and failed to move their head after being prodded in the nose. The final concentrations of methylene blue tested in plates either 6 or 60 μM.

Fluorescence microscopy. For scoring axons from transgenic mFUS and mTDP-43 worms, synchronized animals were selected at days 1, 5 and 9 of adulthood for visualization of motor neurons *in vivo* with the *unc-47p*::GFP transgenic reporter. Animals were immobilized in M9 with 5 mM levamisole and mounted on slides with 2% agarose pads. Motor neurons were visualized with a Leica CTR 6000 and a Leica DFC 480 camera. A minimum of 100 animals was scored per treatment over 4–6 trials. Animals showing gaps or breaks along motor neuron processes were scored as positive for the degeneration phenotype. The mean and SEM were calculated for each trial and two-tailed *t*-tests were used for statistical analysis. For visualization of fluorescence after treatment with dihydrofluorescein diacetate, L4 animals were grown on NGM plates or NGM plates with methylene blue and examined for fluorescence with the Leica system described above.

Lifespan assays. Worms were grown on NGM or NGM+60 μM methylene blue and transferred on NGM-FUDR or NGM-FUDR+60 μM methylene blue. 20 animals/plate by

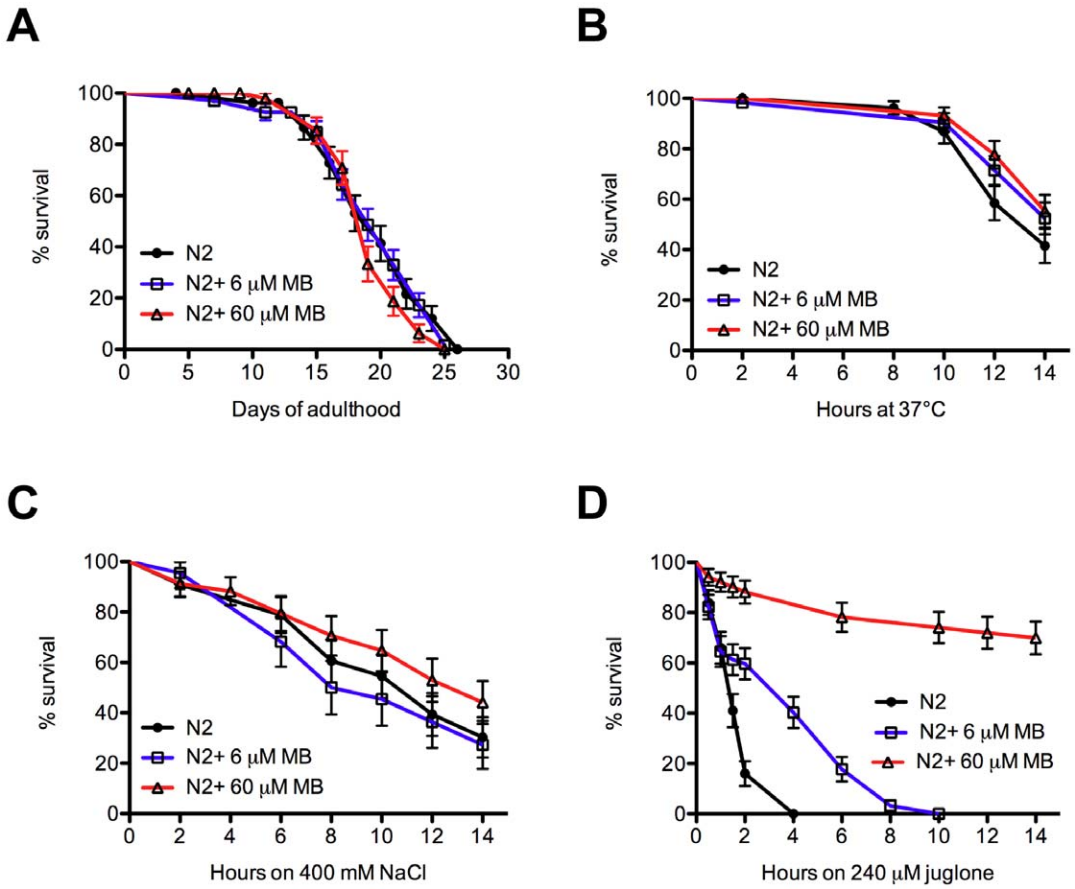

Figure 5. Methylene blue protects against oxidative stress in *C. elegans*. (**A**) N2 worms grown on plates with MB had lifespans indistinguishable from untreated worms (see also Table S1). (**B**) Worms grown on MB and subjected to thermal stress showed similar survival rates compared to untreated N2 worms. (**C**) N2 worms treated with MB showed similar rates of survival compared to untreated worms when subjected to hyperosmolarity. (**D**) MB had a dose-dependent protective effect on N2 worms against oxidative stress and mortality when grown on plates containing juglone ($P<0.001$ for MB treated N2 worms compared to untreated worms).
doi:10.1371/journal.pone.0042117.g005

triplicates were tested at 20°C from adult day 1 until death. Worms were declared dead if they were immotile and did not respond to tactile or heat stimulus.

Stress assays. For oxidative stress tests, worms were grown on NGM or NGM+60 μM methylene blue and transferred to NGM plates +240 μM juglone at adult day 1. For thermal resistance worms were grown on NGM or NGM 60 μM methylene blue and put at 37°C at adult day 1. For osmotic resistance worms were grown on NGM or NGM+60 μM methylene blue and put on 400 mM NaCl plates at adult day 1. For all assays, worms were evaluated for survival every 30 min for the first 2 hours and every 2 hours after up to 14 hours. Nematodes were scored as dead if they were immotile and unable to move in response to heat or tactile stimuli. For all tests worms, 20 animals/plate by triplicates were scored.

Dihydrofluorescein diacetate assay. For visualization of oxidative damage in the transgenic strains the worms were incubated on a slide for 30 min with 5 μM dihydrofluorescein diacetate dye and then washed with 1× PBS three times. After the slide was fixed, fluorescence was observed with the Leica system described above.

Worm lysates. Worms were collected in M9 buffer, washed 3 times with M9 and pellets were placed at −80°C overnight. Pellets were lysed in RIPA buffer (150 mM NaCl, 50 mM Tris pH 7.4, 1% Triton X-100, 0.1% SDS, 1% sodium deoxycholate)+protease inhibitors (10 mg/ml leupeptin, 10 mg/ml pepstatin A, 10 mg/ml chymostatin LPC;1/1000). Pellets were passed through a $27_{1/2}$ G syringe 10 times, sonicated and centrifuged at 16,000× *g*. Supernatants were collected.

Immunoblot. Worm RIPA samples (175 μg/well), lymphoblast cell RIPA samples (15 μg/well) were resuspended directly in 1× Laemmli sample buffer, migrated in 12.5% polyacrylamide gels, transferred to nitrocellulose membranes (BioRad) and immunoblotted. Antibodies used: rabbit anti-TDP-43 (1:200; Proteintech), rabbit anti-FUS/TLS (1:200; AbCam), and mouse anti-actin (1:10000 for worms, MP Biomedicals). Blots were visualized with peroxidase-conjugated secondary antibodies and ECL Western Blotting Substrate (Thermo Scientific).

Statistical analysis. For paralysis and stress-resistance tests, survival curves were generated and compared using the Log-rank (Mantel-Cox) test, and a 60–100 animals were tested per genotype and repeated at least three times.

Zebrafish experiments

Zebrafish maintenance. Zebrafish (*Danio rerio*) embryos were raised at 28.5°C, and collected and staged using standard methods [34]. The Comité de Déontologie de l'Expérimentation sur les Animaux (CDEA), the local animal care committee at the Université de Montréal, having received the protocol relevant to

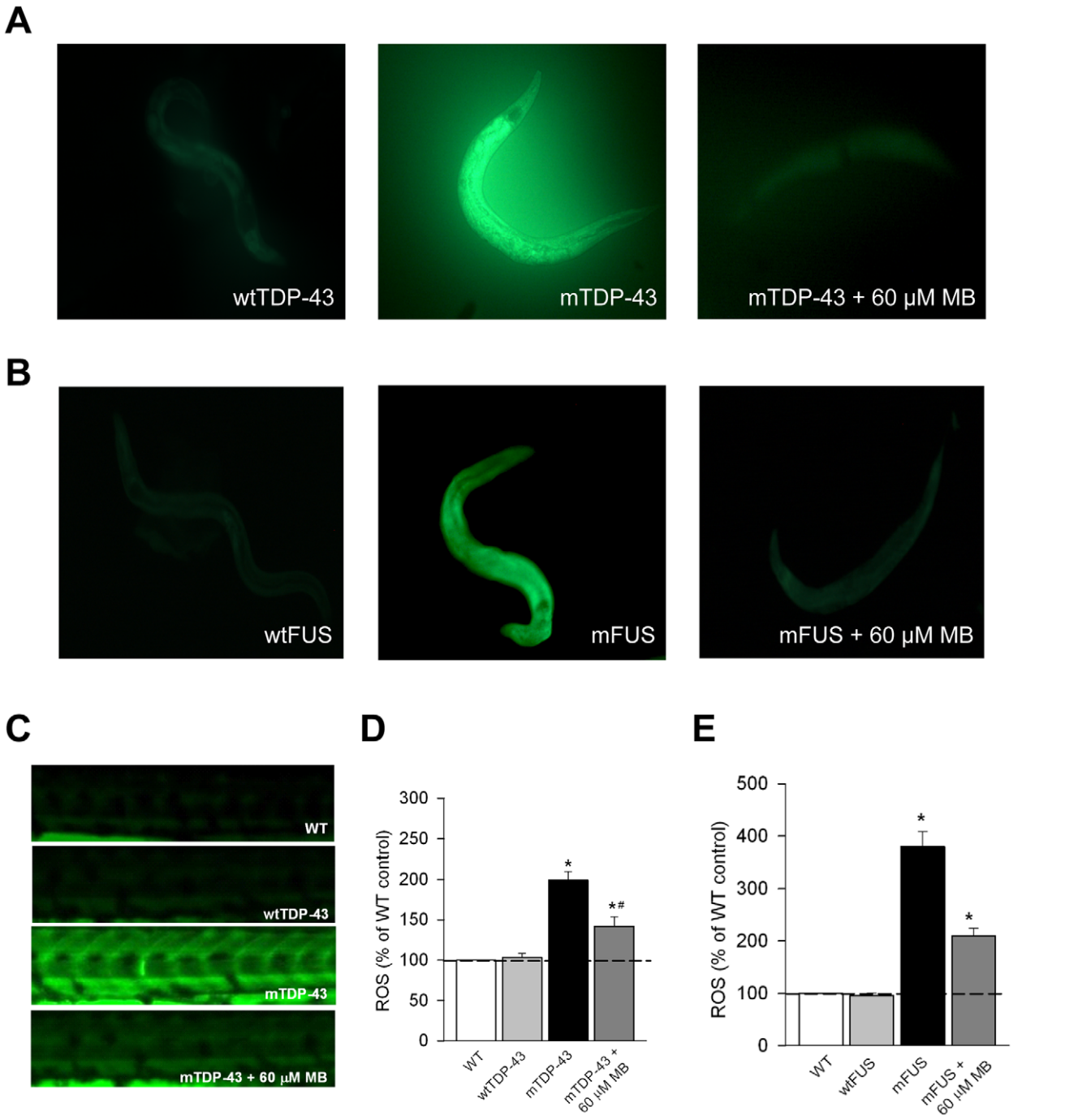

Figure 6. Methylene blue reduces oxidative stress in *C. elegans* and zebrafish transgenics. Oxidative stress was measured in transgenic worms and zebrafish with the dihydrofluorescein diacetate (DHF) that fluoresces when exposed to intracellular peroxide. (A) mTDP-43 worms, but not wtTDP-43 transgenics have a higher level of oxidative stress when stained with DHF. mTDP-43 worms treated with MB and then stained with DHF show a remarkable reduction in fluorescence. (B) wtFUS worms show no fluorescence when stained with DHF compared to mFUS worms. mFUS worms treated with MB and then stained with DHF showed reduced fluorescence. (**C**) Wild type (WT) zebrafish and zebrafish expressing wtTDP-43 show very low levels of fluorescence when stained with DHF compared to mTDP-43 fish. Treatment with MB reduced fluorescence in DHF stained fish. (**D**) Quantification of fluorescence of DHF stained fish shows that MB treatment significantly reduced fluorescence in mTDP-43 fish (*$P<0.001$, *#$P<0.01$). (**E**) MB significantly reduced fluorescence in DHF stained mFUS zebrafish (*$P<0.001$).
doi:10.1371/journal.pone.0042117.g006

this project relating to animal care and treatment, certified that the care and treatment of animals was in accordance with the guidelines and principles of the Canadian Council on Animal Care. Further, all matters arising from this proposal that related to animal care and treatment, and all experimental procedures proposed for use with animals were reviewed and approved by the CDEA before they were initiated or undertaken. This review process was ongoing on a regular basis during the entire period

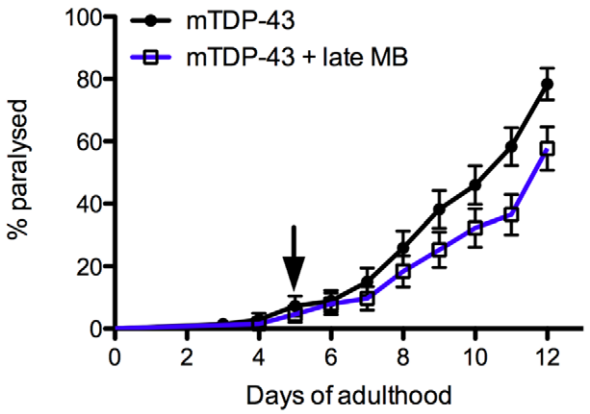

Figure 7. Diminished neuroprotection from late administration of methylene blue. mTDP-43 worms grown on normal plates and switched to plates supplemented with 60 μM MB at day 5 (indicated by the arrow) of adulthood (late MB) showed a modest but significant reduction in paralysis compared to untreated worms ($P<0.05$).
doi:10.1371/journal.pone.0042117.g007

that the research was being undertaken. Zebrafish embryos (no adults were used) are insentient to pain. Fish embryos were incubated overnight in each compound and examined the next day and then disposed. Zebrafish embryos were used over a two-day period then terminated.

In-vitro mRNA synthesis and embryo microinjection. Human FUS wild type and mutant [R521H], human TDP-43 wild type and mutant [G348C] mRNAs were transcribed from NotI-linearized pCS2+ using SP6 polymerase with the mMESSAGE Machine Kit (Ambion). This was followed by a phenol:chloroform extraction and isopropanol precipitation, and diluted in nuclease-free water (Ambion). The mRNAs were diluted in nuclease free water (Ambion) with 0.05% Fast Green vital dye (Sigma-Aldrich) at a concentration of 60 ng/μl (FUS), 25 ng/μl (TDP-43) and were pulse-injected into 1–2 cell stage embryos using a Picospritzer III pressure ejector.

Chemical treatments. Transient transgenics for TDP-43 [G348C] and FUS [R521H] embryos at 24 hpf were placed in individual wells in a 24 well plate and were treated overnight with methylene blue diluted in Evans solution (in mM): 134 NaCl, 2.9 KCl, 2.1 $CaCl_2$, 1.2 $MgCl_2$, 10 HEPES, 10 glucose, pH 7.8, 290 mOsm, with 0.1% DMSO. Behavioural touch responses were then assessed at 52–56 hpf as described in the following section.

Touch-evoked escape response. Zebrafish larvae were touched lightly at the level of the tail with a pair of blunt forceps and their locomotor behavior was recorded with a Grasshopper 2 Camera (Point Grey Research) at 30 Hz. The movies were then analyzed using the manual tracking plugin of ImageJ 1.45r software (NIH) and the swim duration, swim distance and maximum swim velocity of the fish were calculated.

Unbranched axonal length measurements. For immunohistochemical analysis of axonal projections of motor neurons, monoclonal antibody anti-SV2 (Developmental Studies Hybridoma) were used to assess the motor neuron morphology at 48 and 72 hpf. Fluorescent images of fixed embryos were taken using a Quorum Technologies spinning-disk confocal microscope mounted on an upright Olympus BX61W1 fluorescence microscope equipped with an Hamamatsu ORCA-ER camera. Image acquisition was performed with Volocity software (PerkinElmer). As previously described [16], axonal projections from primary and secondary motor neurons at a defined location in the inter somitic segments were determined. Analysis of Z-stacks by confocal microscopy was performed in three to four axonal projections per animal. The axonal length to the first branching (UAL) was determined by tracing the labeled axon from the spinal cord to the point where it branches using ImageJ (NIH). These values were averaged for each of the animal analyzed (10–30 zebrafish per condition) for the various conditions in our study.

Reactive Oxygen Species measurements. For *in vivo* detection of reactive oxygen species, live 2 day old embryos (2 dpf) were incubated in 5 μM 2′,7′-dichlorofluorescein diacetate (Sigma-Aldrich) for 20 minutes at 28.5°C and washed three times for 5 min with embryo media. Fluorescence was observed under a 488 nm wavelength excitation. The generation of reactive oxygen species in the larvae exposed to the chemicals was also quantitatively assessed as described elsewhere [35]. Briefly, 15 embryos were washed with cold Phosphate Buffer solution (PBS; pH 7.4) twice and then homogenized in cold buffer (0.32 mM of sucrose, 20 mM of HEPES, 1 mM of $MgCl_2$, and 0.5 mM of phenylmethyl sulfonylfluoride (PMSF), pH 7.4). The homogenate was centrifuged at 15,000× g at 4°C for 20 min, and the supernatant was transferred to new tubes for further experimentation. Twenty microliters of the homogenate was added to a 96-well plate and incubated at room temperature for 5 min, after which 100 μl of PBS (pH 7.4) and 8.3 μl of DFH stock solution (10 mg/ml) were added to each well. The plate was incubated at 37°C for 30 minutes. The fluorescence intensity was measured using a microplate reader (SpectraMax M2, Molecular Device, Union City, CA, USA) with excitation and emission at 485 and 530 nm, respectively. The reactive oxygen species concentration was expressed as arbitrary emission units per mg protein.

Statistical analysis. All data values are given as means ± SEM. Significance was determined using one-way ANOVAs and Fisher LSD tests for normally distributed and equal variance data, Kruskal–Wallis ANOVA and Dunn's method of comparison were used for non-normal distributions.

Supporting Information

Figure S1 Methylene blue has no effect on wild type motility phenotypes in worms or zebrafish. (**A**) MB had no significant effect on the motility phenotype of wild type (WT) non-transgenic N2 worms. (**B**) Representative traces of TEER phenotypes in WT zebrafish with and without MB treatment. MB did not affect the swim duration (**C**), distance swam (**D**) or maximum swimming velocity (**E**) of WT zebrafish.
(TIF)

Table S1 Lifespan analysis for all experiments. Related to Figure 5A. Animals that died prematurely (ruptured, internal hatching) or were lost (crawled off the plate) were censored at the time of scoring. All control and experimental animals were scored and transferred to new plates at the same time. ns: not significant.
(PDF)

Acknowledgments

We would like to thank M. Drits and G. Laliberte for help with zebrafish. P.D holds a Canada Research Chair in Neuroscience, E.K. holds a MDA Development Grant as well as an AVENIR and Jeune Chercheur contracts with INSERM, J.A.P is a CIHR New Investigator.

Author Contributions

Conceived and designed the experiments: EK PD JAP MT. Performed the experiments: AV SAP CM EK SC MT. Analyzed the data: AV SAP EK JAP MT. Wrote the paper: AV SAP PD EK JAP MT.

References

1. Boillee S, Vande Velde C, Cleveland DW (2006) ALS: a disease of motor neurons and their nonneuronal neighbors. Neuron 52: 39–59.
2. Lomen-Hoerth C (2008) Amyotrophic lateral sclerosis from bench to bedside. Semin Neurol 28: 205–211.
3. Neumann M, Sampathu DM, Kwong LK, Truax AC, Micsenyi MC, et al. (2006) Ubiquitinated TDP-43 in frontotemporal lobar degeneration and amyotrophic lateral sclerosis. Science 314: 130–133.
4. Gitcho MA, Baloh RH, Chakraverty S, Mayo K, Norton JB, et al. (2008) TDP-43 A315T mutation in familial motor neuron disease. Ann Neurol.
5. Kabashi E, Valdmanis PN, Dion P, Spiegelman D, McConkey BJ, et al. (2008) TARDBP mutations in individuals with sporadic and familial amyotrophic lateral sclerosis. Nat Genet.
6. Sreedharan J, Blair IP, Tripathi VB, Hu X, Vance C, et al. (2008) TDP-43 mutations in familial and sporadic amyotrophic lateral sclerosis. Science 319: 1668–1672.
7. Kwiatkowski TJ Jr, Bosco DA, Leclerc AL, Tamrazian E, Vanderburg CR, et al. (2009) Mutations in the FUS/TLS gene on chromosome 16 cause familial amyotrophic lateral sclerosis. Science 323: 1205–1208.
8. Lagier-Tourenne C, Polymenidou M, Cleveland DW (2010) TDP-43 and FUS/TLS: emerging roles in RNA processing and neurodegeneration. Hum Mol Genet 19: R46–64.
9. Kabashi E, Bercier V, Lissouba A, Liao M, Brustein E, et al. (2011) FUS and TARDBP but not SOD1 interact in genetic models of Amyotrophic Lateral Sclerosis. PLoS Genet in press.
10. Wang JW, Brent JR, Tomlinson A, Shneider NA, McCabe BD (2011) The ALS-associated proteins FUS and TDP-43 function together to affect Drosophila locomotion and life span. J Clin Invest.
11. Owens KN, Santos F, Roberts B, Linbo T, Coffin AB, et al. (2008) Identification of genetic and chemical modulators of zebrafish mechanosensory hair cell death. PLoS Genet 4: e1000020.
12. Peterson RT, Link BA, Dowling JE, Schreiber SL (2000) Small molecule developmental screens reveal the logic and timing of vertebrate development. Proc Natl Acad Sci U S A 97: 12965–12969.
13. Jones AK, Buckingham SD, Sattelle DB (2005) Chemistry-to-gene screens in Caenorhabditis elegans. Nat Rev Drug Discov 4: 321–330.
14. Kwok TC, Ricker N, Fraser R, Chan AW, Burns A, et al. (2006) A small-molecule screen in C. elegans yields a new calcium channel antagonist. Nature 441: 91–95.
15. Vaccaro A, Tauffenberger A, Aggad D, Rouleau G, Drapeau P, et al. (2012) Mutant TDP-43 and FUS cause age-dependent paralysis and neurodegeneration in C. elegans. PLoS ONE 7: e31321.
16. Kabashi E, Lin L, Tradewell ML, Dion PA, Bercier V, et al. (2009) Gain and loss of function of ALS-related mutations of TARDBP (TDP-43) cause motor deficits in vivo. Hum Mol Genet 19: 671–683.
17. Kabashi E, Bercier V, Lissouba A, Liao M, Brustein E, et al. (2011) FUS and TARDBP but not SOD1 interact in genetic models of amyotrophic lateral sclerosis. PLoS Genet 7: e1002214.
18. Schirmer RH, Adler H, Pickhardt M, Mandelkow E (2011) "Lest we forget you - methylene blue …". Neurobiol Aging.
19. Cheah BC, Vucic S, Krishnan AV, Kiernan MC (2010) Riluzole, neuroprotection and amyotrophic lateral sclerosis. Curr Med Chem 17: 1942–1199.
20. Van Raamsdonk JM, Hekimi S (2009) Deletion of the mitochondrial superoxide dismutase sod-2 extends lifespan in Caenorhabditis elegans. PLoS Genet 5: e1000361.
21. Harding HP, Zhang Y, Zeng H, Novoa I, Lu PD, et al. (2003) An integrated stress response regulates amino acid metabolism and resistance to oxidative stress. Mol Cell 11: 619–633.
22. Necula M, Breydo L, Milton S, Kayed R, van der Veer WE, et al. (2007) Methylene blue inhibits amyloid Abeta oligomerization by promoting fibrillization. Biochemistry 46: 8850–8860.
23. Wischik CM, Edwards PC, Lai RY, Roth M, Harrington CR (1996) Selective inhibition of Alzheimer disease-like tau aggregation by phenothiazines. Proc Natl Acad Sci U S A 93: 11213–11218.
24. Yamashita M, Nonaka T, Arai T, Kametani F, Buchman VL, et al. (2009) Methylene blue and dimebon inhibit aggregation of TDP-43 in cellular models. FEBS Lett 583: 2419–2424.
25. Arai T, Hasegawa M, Nonoka T, Kametani F, Yamashita M, et al. (2010) Phosphorylated and cleaved TDP-43 in ALS, FTLD and other neurodegenerative disorders and in cellular models of TDP-43 proteinopathy. Neuropathology 30: 170–181.
26. Audet JN, Soucy G, Julien JP (2012) Methylene blue administration fails to confer neuroprotection in two amyotrophic lateral sclerosis mouse models. Neuroscience.
27. Medina DX, Caccamo A, Oddo S (2011) Methylene blue reduces abeta levels and rescues early cognitive deficit by increasing proteasome activity. Brain Pathol 21: 140–149.
28. van Bebber F, Paquet D, Hruscha A, Schmid B, Haass C (2010) Methylene blue fails to inhibit Tau and polyglutamine protein dependent toxicity in zebrafish. Neurobiol Dis 39: 265–271.
29. Simpson EP, Yen AA, Appel SH (2003) Oxidative Stress: a common denominator in the pathogenesis of amyotrophic lateral sclerosis. Curr Opin Rheumatol 15: 730–736.
30. Lin MT, Beal MF (2006) Mitochondrial dysfunction and oxidative stress in neurodegenerative diseases. Nature 443: 787–795.
31. Naganska E, Matyja E (2011) Amyotrophic lateral sclerosis - looking for pathogenesis and effective therapy. Folia Neuropathol 49: 1–13.
32. Rojas JC, Bruchey AK, Gonzalez-Lima F (2012) Neurometabolic mechanisms for memory enhancement and neuroprotection of methylene blue. Prog Neurobiol 96: 32–45.
33. Rojas JC, Simola N, Kermath BA, Kane JR, Schallert T, et al. (2009) Striatal neuroprotection with methylene blue. Neuroscience 163: 877–889.
34. Kimmel CB, Ballard WW, Kimmel SR, Ullmann B, Schilling TF (1995) Stages of embryonic development of the zebrafish. Dev Dyn 203: 253–310.
35. Deng J, Yu L, Liu C, Yu K, Shi X, et al. (2009) Hexabromocyclododecane-induced developmental toxicity and apoptosis in zebrafish embryos. Aquat Toxicol 93: 29–36.

Neurobiology of Aging 34 (2013) 2175–2182

Contents lists available at SciVerse ScienceDirect

Neurobiology of Aging

journal homepage: www.elsevier.com/locate/neuaging

Evaluation of longevity enhancing compounds against transactive response DNA-binding protein-43 neuronal toxicity

Arnaud Tauffenberger [a,b,c], Carl Julien [a,b,c], J. Alex Parker [a,b,c,*]

[a] CRCHUM, Montréal, Québec, Canada
[b] Center of Excellence in Neuromics, Université de Montréal, Montréal, Québec, Canada
[c] Département de Pathologie et Biolologie Cellulaire, Université de Montréal, Montréal, Québec, Canada

ARTICLE INFO

Article history:
Received 21 September 2012
Received in revised form 2 March 2013
Accepted 11 March 2013
Available online 13 April 2013

Keywords:
TDP-43
Amyotrophic lateral sclerosis
C. elegans
Neurodegeneration
Longevity
Proteotoxicity

ABSTRACT

In simple systems, lifespan can be extended by various methods including dietary restriction, mutations in the insulin/insulin-like growth factor (IGF) pathway or mitochondria among other processes. It is widely held that the mechanisms that extend lifespan may be adapted for diminishing age-associated pathologies. We tested whether a number of compounds reported to extend lifespan in *C. elegans* could reduce age-dependent toxicity caused by mutant TAR DNA-binding protein-43 in *C. elegans* motor neurons. Only half of the compounds tested show protective properties against neurodegeneration, suggesting that extended lifespan is not a strong predictor for neuroprotective properties. We report here that resveratrol, rolipram, reserpine, trolox, propyl gallate, and ethosuximide protect against mutant TAR DNA-binding protein-43 neuronal toxicity. Finally, of all the compounds tested, only resveratrol required *daf-16* and *sir-2.1* for protection, and ethosuximide showed dependence on *daf-16* for its activity.

1. Introduction

For more than 75 years, people have been fascinated by the discovery that rats living on a restricted diet (dietary restriction) showed increased lifespan (McCay et al., 1989), a phenomenon that is under investigation in primates (Colman et al., 2009; Mattison et al., 2012). Of great interest is the fact that not only do many organisms show increased lifespan under dietary restriction conditions but they also show decreased incidences of age-related pathologies (Anderson and Weindruch, 2012). Additional mechanisms that regulate longevity have been discovered including mitochondrial function and the insulin/insulin-like growth factor (IGF) signaling pathway. Molecular and genetic approaches have begun to decipher the cellular mechanisms of lifespan extension and this has led to the development of an industry hoping to find and develop longevity mimetics as potential therapeutic agents against age-related disease (Mercken et al., 2012). Work from model organisms like *C. elegans* has identified numerous compounds that extend lifespan by influencing conserved longevity mechanisms and we wondered if these compounds would be effective against age-dependent proteotoxicity. To evaluate these compounds we turned to a *C. elegans* model of age-dependent motor neuron toxicity (Vaccaro et al., 2012a) and tested 11 compounds reported to extend lifespan. We identified 6 compounds that reduced mutant transactive response (TAR) DNA-binding protein-43 (TDP-43) neuronal toxicity and might be useful as candidates for testing and drug development in mammalian models of neurodegeneration.

2. Methods

2.1. C. elegans *strains and genetics*

Standard methods of culturing and handling worms were used. Worms were maintained on standard nematode growth media plates streaked with OP50 *E. coli*. All strains were scored at 20 °C. Mutations and transgenes used in this study were: *daf-16(mu86)*, *hsf-1(sy441)*, *rrf-3(pk1426)*, *sir-2.1(ok434)*, and *xqIs133[unc-47::TDP-43[A315T];unc-119(+)]*. Most of the strains were obtained from the *C. elegans* Genetics Center (University of Minnesota, Minneapolis, MN, USA). Mutants or transgenic worms were verified by visible phenotypes, polymerase chain reaction analysis for deletion mutants, sequencing for point mutations, or a combination thereof. Deletion mutants were outcrossed a minimum of 3 times to wild type N2 worms before use.

2.2. Paralysis assays

Worms were counted as paralyzed if they failed to move when prodded with a worm pick. Worms were scored as dead if they

* Corresponding author at: CRCHUM, Hopital Notre Dame, 1560 rue Sherbrooke Est, M-5226, Montreal, Québec H2L 4M1, Canada. Tel.: +1 514 890 8000 ×28826; fax: +1 514 412-7602.
E-mail address: ja.parker@umontreal.ca (J.A. Parker).

0197-4580/$ – see front matter
http://dx.doi.org/10.1016/j.neurobiolaging.2013.03.014

failed to move their head after being prodded in the nose and showed no pharyngeal pumping. For the paralysis tests worms grown on the specific compound from hatching were transferred to the appropriate experimental plate for scoring.

2.3. Neurodegeneration assays

For scoring of neuronal processes, TDP-43 transgenic animals were selected at day 9 of adulthood for visualization of motor neurons processes in vivo. Animals were immobilized in M9 with 5 mM levamisole and mounted on slides with 2% agarose pads. Neurons were visualized using a Leica DM6000 microscope and a Leica DFC 480 camera. A minimum of 100 animals were scored per treatment over 4–6 trials. The mean and standard error of the mean were calculated for each trial and 2-tailed *t* tests were used for statistical analysis.

2.4. RNAi experiments

RNA interference (RNAi)-treated strains were fed *E. coli* (HT115) containing an empty vector or *skn-1* (T19E7.2) RNAi clones from the ORFeome RNAi library (Open Biosystems). RNAi experiments were performed at 20 °C. Worms were grown on Nematode Growth Media enriched with 1 mM isopropyl-ß-D-thiogalactopyranoside. All RNAi paralysis tests were performed using a TDP-43 [A315T];*rrf-3(pk1426)* strain. To minimize developmental effects, L4 worms were grown on plates with either *skn-1*(RNAi) or empty vector and assayed for paralysis as adults. *skn-1*(RNAi) activity was confirmed by the observation of lethal and sterile phenotypes in the progeny of treated animals.

2.5. Protein extraction

Worms were lysed in radioimmunoprecipitation assay buffer (150 mM NaCl, 50 mM Tris pH 7.4, 1% Triton X-100, 0.1% sodium dodecyl sulfate, 1% sodium deoxycholate) plus 0.1% protease inhibitors (10 mg/mL leupeptin, 10 mg/mL pepstatin A, 10 mg/mL chymostatin). Nematodes were lysed with a $27_{1/2}$ syringe 10–15 times, incubated on ice for 10 minutes then moved at room temperature for 10 minutes and finally centrifuged at 16,000*g* for 10 minutes. Protein quantification was performed using a BCA protein assay kit (Thermo Scientific). For TDP-43 transgenic worms, soluble and insoluble fractions were obtained using methods previously described (Liachko et al., 2010; Neumann et al., 2006), with modifications. Briefly, worms pellets were homogenized with a pellet mixer (Disposable Pellet Mixer and Cordless Motor, VWR) in 1 volume (wt/vol) of low-salt buffer (Benedetti et al., 2008) (10 mM Tris, 5 mM Ethylene Diamine Triacetic Acid (EDTA), 10% sucrose, pH 7.5) and centrifuged at 25,000*g* for 30 minutes at 4 °C. The supernatant represents the low salt (LS) fraction, containing the soluble proteins.

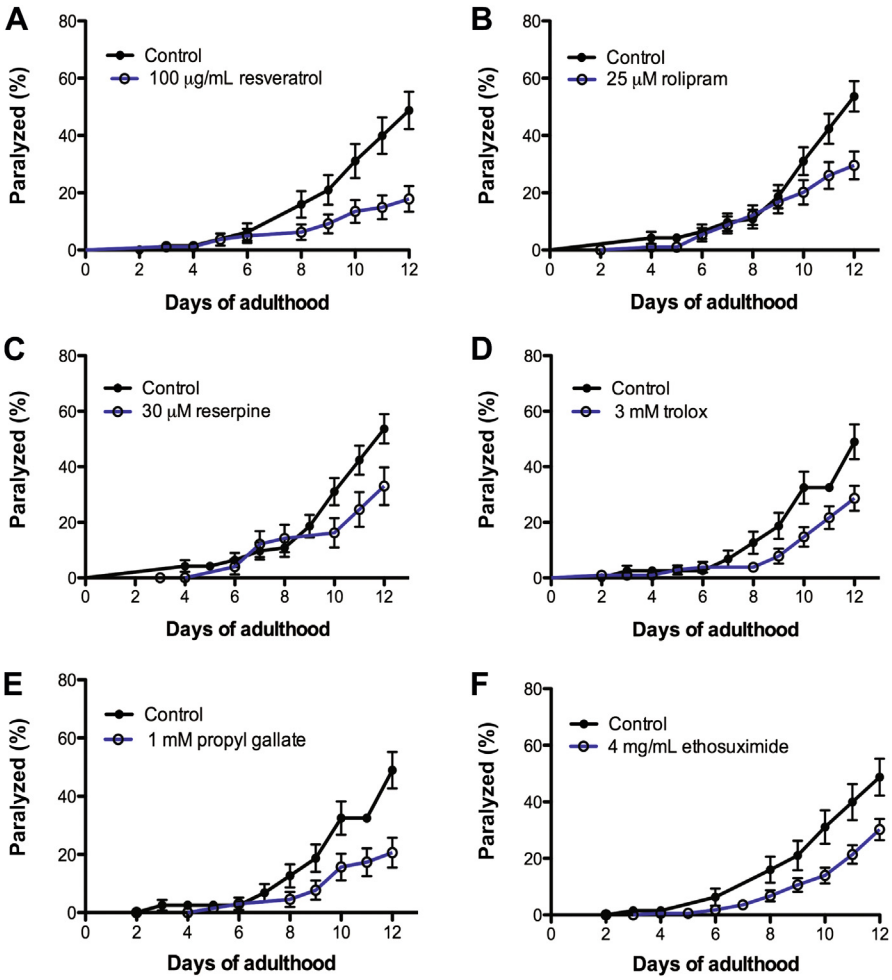

Fig. 1. Lifespan-extending compounds reduce mutant TAR DNA-binding protein–43-induced paralysis. Compounds that reduced mutant TAR DNA-binding protein–43-induced motility defects and paralysis compared with untreated control animals included: (A) 100 µg/mL resveratrol ($p < 0.001$); (B) 25 µM rolipram ($p < 0.001$); (C) 30 µM reserpine ($p < 0.05$); (D) 3 mM trolox ($p < 0.01$); (E) 1 mM propyl gallate ($p < 0.01$); (F) 4 mg/mL ethosuximide ($p < 0.01$). See also Supplementary Table 1.

The pellet was washed with the same volume of LS, centrifuged again, and the supernatant was discarded. The remaining pellet was re-extracted with the same volume of Triton buffer (LS with 1% Triton X-100 and 0.5 M NaCl), centrifuged at 180,000*g* for 30 minutes at 4 °C. The resulting pellet was re-extracted with the same volume of myelin floatation buffer (Triton buffer containing 30% sucrose) and centrifuged at 180,000*g* for 30 minutes at 4 °C. The remaining pellet was re-extracted in the same volume of Sarkosyl buffer (LS with 1% N-Lauroyl-sarcosine and 0.5 M NaCl), incubated with agitation for 1 hour at 22 °C and centrifuged at 180,000*g* for 30 minutes at 22 °C. The detergent-insoluble pellet was weighted and solubilized in 5 volumes (wt/vol) of urea buffer (30 mM Tris, 7 M urea, 2 M thiourea, 4% 3-[(3-cholamidopropyl) dimethylammonio]-1- propanesulfonate, pH 8.5) and sonicated for 5 minutes. All buffers contained 1 mM Dithiothreitol DTT and protease inhibitors (LPC; 1/1000). The soluble LS and the insoluble urea fractions were quantified with the Bradford Protein Assay Kit (Bio-Rad) according to the manufacturer's instructions.

3. Results

3.1. Neuroprotection from select longevity-enhancing compounds

We investigated neurodegeneration with a well-characterized transgenic *C. elegans* strain that expresses the full-length human TDP-43 with the A315T mutation associated with amyotrophic lateral sclerosis in the worm's GABAergic motor neurons (Vaccaro et al., 2012a). These animals display adult-onset motility problems leading to progressive paralysis and neuronal degeneration that can be assessed over a period of 9 to 12 days (Vaccaro et al., 2012a). With this model, we then tested 11 compounds reported to increase lifespan in *C. elegans* for whether they could suppress the progressive paralysis caused by mutant TDP-43 (mTDP-43). The compounds tested included: the antioxidants propyl gallate (PG), trolox (TRO), and α-lipoic acid (Benedetti et al., 2008), the polyphenols resveratrol (RSV) (Morselli et al., 2010) and quercetin (Kampkotter et al., 2008), the anticonvulsant ethosuximide (ETX)

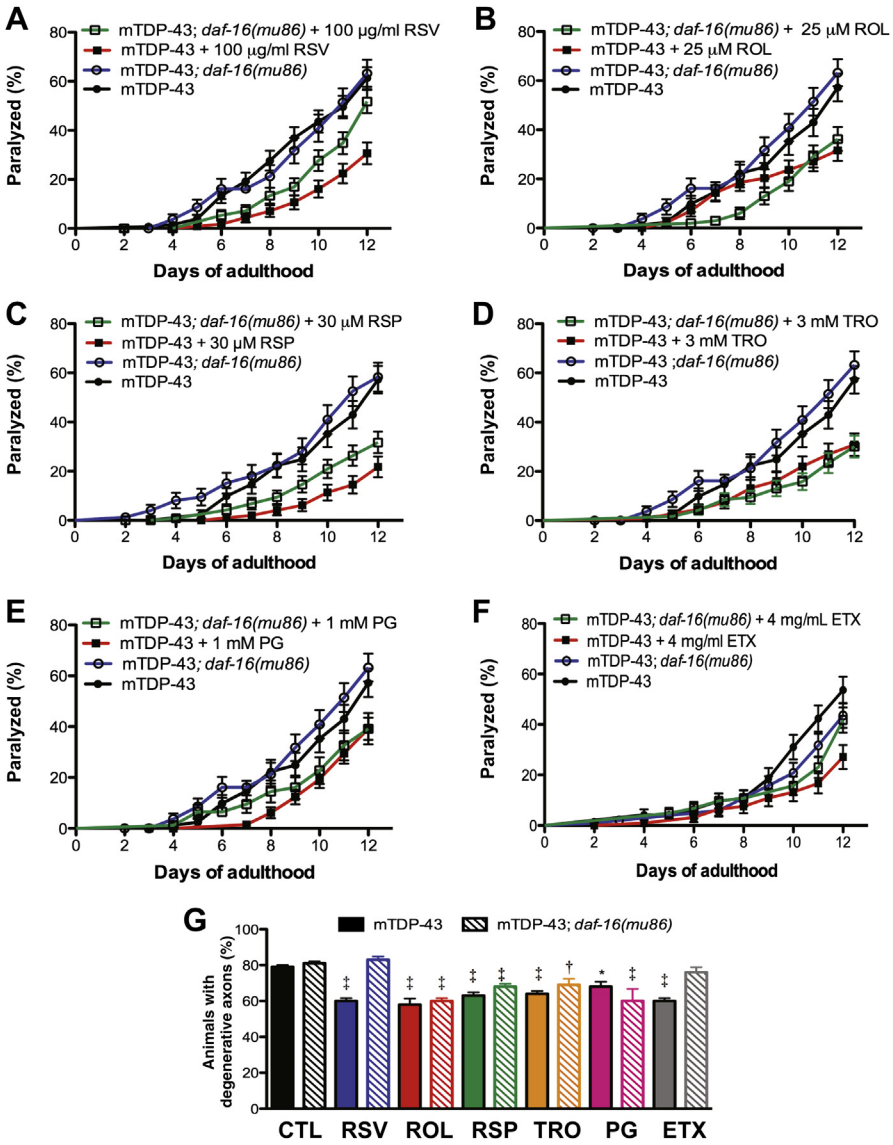

Fig. 2. Transcription factor *daf-16*/Forkhead box O (FOXO mediates RSV and ETX neuroprotection. (A) RSV delayed mutant TAR DNA-binding protein-43 (mTDP-43) paralysis and this effect was dependent on *daf-16*. (B–E) ROL, RSP, TRO, and PG all reduced mTDP-43 paralysis compared with untreated control animals independent of *daf-16*. See Supplementary Table 1 for statistical information. (F) ETX delayed mTDP-43 paralysis and this was dependent on *daf-16*. (G) RSV and ETX failed to rescue neuronal degeneration in *daf-16* mutant animals but all other compounds reduced neuronal degeneration at adult day 9 in *daf-16* mutant animals compared with untreated transgenic animals. * $p < 0.05$; † $p < 0.001$; ‡ $p < 0.0001$. Abbreviations: ETX, ethosuximide; PG, propyl gallate; ROL, rolipram; RSP, reserpine; RSV, resveratrol; TRO, trolox.

(Collins et al., 2008), reserpine (RSP) (Srivastava et al., 2008), spermidine (Eisenberg et al., 2009), valproic acid (Evason et al., 2008), and thioflavin (Alavez et al., 2011), and rolipram (ROL), a Phosphodiesterase 4 inhibitor that mimics the effects of RSV on mitochondrial function and glucose tolerance (Park et al., 2012) (please see Supplementary Table 1 for official names and suppliers). Interestingly, only 6 compounds rescued TDP-43 toxicity: RSV, ROL, RSP, TRO, PG, and ETX (Fig. 1, Supplementary Table 2) rescued mTDP-43 proteotoxicity at dosages previously used to increase lifespan. The 5 remaining compounds did not delay paralysis in the transgenic mTDP-43 worms (Supplementary Fig. 1, Supplementary Table 2). We also tested whether these 6 neuroprotective compounds extended lifespan in our worms and found that all compounds except for RSV increased lifespan (Supplementary Fig. 2, Supplementary Table 3). We also tested whether the reported effects were dependent on changes on protein expression. We found no differences in global protein expression after treatment with the 6 compounds in our transgenic worms (Supplementary Fig. 3). Interestingly, we also observed a reduction in mTDP-43 insolubility in animals treated with TRO, PG, and ETX suggesting these compounds might aid the cellular clearance of toxic protein species (Supplementary Fig. 3). Our data reveal an imperfect correlation between the ability of a compound to extend lifespan and reduce neuronal proteotoxicity.

3.2. *Involvement of* daf-16, hsf-1, sir-2.1, *and* skn-1 *pathways in compound-mediated neuroprotection*

Some of the key regulators of aging and stress signaling in *C. elegans* include the forkhead transcription factor *daf-16*, the heat shock factor transcription factor *hsf-1*, the sirtuin deacetylase *sir-2.1* (Kenyon, 2010), and the Nuclear respiratory factor transcription factor *skn-1* (An and Blackwell, 2003; Bishop and Guarente, 2007). To test if the 6 active compounds functioned within these pathways, we crossed our mTDP-43 transgenic animals with

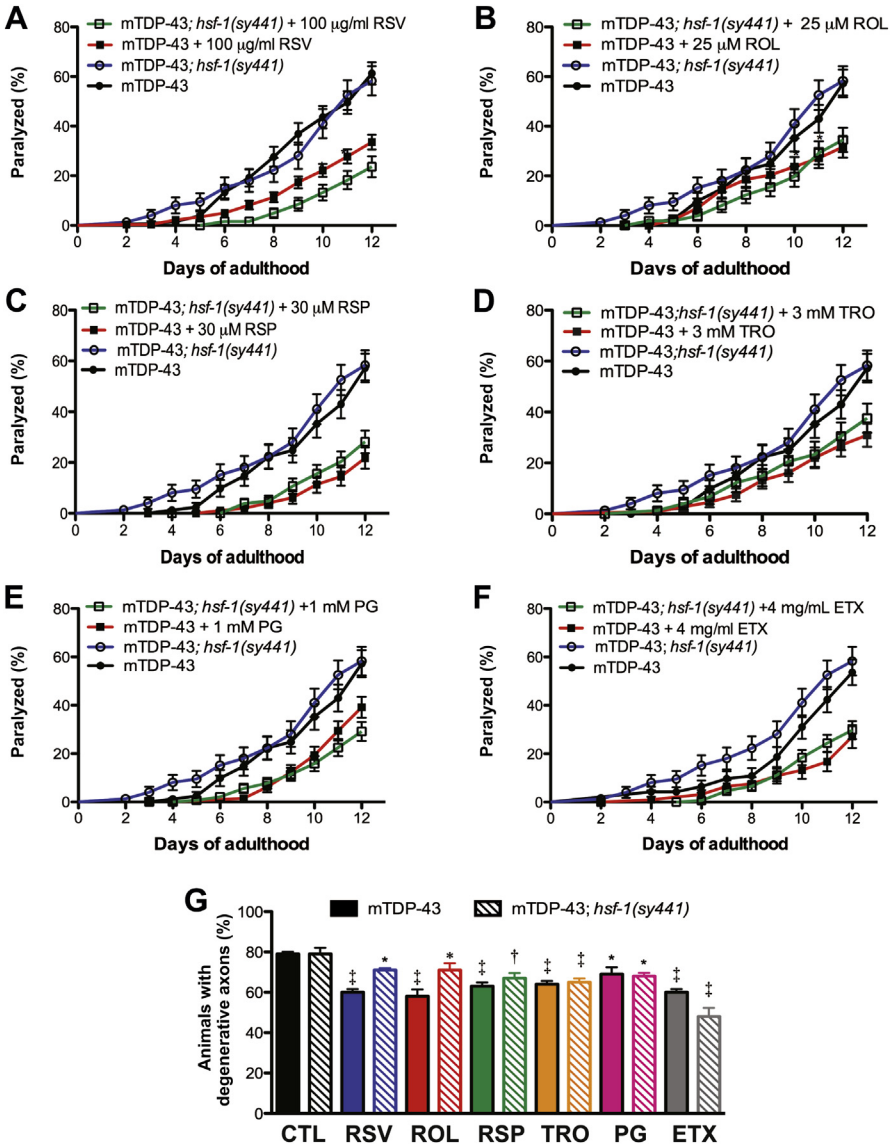

Fig. 3. Neuroprotective effects by the compounds are independent of *hsf-1*. (A–F) All compounds reduced mutant TAR DNA-binding protein-43 (mTDP-43) paralysis compared with untreated control animals independently of *hsf-1*. See Supplementary Table 1 for statistical information. (G) All compounds reduced neuronal degeneration in mTDP-43 animals compared with untreated control animals. * $p < 0.05$; † $p < 0.001$; ‡ $p < 0.0001$. Abbreviations: ETX, ethosuximide; PG, propyl gallate; ROL, rolipram; RSP, reserpine; RSV, resveratrol; TRO, trolox.

loss-of-function mutations or RNAi for each gene and tested if the compounds maintained neuroprotective activity.

3.2.1. *Transcription factor* daf-16 *mediates resveratrol and ETX neuroprotection*

Reduced insulin/IGF pathway signaling has been implicated in aging and stress resistance (Kenyon, 2005; Kenyon et al., 1993). The downstream effector *daf-16*/Forkhead box O has been identified as a key target of RSV neuroprotective effects in polyglutamine toxicity (Parker et al., 2005), and consistently, RSV was less effective at reducing mTDP-43-induced paralysis and axonal degeneration (Fig. 2A and G). Of the remaining compounds we observed that ETX was less effective at suppressing paralysis and neurodegeneration in mTDP-43;*daf-16* mutants suggesting that part of this compound's neuroprotective activity might rest within the insulin/IGF signaling pathway (Fig. 2F and G).

3.2.2. *Neuroprotective effects by compounds are independent of* hsf-1

Chaperones are key regulators of the cellular stress response and the heat shock factor *hsf-1*/Heat shock factor 1 (HSF1) has been implicated in dietary restriction and proteotoxicity (Cohen et al., 2006; Teixeira-Castro et al., 2011). We tested the different compounds in mTDP-43;*hsf-1(sy441)* mutants and observed no differences in the rates of paralysis or neurodegeneration compared with untreated mTDP-43 control animals (Fig. 3 and Supplementary Table 2). Thus, although *hsf-1* is important for proteotoxicity modification, it seems that neuroprotection by the 6 compounds tested here is independent of *hsf-1*.

3.2.3. *Resveratrol reduces neurotoxicity in a* sir-2.1*-dependent manner*

The polyphenol RSV is naturally produced by certain plant species in response to environmental stress (Signorelli and Ghidoni,

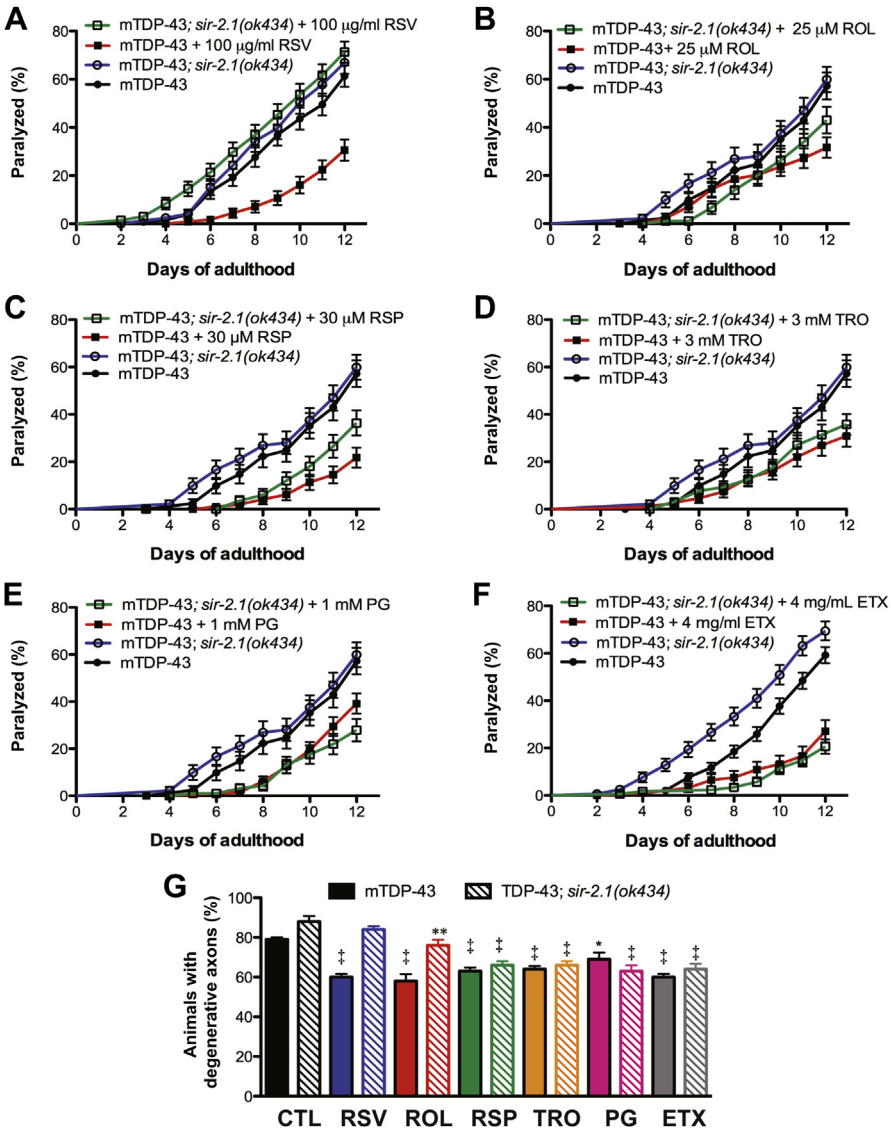

Fig. 4. Resveratrol reduces neurotoxicity in a *sir-2.1*-dependent manner. (A) RSV delayed mutant TAR DNA-binding protein-43 (mTDP-43) paralysis and this was dependent on *sir-2.1*. (B–F) ROL, RSP, TRO, PG, and ETX all reduced mTDP-43 paralysis compared with untreated animals independently of *sir-2.1*. See Supplementary Table 1 for statistical information. (G) RSV failed to rescue axonal degeneration in *sir-2.1* mutant animals but all other compounds reduced neuronal degeneration in mTDP-43 animals compared with untreated control animals. * $p < 0.05$; ** $p < 0.01$; ‡ $p < 0.0001$. Abbreviations: ETX, ethosuximide; PG, propyl gallate; ROL, rolipram; RSP, reserpine; RSV, resveratrol; TRO, trolox.

2005). Subsequent studies have shown that RSV requires sirtuins, a class of nicotinamide adenine dinucleotide-dependent deacetylases, for lifespan extension using dietary restriction (Lin et al., 2000), and was able to rescue neurodegeneration in different late age of onset disease in a Sirtuin 1-dependent manner (Kim et al., 2007; Parker et al., 2005). Thus, consistent with previous studies, RSV failed to rescue paralysis and neurodegeneration in mTDP-43;*sir-2.1(ok434)* mutants (Figs. 4A, 2G and Supplementary Table 2). However, the remaining 5 compounds continued to suppress paralysis and neurodegeneration phenotypes in the absence of *sir-2.1* (Figs. 4B–F and 2G), suggesting they function through alternative pathways.

3.2.4. *Neuroprotective effects by compounds are independent of* skn-1

Many genes involved in aging modulation and stress resistance overlap. We investigated whether the transcription factor *skn-1*, an Nuclear respiratory factor-like response factor that regulates stress resistance and longevity (Tullet et al., 2008; Wang et al., 2010), was required for rescue of neuronal phenotypes in mTDP-43 transgenic worms after treatment with the 6 compounds. However, all the compounds continued to rescue paralysis and axonal degeneration in the absence of *skn-1* (Fig. 5 and Supplementary Table 2).

4. Discussion

Understanding the cellular mechanisms of lifespan extension is an active area of research, as are efforts to apply these findings to age-related pathologies. Because extending lifespan by genetic or dietary methods delays age-associated negative phenotypes from worms to primates, the quest to identify chemicals replicating these effects is a promising area of therapeutic investigation. Supporting this notion are studies from *C. elegans* demonstrating that dietary restriction (Steinkraus et al., 2008), insulin/IGF signaling (Cohen et al., 2006; Morley et al., 2002), *hsf-1* (Cohen et al., 2006; Hsu et al., 2003), *sir-2.1* (Parker et al., 2005), or *skn-1* (Wang et al.,

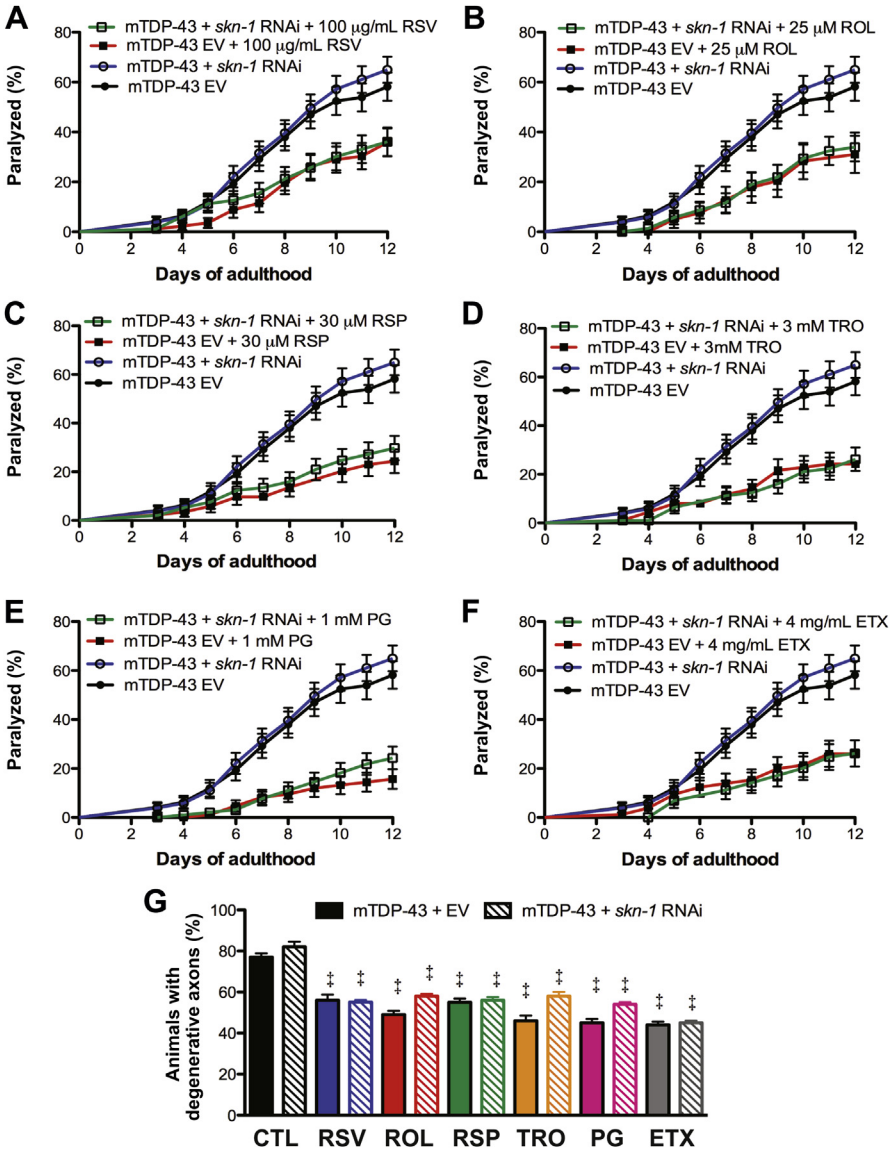

Fig. 5. Neuroprotective effects by compounds are independent of *skn-1*. (A–F) All compounds reduced mutant TAR DNA-binding protein-43 (mTDP-43) paralysis compared with untreated control animals independently of *skn-1*. See Supplementary Table 1 for statistical information. (G) All compounds reduced neuronal degeneration in mTDP-43 animals compared with untreated control animals. ‡ $p < 0.0001$. Abbreviations: ETX, ethosuximide; EV, Empty Vector; PG, propyl gallate; RNAi, RNA interference; ROL, rolipram; RSP, reserpine; RSV, resveratrol; TRO, trolox.

2010) modify proteotoxicity. With this goal in mind, we examined a number of compounds shown to extend lifespan, or in some cases, to reduce polyglutamine or amyloid-ß proteotoxicity in *C. elegans*, and investigated if they could suppress neuronal mTDP-43 toxicity. We identified 6 compounds that suppressed neuronal toxicity, but of these only RSV and ETX showed dependence on the aging genes *daf-16* and *sir-2.1*.

Our data suggest that lifespan extension might not be a strong predictor for neuroprotection. Indeed, recent work has shown that dietary restriction is ineffective against delaying neurodegeneration caused by mTDP-43 or polyglutamine in worms (Tauffenberger et al., 2012), amyloid-ß or tau toxicity in flies (Kerr et al., 2011), or mutant superoxide dismutase 1 in mice (Patel et al., 2010). Regarding the insulin/IGF pathway, reduced signaling has been shown to rescue (Cohen et al., 2006) or enhance proteotoxicity (Vaccaro et al., 2012b), suggesting this pathway might be difficult to manipulate for therapeutic benefit. Part of the discrepancy might be that earlier studies investigating longevity and proteotoxicity relied on models expressing mutant proteins in *C. elegans* body wall muscle cells. Similar results have been observed for *sir-2.1*, where deletion of *sir-2.1* exacerbates polyglutamine toxicity in neurons (Bates et al., 2006; Parker et al., 2005), but rescues polyalanine and α-synuclein toxicity in muscle cells (Catoire et al., 2008; van Ham et al., 2008). The disparity between muscle and neuronal models might apply to drug screening as well, where compounds like thioflavin have been shown to reduce amyloid-ß and polyglutamine toxicity in muscle cells (Alavez et al., 2011), but we observed no activity in our neuronal TDP-43 model. Neurons and muscle cells have different functions and metabolic requirements so it might not be surprising that they respond differently to manipulations promoting overall lifespan extensions in the context of proteotoxicity. Indeed, neurons and muscle cells appear to have different capabilities in responding to protein misfolding during aging (Kern et al., 2010). Thus, the predictive value of muscle-based models for neurodegenerative disorders needs to be interpreted with caution.

Although we describe an imperfect correlation between longevity and neuroprotection, we have identified 6 compounds that protect against mTDP-43 toxicity in motor neurons. Further investigation and validation in vertebrate systems will be required to gauge the effectiveness of these compounds as early leads for drug discovery and development in amyotrophic lateral sclerosis and other late-onset proteinopathies.

Disclosure statement

All authors have no conflicts of interest to disclose.
No approvals were required for the work described in this report.

Acknowledgements

The authors thank S. Peyrard for technical support. A.T. is supported by a CIHR and Huntington's Society of Canada fellowship. J.A.P. is a CIHR New Investigator. The CHUM Foundation, a CIHR Catalyst Grant, the Bernice Ramsay Discovery Grant from the ALS Society of Canada, and the Congressionally Directed Medical Research Program (CDMRP) Amyotrophic Lateral Sclerosis Research Program (USA) supported this work.

Appendix A. Supplementary data

Supplementary data associated with this article can be found, in the online version, at http://dx.doi.org/10.1016/j.neurobiolaging.2013.03.014.

References

Alavez, S., Vantipalli, M.C., Zucker, D.J., Klang, I.M., Lithgow, G.J., 2011. Amyloid-binding compounds maintain protein homeostasis during ageing and extend lifespan. Nature 472, 226–229.
An, J.H., Blackwell, T.K., 2003. SKN-1 links C. elegans mesendodermal specification to a conserved oxidative stress response. Genes Dev. 17, 1882–1893.
Anderson, R.M., Weindruch, R., 2012. The caloric restriction paradigm: implications for healthy human aging. Am. J. Hum. Biol. 24, 101–106.
Bates, E.A., Victor, M., Jones, A.K., Shi, Y., Hart, A.C., 2006. Differential contributions of Caenorhabditis elegans histone deacetylases to huntingtin polyglutamine toxicity. J. Neurosci. 26, 2830–2838.
Benedetti, M.G., Foster, A.L., Vantipalli, M.C., White, M.P., Sampayo, J.N., Gill, M.S., Olsen, A., Lithgow, G.J., 2008. Compounds that confer thermal stress resistance and extended lifespan. Exp. Gerontol. 43, 882–891.
Bishop, N.A., Guarente, L., 2007. Two neurons mediate diet-restriction-induced longevity in C. elegans. Nature 447, 545–549.
Catoire, H., Pasco, M.Y., Abu-Baker, A., Holbert, S., Tourette, C., Brais, B., Rouleau, G.A., Parker, J.A., Neri, C., 2008. Sirtuin inhibition protects from the polyalanine muscular dystrophy protein PABPN1. Hum. Mol. Genet. 17, 2108–2117.
Cohen, E., Bieschke, J., Perciavalle, R.M., Kelly, J.W., Dillin, A., 2006. Opposing activities protect against age-onset proteotoxicity. Science 313, 1604–1610.
Collins, J.J., Evason, K., Pickett, C.L., Schneider, D.L., Kornfeld, K., 2008. The anticonvulsant ethosuximide disrupts sensory function to extend C. elegans lifespan. PLoS Genet. 4, e1000230.
Colman, R.J., Anderson, R.M., Johnson, S.C., Kastman, E.K., Kosmatka, K.J., Beasley, T.M., Allison, D.B., Cruzen, C., Simmons, H.A., Kemnitz, J.W., Weindruch, R., 2009. Caloric restriction delays disease onset and mortality in rhesus monkeys. Science 325, 201–204.
Eisenberg, T., Knauer, H., Schauer, A., Buttner, S., Ruckenstuhl, C., Carmona-Gutierrez, D., Ring, J., Schroeder, S., Magnes, C., Antonacci, L., Fussi, H., Deszcz, L., Hartl, R., Schraml, E., Criollo, A., Megalou, E., Weiskopf, D., Laun, P., Heeren, G., Breitenbach, M., Grubeck-Loebenstein, B., Herker, E., Fahrenkrog, B., Frohlich, K.U., Sinner, F., Tavernarakis, N., Minois, N., Kroemer, G., Madeo, F., 2009. Induction of autophagy by spermidine promotes longevity. Nature Cell Biol. 11, 1305–1314.
Evason, K., Collins, J.J., Huang, C., Hughes, S., Kornfeld, K., 2008. Valproic acid extends Caenorhabditis elegans lifespan. Aging Cell 7, 305–317.
Hsu, A.L., Murphy, C.T., Kenyon, C., 2003. Regulation of aging and age-related disease by DAF-16 and heat-shock factor. Science 300, 1142–1145.
Kampkotter, A., Timpel, C., Zurawski, R.F., Ruhl, S., Chovolou, Y., Proksch, P., Watjen, W., 2008. Increase of stress resistance and lifespan of Caenorhabditis elegans by quercetin. Comp. Biochem. Physiol. B Biochem. Mol. Biol. 149, 314–323.
Kenyon, C., 2005. The plasticity of aging: insights from long-lived mutants. Cell 120, 449–460.
Kenyon, C., Chang, J., Gensch, E., Rudner, A., Tabtiang, R., 1993. A C. elegans mutant that lives twice as long as wild type. Nature 366, 461–464.
Kenyon, C.J., 2010. The genetics of ageing. Nature 464, 504–512.
Kern, A., Ackermann, B., Clement, A.M., Duerk, H., Behl, C., 2010. HSF1-controlled and age-associated chaperone capacity in neurons and muscle cells of C. elegans. PLoS One 5, e8568.
Kerr, F., Augustin, H., Piper, M.D., Gandy, C., Allen, M.J., Lovestone, S., Partridge, L., 2011. Dietary restriction delays aging, but not neuronal dysfunction, in Drosophila models of Alzheimer's disease. Neurobiol. Aging 32, 1977–1989.
Kim, D., Nguyen, M.D., Dobbin, M.M., Fischer, A., Sananbenesi, F., Rodgers, J.T., Delalle, I., Baur, J.A., Sui, G., Armour, S.M., Puigserver, P., Sinclair, D.A., Tsai, L.H., 2007. SIRT1 deacetylase protects against neurodegeneration in models for Alzheimer's disease and amyotrophic lateral sclerosis. EMBO J. 26, 3169–3179.
Liachko, N.F., Guthrie, C.R., Kraemer, B.C.,, 2010. Phosphorylation promotes neurotoxicity in a Caenorhabditis elegans model of TDP-43 proteinopathy. J. Neurosci. 30, 16208–16219.
Lin, S.J., Defossez, P.A., Guarente, L., 2000. Requirement of NAD and SIR2 for lifespan extension by calorie restriction in Saccharomyces cerevisiae. Science 289, 2126–2128.
Mattison, J.A., Roth, G.S., Beasley, T.M., Tilmont, E.M., Handy, A.M., Herbert, R.L., Longo, D.L., Allison, D.B., Young, J.E., Bryant, M., Barnard, D., Ward, W.F., Qi, W., Ingram, D.K., de Cabo, R., 2012. Impact of caloric restriction on health and survival in rhesus monkeys from the NIA study. Nature 489, 318–321.
McCay, C.M., Crowell, M.F., Maynard, L.A., 1989. The effect of retarded growth upon the length of life span and upon the ultimate body size. 1935. Nutrition 5, 155–171; discussion, 172.
Mercken, E.M., Carboneau, B.A., Krzysik-Walker, S.M., de Cabo, R., 2012. Of mice and men: the benefits of caloric restriction, exercise, and mimetics. Ageing Res. Rev. 11, 390–398.
Morley, J.F., Brignull, H.R., Weyers, J.J., Morimoto, R.I., 2002. The threshold for polyglutamine-expansion protein aggregation and cellular toxicity is dynamic and influenced by aging in Caenorhabditis elegans. Proc. Natl. Acad. Sci. U. S. A. 99, 10417–10422.
Morselli, E., Maiuri, M.C., Markaki, M., Megalou, E., Pasparaki, A., Palikaras, K., Criollo, A., Galluzzi, L., Malik, S.A., Vitale, I., Michaud, M., Madeo, F., Tavernarakis, N., Kroemer, G., 2010. Caloric restriction and resveratrol promote longevity through the Sirtuin-1-dependent induction of autophagy. Cell Death Dis. 1, e10.

Neumann, M., Sampathu, D.M., Kwong, L.K., Truax, A.C., Micsenyi, M.C., Chou, T.T., Bruce, J., Schuck, T., Grossman, M., Clark, C.M., McCluskey, L.F., Miller, B.L., Masliah, E., Mackenzie, I.R., Feldman, H., Feiden, W., Kretzschmar, H.A., Trojanowski, J.Q., Lee, V.M., 2006. Ubiquitinated TDP-43 in frontotemporal lobar degeneration and amyotrophic lateral sclerosis. Science 314, 130–133.

Park, S.J., Ahmad, F., Philp, A., Baar, K., Williams, T., Luo, H., Ke, H., Rehmann, H., Taussig, R., Brown, A.L., Kim, M.K., Beaven, M.A., Burgin, A.B., Manganiello, V., Chung, J.H., 2012. Resveratrol ameliorates aging-related metabolic phenotypes by inhibiting cAMP phosphodiesterases. Cell 148, 421–433.

Parker, J.A., Arango, M., Abderrahmane, S., Lambert, E., Tourette, C., Catoire, H., Neri, C., 2005. Resveratrol rescues mutant polyglutamine cytotoxicity in nematode and mammalian neurons. Nat. Genet. 37, 349–350.

Patel, B.P., Safdar, A., Raha, S., Tarnopolsky, M.A., Hamadeh, M.J., 2010. Caloric restriction shortens lifespan through an increase in lipid peroxidation, inflammation and apoptosis in the G93A mouse, an animal model of ALS. PLoS One 5, e9386.

Signorelli, P., Ghidoni, R., 2005. Resveratrol as an anticancer nutrient: molecular basis, open questions and promises. J. Nutr. Biochem. 16, 449–466.

Srivastava, D., Arya, U., SoundaraRajan, T., Dwivedi, H., Kumar, S., Subramaniam, J.R., 2008. Reserpine can confer stress tolerance and lifespan extension in the nematode C. elegans. Biogerontology 9, 309–316.

Steinkraus, K.A., Smith, E.D., Davis, C., Carr, D., Pendergrass, W.R., Sutphin, G.L., Kennedy, B.K., Kaeberlein, M., 2008. Dietary restriction suppresses proteotoxicity and enhances longevity by an hsf-1-dependent mechanism in Caenorhabditis elegans. Aging Cell 7, 394–404.

Tauffenberger, A., Vaccaro, A., Aulas, A., Vande Velde, C., Parker, J.A., 2012. Glucose delays age-dependent proteotoxicity. Aging Cell 11, 856–866.

Teixeira-Castro, A., Ailion, M., Jalles, A., Brignull, H.R., Vilaca, J.L., Dias, N., Rodrigues, P., Oliveira, J.F., Neves-Carvalho, A., Morimoto, R.I., Maciel, P., 2011. Neuron-specific proteotoxicity of mutant ataxin-3 in C. elegans: rescue by the DAF-16 and HSF-1 pathways. Hum. Mol. Genet. 20, 2996–3009.

Tullet, J.M., Hertweck, M., An, J.H., Baker, J., Hwang, J.Y., Liu, S., Oliveira, R.P., Baumeister, R., Blackwell, T.K., 2008. Direct inhibition of the longevity-promoting factor SKN-1 by insulin-like signaling in C. elegans. Cell 132, 1025–1038.

Vaccaro, A., Tauffenberger, A., Aggad, D., Rouleau, G., Drapeau, P., Parker, J.A., 2012a. Mutant TDP-43 and FUS cause age-dependent paralysis and neurodegeneration in C. elegans. PloS One 7, e31321.

Vaccaro, A., Tauffenberger, A., Ash, P.E., Carlomagno, Y., Petrucelli, L., Parker, J.A., 2012b. TDP-1/TDP-43 regulates stress signaling and age-dependent proteotoxicity in Caenorhabditis elegans. PLoS Genet. 8, e1002806.

van Ham, T.J., Thijssen, K.L., Breitling, R., Hofstra, R.M., Plasterk, R.H., Nollen, E.A., 2008. C. elegans model identifies genetic modifiers of alpha-synuclein inclusion formation during aging. PLoS Genet. 4, e1000027.

Wang, J., Robida-Stubbs, S., Tullet, J.M., Rual, J.F., Vidal, M., Blackwell, T.K., 2010. RNAi screening implicates a SKN-1-dependent transcriptional response in stress resistance and longevity deriving from translation inhibition. PLoS Genet. 6, e1001048.

Neuroscience 209 (2012) 136–143

METHYLENE BLUE ADMINISTRATION FAILS TO CONFER NEUROPROTECTION IN TWO AMYOTROPHIC LATERAL SCLEROSIS MOUSE MODELS

J.-N. AUDET, G. SOUCY AND J.-P. JULIEN*

Research Centre of CHUQ and Department of Psychiatry and Neurosciences, Laval University, 2705 Laurier Boulevard, QC, Canada G1V 4G2

Abstract—Approximately 20% cases of familial amyotrophic lateral sclerosis (ALS) are caused by mutations in the gene encoding Cu/Zn superoxide dismutase (SOD1). Recent studies have shown that methylene blue (MB) was efficient in conferring protection in several neurological disorders. MB was found to improve mitochondrial function, to reduce reactive oxygen species, to clear aggregates of toxic proteins, and to act as a nitric oxide synthase inhibitor. These pleiotropic effects of relevance to ALS pathogenesis led us to test MB in two models of ALS, SOD1^{G93A} mice and TDP-43^{G348C} transgenic mice. Intraperitoneal administration of MB at two different doses was initiated at the beginning of disease onset, at 90 days of age in SOD1^{G93A} and at 6 months of age in TDP-43^{G348C} mice. Despite its established neuroprotective properties, MB failed to confer protection in both mouse models of ALS. The lifespan of SOD1^{G93A} mice was not affected by MB treatment. The declines in motor function, reflex score, and body weight of SOD1^{G93A} mice remained unchanged. MB treatment had no effect on motor neuron loss and aggregation or misfolding of SOD1. A combination of MB with lithium also failed to provide benefits in SOD1^{G93A} mice. In TDP-43^{G348C} mice, MB failed to improve motor function. Cytosolic translocation of TDP-43, ubiquitination and inflammation remained also unchanged after MB treatment of TDP-43^{G348C} mice.

Key words: methylene blue, superoxide dismutase, TDP-43, ALS, neuroinflammation.

Amyotrophic lateral sclerosis (ALS) is the most common adult-onset motor neuron disease, leading to progressive paralysis and death. Ninety percent of the cases are sporadic (sALS), and the remaining are familial (fALS), but the two forms are clinically and pathologically undistinguishable. Twenty percent of the familial cases are related to mutations in the Cu/Zn superoxide dismutase gene (*SOD1*) gene, although the mechanisms leading to pathology remain unclear (Boillee et al., 2006). Transgenic mice expressing several SOD1 mutants have been widely used to understand the ALS pathology because they were found to develop motor neuron disease very similar to the human disease (Turner and Talbot, 2008). Various hypotheses have been proposed to explain the toxicity of SOD1 mutant protein including aggregation (reviewed in Chattopadhyay and Valentine, 2009; Ticozzi et al., 2010), oxidative stress (reviewed in Barber and Shaw, 2010) and mitochondrial dysfunction (reviewed in Pizzuti and Petrucci, 2011), excitotoxicity (reviewed in Bogaert et al., 2010), and more recently RNA processing through TDP-43 and FUS/TLS abnormalities (reviewed in Baumer et al., 2010; Lagier-Tourenne et al., 2010). Although pathological pathways leading to ALS seem to differ between SOD1 and TDP-43 cases, a common hallmark resides in toxic protein aggregation (Chattopadhyay and Valentine, 2009; Johnson et al., 2009).

Although numerous compounds have been tested to treat ALS, most of them were proven ineffective, except riluzole, which slightly prolongs survival of patients (Miller et al., 2007). Methylene blue (MB), a monoamine oxidase inhibitor, has been used for more than a century to treat several diseases and infections. It acts as an inhibitor of NO synthase, whose upregulation occurs in motoneurons and reactive astrocytes of ALS patients (Anneser et al., 2001; Sasaki et al., 2001), as well as in SOD1^{G93A} mice (Cha et al., 1998; Almer et al., 1999; Sasaki et al., 2002). MB can also improve mitochondrial function and be an effective electron carrier, thus acting on reactive oxygen species (Atamna et al., 2008; Wen et al., 2011), which can also be linked to ALS. Increasing evidence shows that methylene blue has strong neuroprotective effects in a growing list of neurological disorders, including Alzheimer's disease (Wischik et al., 1996; Atamna and Kumar, 2010; Medina et al., 2011), Parkinson's disease (Wen et al., 2011), cerebral ischemia (Wiklund et al., 2007; Miclescu et al., 2010; Wen et al., 2011), amnesia (Riha et al., 2011), and bipolar disorder (Naylor et al., 1981; Narsapur and Naylor, 1983; Eroglu and Caglayan, 1997). Furthermore, MB has already been proposed as a potential treatment for ALS, as it clears TDP-43 aggregates in cellular models (Yamashita et al., 2009). Moreover, MB has been shown to prolong survival of normal mice and rats (National Toxicology Program, 2008). The latter may also be relevant to ALS, as a premature senescence of motoneurons may be a cause of ALS (McComas et al., 1973).

During the last years, lithium has also raised a lot of attention as a potential treatment for ALS. Positive results were reported from mouse studies and a clinical trial (Shin et al., 2007; Feng et al., 2008; Fornai et al., 2008), but this was followed more recently by negative results with mice (Gill et al., 2009; Pizzasegola et al., 2009) and humans (Aggarwal et al., 2010; Chio et al., 2010). Various hypoth-

*Corresponding author. Tel: +1-418-654-2296; fax: +1-418-654-2761.
E-mail address: jean-pierre.julien@crchul.ulaval.ca (J.-P. Julien).
Abbreviations: ALS, amyotrophic lateral sclerosis; DRG, dorsal root ganglia; IR, immunoreactivity; MB, methylene blue; SOD1, Cu/Zn superoxide dismutase; VR, ventral root.

0306-4522/12 $36.00
doi:10.1016/j.neuroscience.2011.12.047

esizes were formulated to explain those divergent outcomes. However it seems that paradigms combining lithium treatment with other compounds often result in improvement of the disease (Shin et al., 2007; Feng et al., 2008). Besides, in an attempt to diminish seizures in an epilepsy model in mice, a combination of lithium with MB produced a significant decrease of seizures when compared with lithium alone (Bahremand et al., 2010). Thus, it may be relevant to assess the synergic potential of lithium with MB.

Here, we evaluated the efficiency of MB alone or in combination with lithium in mouse SOD1^{G93A}, a well-established and characterized model of ALS. Because there is growing evidence that sporadic ALS cases with TDP-43 abnormalities have a different etiology than familial ALS caused by SOD1 (Neumann et al., 2006; Orrell, 2010), we also tested the effectiveness of MB in the new TDP-43^{G348C} model of ALS (Swarup et al., 2011). These TDP-43 transgenic mice recapitulate well pathological hallmarks of ALS/FTD, making it a good model to further validate the efficiency of MB. In contrast to many other neurological disorders, we report that administration of MB, alone or in combination with lithium, conferred no protection in ALS pathogenesis caused by mutant SOD1 or by mutant TDP-43.

EXPERIMENTAL PROCEDURES

Animals

SOD1^{G93A} mice [stock number 002726] were acquired from the Jackson Laboratory (Bar Harbor, ME, USA) and enriched in C57BL/6HSd strain ($n>20$). SOD1^{G93A} mice were genotyped in accordance with Jackson Laboratory protocols. SOD1^{G93A} mice were injected at the beginning of the symptomatic stage (90 days) every 2 days until their death. TDP-43^{G348C} mice were generated in C3B6 background (described in Swarup et al., 2011) and backcrossed in C57BL/6 background for at least 10 generations. TDP-43^{G348C} mice were injected at the beginning of the symptomatic stage (6 months) every 2 days until 12 months. Methylene blue (Sigma, St-Louis, MO, USA) was dissolved in 0.9% saline, and mice were given 1 mg/kg (SOD1^{G93A} and TDP-43^{G348C} mice) or 10 mg/kg (SOD1^{G93A} mice) intraperitoneally. Lithium (Sigma) was dissolved in 0.9% saline and injected intraperitoneally at a dose of 10 mg/kg (SOD1^{G93A} mice). The use and maintenance of the mice described in this article were performed in accordance to the Guide of Care and Use of Experimental Animals of the Canadian Council on Animal Care. The number of animals and their suffering has been minimized.

Analysis of disease progression

Measurements of body weight, hind limb reflex, and rotarod performance were used to score the clinical effects of SOD1^{G93A} mice. The extensibility and postural reflex of the hind limbs when mice were held up with their tails were scored as described previously (Urushitani et al., 2006). The SOD1^{G93A} reflex score and body weight were measured every 2 days, beginning at 90 days. Scoring was performed in a blind manner by animal technicians who had no information about the genotype but had experience in grading SOD1 mice paralysis. Analysis of TDP-43^{G348C} and SOD1^{G93A} mice disease progression was performed with an accelerated rotarod, starting at 4 rpm with a 0.25 rpm/s acceleration, and time was noted when the mice fell off the roll. Three trials were done per animal, and the mean value was calculated for statistics and graphs. Rotarod tests for SOD1^{G93A} and TDP-43^{G348C} mice were performed once a week.

Tissue collection and immunohistochemical analyses

Mice were anesthetized and transcardially perfused with NaCl 0.9% and fixed with 4% paraformaldehyde. Dissected spinal cord tissues were postfixed for 24 h in 4% paraformaldehyde and equilibrated in a solution of PBS-sucrose (20%) for 48 h. Spinal cord tissues were cut in 25 μm thick sections with a Leica frozen microtome and kept in a cryoprotective solution at −20 °C. For SOD1^{G93A} mice, sections were incubated with anti-misfolded SOD1 antibody A5C3 (Gros-Louis et al., 2010) (Medimabs, Montreal, Canada), stained with the fluorophore-coupled secondary antibody Alexa-488 (Invitrogen, Carlsbad, CA, USA), and counterstained with DAPI. For TDP-43^{G348C} mice, sections were incubated with monoclonal anti-human TDP-43 (Abnova, Taipei, Taiwan), anti-ubiquitin (Abcam, Cambridge, MA, USA), anti-GFAP (formerly Chemicon—Millipore, Billerica, MA, USA), or anti-Iba1 (Wako, Osaka, Japan) antibodies stained with the fluorophore-coupled secondary antibody Alexa-488 or Alexa-594 (Invitrogen). Dissected dorsal root ganglia (DRG) were postfixed in a solution of 3% glutaraldehyde for a period of 48 h, washed in PBS, treated with 1% osmium tetraoxide for 2 h, and dehydrated through graded alcohol solutions. Before Epon plastic embedding, DRG were further dissected to ensure that all ventral root (VR) axons would be sampled at a distance of 3 mm from the DRG cell body. Semi-thin cross sections (1 μm) were stained with Toluidine Blue, rinsed, and coverslipped. To quantify the immunoreactivity (IR) score on immunohistochemistries, we measured the optical densities of each staining with ImageJ software (NIH). For A5C3, Iba1, and GFAP immunofluorescences, the whole signal intensity was read. To quantify cytoplasmic TDP-43, we surrounded all motoneurons in the spinal cord slices based on their morphology and removed from selection the nucleus for the cytoplasmic measurement. We then read the whole cell intensity and divided the cytoplasm on the whole cell signal to obtain a percentage of cytoplasmic TDP-43 translocalization. For ubiquitin quantification, we measured the amount of ubiquitin-positive inclusions exclusively in the cytoplasmic part of motoneurons.

Western blotting

Total spinal cord lysates from SOD1^{G93A} transgenic mice and from non-transgenic littermates were prepared by homogenization in 1 mL of TNG-T buffer consisting of 50 mM Tris–HCl, pH 7.4; 150 mM NaCl; 10% glycerol; 1% Triton X-100; protease inhibitor mixture (Roche, Indianapolis, IN, USA). After homogenization, the tissue suspension was centrifuged for 15 min at 1000 g at 4 °C. The supernatant (soluble fraction) and the pellet (insoluble fraction) were denatured in the sampling buffer containing 2-mercaptoethanol and SDS with boiling. After migration on standard SDS-PAGE gels, the proteins were blotted on PVDF (PerkinElmer, Waltham, MA, USA) membrane. The membranes were labeled with commercially available anti-SOD1 (Stressgen, Ann Arbor, MI, USA). The amount of loaded protein was verified by stripping the same membranes and incubating with anti-actin antibody (Chemicon). The blots were detected using IgG conjugated with peroxidase and chemiluminescent assay (PerkinElmer). The Western bands were scanned and analyzed by densitometry using ImageJ software (National Institutes of Health, Bethesda, MD, USA).

Statistical analyses

Data were analyzed using Prism 5.0 software (GraphPad Software, LaJolla, CA, USA). Behavioral data were computed by performing two-way ANOVAs (except when specified) followed by Bonferroni post-tests and survival data using Mantel-Cox log-rank tests. VR axon counts were compared using two-tailed Student's t-tests. Data are expressed as mean±SEM; $P<0.05$ was considered statistically significant. One-way ANOVA followed by Bonfer-

roni post-test was performed on A5C3 IR scores (SOD1^{G93A} mice) and unpaired *t*-tests were performed on all other IR scores (TDP-43^{G348C} mice).

RESULTS

Methylene blue treatment, alone or in combination with lithium, did not affect lifespan or phenotype of SOD1^{G93A} mice

Following injection of SOD1^{G93A} mice with methylene blue, lithium, or both drugs starting at 90 days of age, we analyzed the lifespan of transgenic mice (Fig. 1A). Mice treated with methylene blue (1 mg/kg) had a lifespan of 141 days, those treated with a combination of methylene blue (1 mg/kg) and lithium (10 mg/kg) had a lifespan of 141.5, those treated with lithium (10 mg/kg) alone lived 139 days; whereas saline injected mice had a median survival of 141 days. The difference was not significant between any of the groups ($P=0.7337$; $n=10$, $n=8$, $n=9$, and $n=18$, respectively). Moreover, analysis of phenotype by reflex scores and rotarod scores showed no difference between any of the groups ($P=0.3173$ and $P=0.8366$, respectively) (Fig. 1B, C). Correspondingly, body weight measures revealed no difference in disease progression of transgenic mice following any of the treatment ($P=0.5070$) (Fig. 1D). To make sure that the dose of methylene blue was sufficient to induce an effect, we also treated SOD1^{G93A} mice with a 10 mg/kg dose of methylene blue under the same parameters (data not shown). The treated animal had a lifespan of 137.5 days compared with 141 days for the saline treated mice, and again this difference was not statistically significant ($P=0.3268$, $n=8$ and $n=18$, respectively).

MB administration had no effect on motor function of TDP-43^{G348C} mice

As expected, TDP-43^{G348C} transgenic mice performed less well on rotarod assessment than wild-type (WT) mice during all the tested period ($P<0.0001$, $n=9$ and $n=6$,

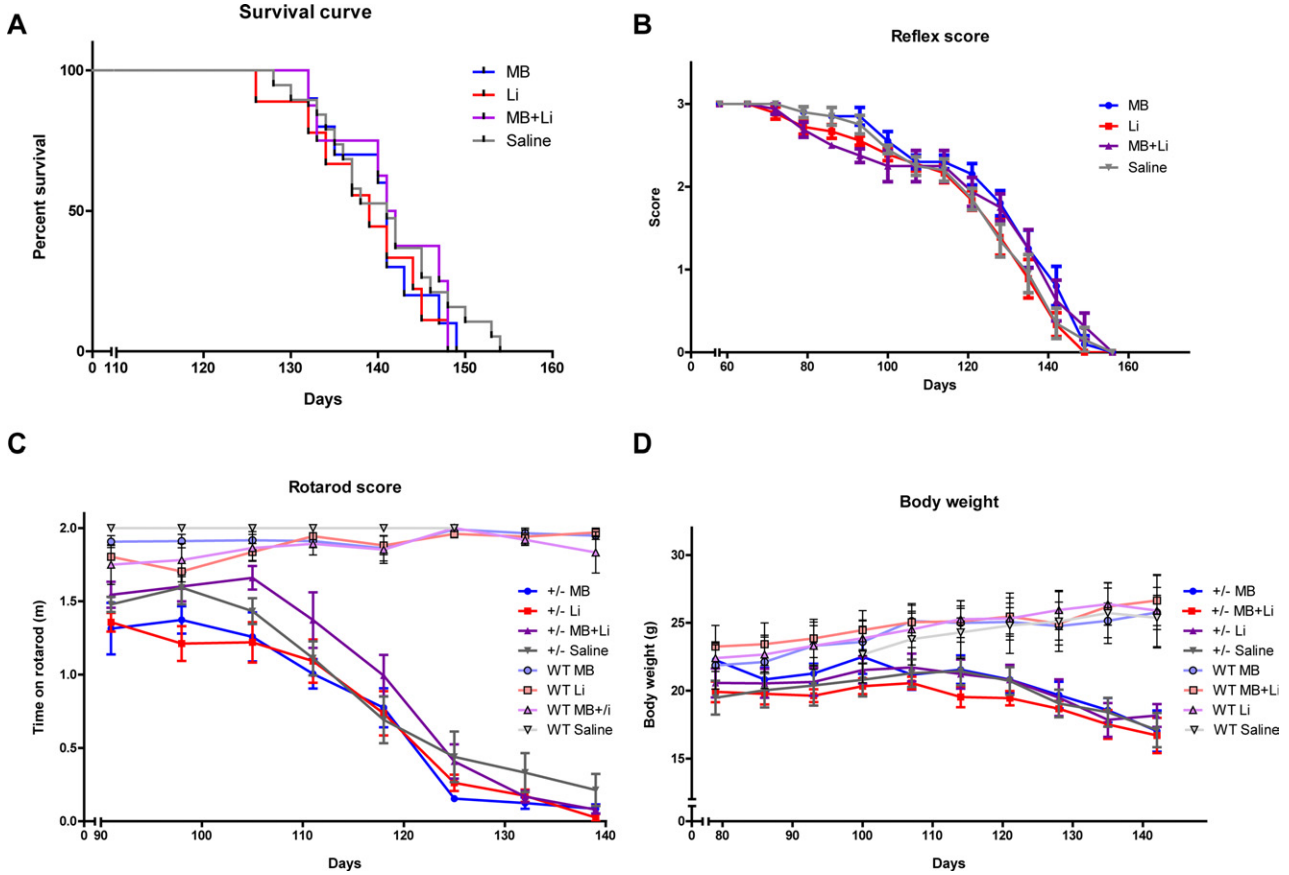

Fig. 1. Treatment with MB, lithium, or both drugs simultaneously does not affect survival or phenotypes of SOD1^{G93A} mice. (A) Survival: Kaplan–Meier survival curve shows that saline treated transgenic mice Sod1^{G93A} ($n=19$) had a mean survival of 141.0 d, whereas MB ($n=10$), Li ($n=9$), or MB+Li ($n=8$) treated mice lived for 141.0, 139.0, and 141.5 d, respectively. Log-rank test shows no significance ($P=0.7337$). (B) Reflex score: two-way ANOVA revealed that the treatment had no effect on the reflex score throughout the time points ($P=0.3173$). (C) Rotarod score: Regardless of the treatment, the performance of the transgenic mice (±) was similar on the rotarod until the end of the measurements ($P=0.8366$). Wild-type (WT) mice almost always perform at maximum value (2 min) irrespective of the treatment. (D) Body weight. WT mice consistently gain weight with age unrelatedly of the treatment, whereas transgenic mice lose weight as the paralysis progresses. However, the progressive decrease in the bodyweight of transgenic mice after the onset was comparable between all the groups ($P=0.5070$). For interpretation of the references to color in this figure legend, the reader is referred to the Web version of this article.

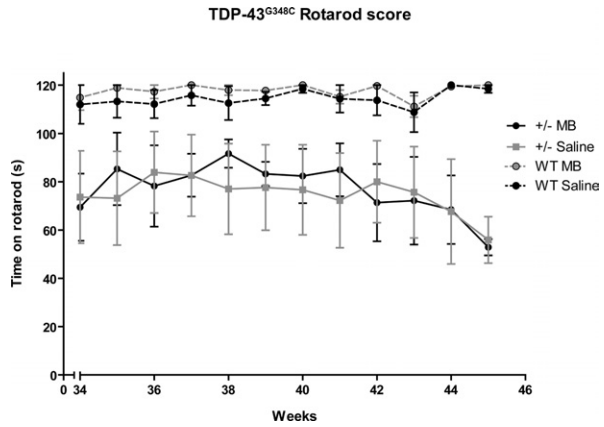

Fig. 2. MB did not improve motor function of TDP-43^{G348C} mice. Rotarod tests were assessed in three consecutive trials every week and the mean value is plotted. WT mice performs significantly better than TDP-43^{G348C} transgenic mice (±) ($P<0.0001$, $n=6$ and $n=9$, respectively). There was no difference between MB treated transgenic mice and saline treated transgenic mice neither in any of the time points nor in the overall curve ($P=0.8801$, $n=4$ and $n=5$, respectively).

respectively) (Fig. 2). However, there was no difference between the performances of saline-treated transgenic (±) animals versus MB-treated transgenic (±) animals ($P=0.8801$, $n=5$ and $n=4$, respectively).

Cellular hallmarks of ALS were unchanged after MB treatment

Misfolded SOD1 is a pathological hallmark of ALS, even in sporadic cases (Bosco et al., 2010; Forsberg et al., 2010). For this reason, we examined its presence with a monoclonal antibody (A5C3) that is specific to misfolded SOD1 (Fig. 3A). However, following any of the treatments, the amount of misfolded SOD1 found in the spinal cord of SOD1^{G93A} mice was not diminished. Comparison of IR scores showed no difference in A5C3 signal for all treatments ($P=0.4593$, $n=3$) (Fig. 3C). In TDP-43 transgenic mice as well as in ALS patients, cytosolic TDP-43 translocalization is a well-known pathological hallmark of ALS (Arai et al., 2006; Neumann et al., 2006; Swarup et al., 2011). Monoclonal antibody against human TDP-43 revealed no observable difference in the amount of translocated TDP-43 between treated transgenic animal versus transgenic controls (Fig. 3B), and this was confirmed by quantification of the percentage of TDP-43 found in cytoplasm ($P=0.8662$, $n=3$, see figure legend for details) (Fig. 3D). Similarly, the extent of ubiquitination was not diminished by MB treatment in transgenic mice ($P=0.5467$, $n=3$). Microgliosis and astrocytosis, also associated ALS pathology, were not reduced nor aggravated as revealed by Iba1 and GFAP antibodies in immunofluorescence (Fig. 3B) and their quantification (respectively: $P=0.9644$, $n=4$; $P=0.8263$, $n=5$) (Fig. 3D).

MB does not affect the number of surviving axons in the dorsal root ganglia of SOD1^{G93A} mice

Axonal degeneration correlates with the disease severity in SOD1 mutant mice (Gurney et al., 1994; Wong et al., 1995; Bruijn et al., 1997). Therefore, we performed transversal sections of the dorsal root ganglia and assessed the axonal degeneration in the VR (Fig. 4A). While the non-transgenic mice had nearly a thousand motoneurons in the VR, SOD1^{G93A} mice had more or less 35% of their axons remaining (Fig. 4B). However, there was no difference in the number of axons of mice treated with MB, lithium, or both drugs together (MB: 357, Li: 357.5, MB+Li: 346.5, Saline: 378.0; $P=0.5157$).

Accumulation of insoluble SOD1 is not diminished by MB treatment

It has been proposed that MB may play a role in clearance of a variety of toxic insoluble aggregates. In fact, it was demonstrated that MB can inhibit aggregate formation of a variety of proteins (Wischik et al., 1996; Taniguchi et al., 2005; Yamashita et al., 2009). To verify this hypothesis in SOD1^{G93A} mice, we compared the ratio of soluble versus insoluble fractions of SOD1 in the spinal cord of SOD1^{G93A} mice, treated or not (Fig. 5). In the non-transgenic (WT) mice we mostly detected soluble Sod1, whereas transgenic SOD1^{G93A} mice had a considerable amount insoluble SOD1, as expected. However, the extent of aggregation was not lessened by MB treatment, lithium, or both treatments together.

DISCUSSION

Here we demonstrate that MB, Li, or both drugs administered jointly had no effect on the disease caused by SOD1^{G93A} in mice. MB also failed to alleviate disease caused by TDP-43^{G348C} in mice. Our analyses demonstrated that MB was unable to attenuate pathological hallmarks of ALS in either SOD1^{G93A} mice or TDP-43^{G348C} mice.

An earlier study concluded of MB ineffectiveness in conferring protection by oral administration at a dose of 25 mg/kg, which is much higher than the safe working dose already used in mice and in humans for other pathologies (Lougheed and Turnbull, 2011). This could have led to a toxic outcome, masking potential beneficial effects of MB. In another paradigm, a low dose of MB was efficient, whereas the high dose was not able to induce any beneficial effects (Callaway et al., 2004). Actually, toxicity of MB generally occurs at a dosage above 6–12.5 mg/kg (depending on the studies), and the recommended dosage is 1–2 mg/kg (Wiklund et al., 2007; National Toxicology Program, 2008). In this study we treated all mice with a dose of 1 mg/kg of MB, which is within the mean working dose range used in most other paradigms in mice and humans when injected (0.5–2.5 mg/kg) (Clifton and Leikin, 2003; Callaway et al., 2004; Wiklund et al., 2007; Miclescu et al., 2010; Wen et al., 2011). Moreover, it has been demonstrated that MB crosses easily the blood–brain barrier, resulting in high concentrations in the CNS even at low dose administration (Peter et al., 2000). Nevertheless, to make sure that this dose was not too low, we repeated the experiment in SOD1^{G93A} mice with a dose of 10 mg/kg. Upon measuring the lifespan of this high-dose cohort of

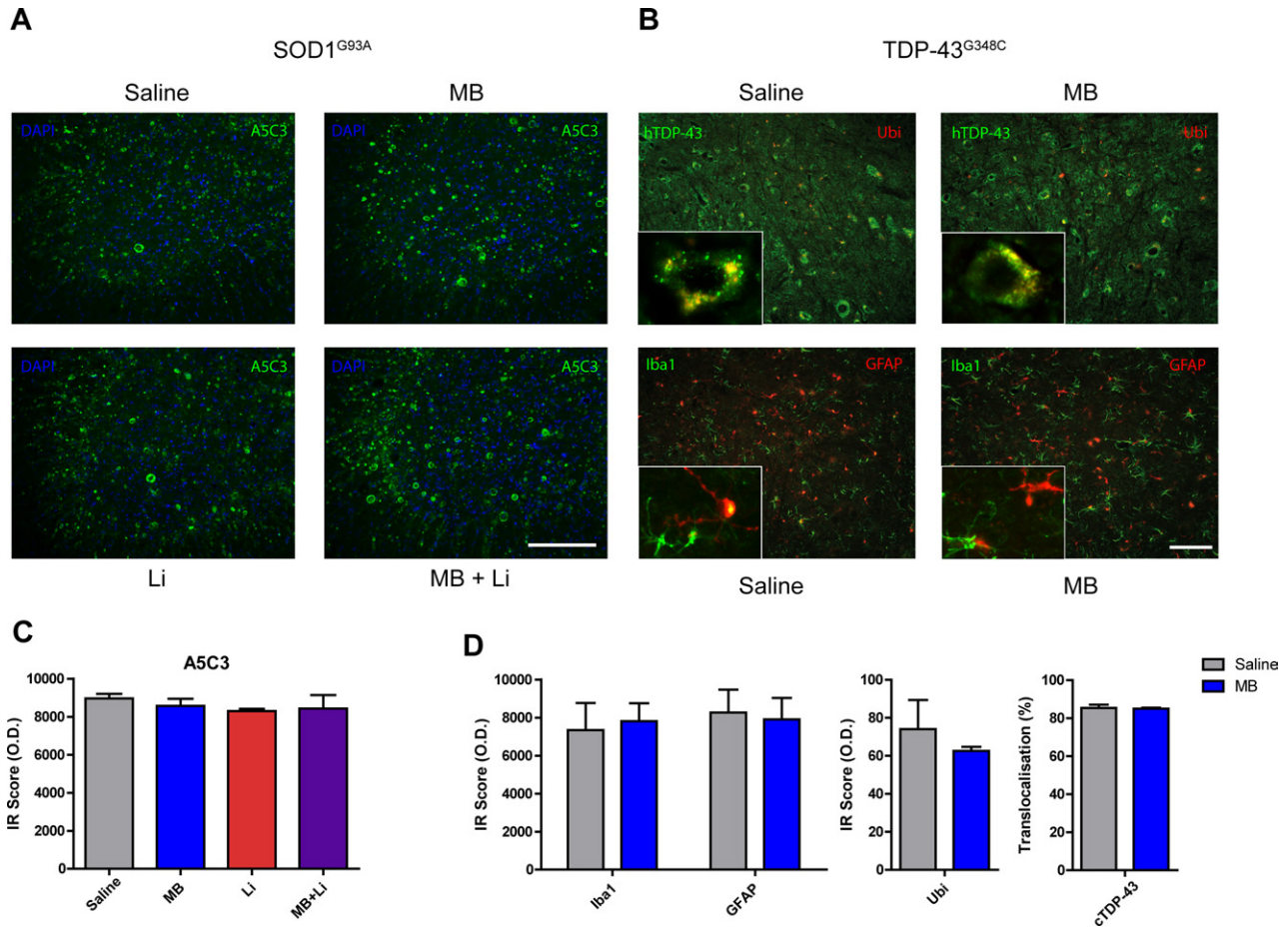

Fig. 3. Cellular pathological hallmarks of ALS are not diminished by MB and/or Li in SOD1^{G93A} or by MB in TDP-43^{G348C} mice. (A) Misfolded SOD1, detected by the A5C3 antibody, is found abundantly in spinal cords of SOD1^{G93A} mice. However, the intensity of the signal is very similar following any of the treatments. Scale bar=50 μm. (B) Abnormal cytoplasmic hTDP-43 is found plentifully in spinal cord motoneurons of TDP-43^{G348C} mice, and aggregates are sometimes found ubiquitinated (hTDP-43 and Ubi colocalization is shown in inlay magnification of a representative cell). Still, there is no reduction of cytoplasmic TDP-43 or ubiquitination extent by MB treatment. GFAP and Iba1 immunofluorescences are also similar after MB treatment. Scale bar=10 μm. (C) Quantification of A5C3 immunoreactivity (IR) in SOD1^{G93A} mice reveals no difference among the different treatments (P=0.4593, n=3) [OD: optical density arbitrary units]. (D) There was no difference in the immunoreactivity scores of MB and saline-treated TDP-43^{G348C} mice for Iba1, GFAP, and ubiquitin (respectively: P=0.9644, n=4; P=0.8263, n=5; P=0.5467, n=3). The amount of hTDP-43 cellular translocalization (cTDP-43, calculated as the percentage of cellular TDP-43 divided by the total cell TDP-43 in motoneurons) was also very comparable in both treatments (P=0.8662, n=3). For interpretation of the references to color in this figure legend, the reader is referred to the Web version of this article.

animals, we consistently saw no difference in the MB-treated animals compared with saline-treated animals (MB: mean=137.5, saline: mean=141.0, P=0.3268).

Lougheed and Turnbull (2011) did not report the physiological outcomes of the treatment. Hence, the possibility that MB could have ameliorated some aspects of the disease has not been addressed in that study. Here, we have examined the major pathological hallmarks of ALS in SOD1^{G93A} and in TDP^{G348C} mice. First, the number of motor neurons remained unchanged in SOD1^{G93A} (Fig. 4) after MB treatments. Besides, the extent of misfolding and aggregation of SOD1 proteins correlates with the disease in mutant SOD1 mice (Gurney, 1997; Bruijn et al., 1998; Wang et al., 2005; Prudencio et al., 2009). Accordingly, we investigated that feature and we showed that treatment with MB does not reduce aggregation/misfolding of SOD1 (Figs. 3A and 5).

There is evidence that misfolded SOD1 may be a common feature of most ALS patient, familial or even sporadic (Bosco et al., 2010; Forsberg et al., 2010). However, it has been proposed that sporadic ALS cases with TDP-43 abnormalities have a different etiology than familial ALS caused by SOD1 (Neumann et al., 2006; Orrell, 2010). Consequently, the possibility that MB may have protective effects in ALS of other etiologies than mutant SOD1 could not be excluded. For instance, MB was able to clear aggregates of TDP-43 in a cellular model of ALS (Yamashita et al., 2009). In contrast, we report that MB had no effect on disease symptoms or on formation of cytoplasmic TDP-43 inclusions in transgenic mice expressing TDP-43^{G348C}.

The TDP-43^{G348C} mice develop during aging motor dysfunction, a main feature of ALS disease (Swarup et al., 2011). The TDP-43^{G348C} mice treated with MB for 6 months exhib-

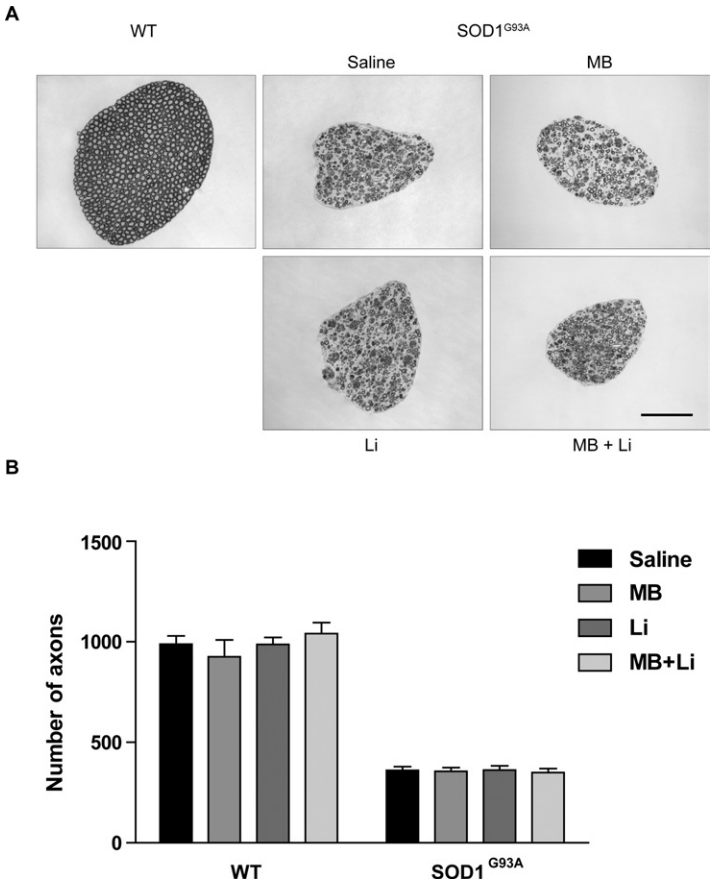

Fig. 4. No change in motor axons of SOD1^{G93A} mice. (A) Although the vast majority of axons appear intact in WT mice, transgenic SOD1^{G93A} mice exhibit massive degeneration of axons in the transversally sliced L5 ventral roots. (B) Quantification of the number of surviving axons in the ventral root shows that SOD1^{G93A} mice had 2.76 times less axons than the WT mice ($P<0.0001$, $n=19$ and $n=13$, respectively). However, the number of axons in the ventral root is similar in all the SOD1^{G93A} mice either for the saline (mean=361.0, $n=6$), MB (mean=356.2, $n=5$), Li (mean=362.3, $n=4$), or MB+Li (mean=349.0, $n=4$) treatments ($P=0.9672$). Scale bar=50 μm.

ited the same motor performance as saline-treated TDP-43^{G348C} mice (Fig. 2). Moreover, immunodetection of cytoplasmic TDP-43, of ubiquitin and of inflammation remained unchanged by the MB treatment (Fig. 3B, D).

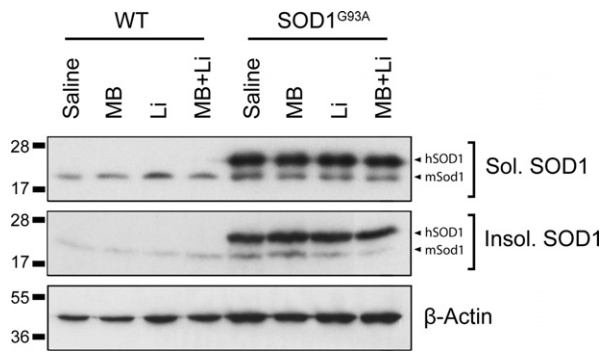

Fig. 5. Insoluble SOD1 is not cleared by MB and/or Li in SOD1^{G93A} mice. Insoluble SOD1 is predominantly found in SOD1^{G93A} mice and is mainly formed of human mutant SOD1 (hSOD1, upper bands in SOD1 panels). However, the ratio insoluble/soluble is consistent for any of the treatments (Saline, MB, Li, or MB+Li). Endogenous mouse SOD1 (mSOD1, lower bands in SOD1 panels) is relatively constant among all the mice.

The fact that lithium did not alleviate ALS symptoms in SOD1^{G93A} mice is concordant with recent negative results by independent groups (Gill et al., 2009; Pizzasegola et al., 2009; Aggarwal et al., 2010; Chio et al., 2010). These negative results were based on studies with larger cohorts of mice than earlier positive studies (Shin et al., 2007; Feng et al., 2008; Fornai et al., 2008). The scope of our experiments was mainly to investigate the possible synergic effect of MB with Li, because both were shown to achieve such effects in other paradigms (Shin et al., 2007; Feng et al., 2008; Bahremand et al., 2010). Based on our results we concluded that this was not the case in G93A mice and consequently we did not pursue further lithium tests in another ALS mouse model, the TDP-43 transgenic mice.

It is surprising that despite the existence of potential therapeutic targets for MB in ALS pathology, this compound could not improve the disease phenotypes in two different mouse models, the G93A mice and TDP-43 mice. There are still much uncertainties about pathogenic mechanisms that contribute directly to neurodegeneration process (Chattopadhyay and Valentine, 2009; Barber and Shaw, 2010; Baumer et al., 2010; Bogaert et al., 2010;

Lagier-Tourenne et al., 2010; Ticozzi et al., 2010; Pizzuti and Petrucci, 2011). Therefore, a possible explanation for the MB failure to alleviate ALS features could be that MB targets such as NOs, oxidative stress, mitochondria deficits, and protein aggregation are not the key contributors of motor neuron loss in these mouse models.

In summary, our results suggest that, despite its recognized protective properties (Schirmer et al., 2011), MB is inappropriate for treatment of ALS associated with either SOD1 mutations or TDP-43 abnormalities.

Acknowledgments—We gratefully thank Mélanie Couture, Christine Bareil, Marie-Ève Boulanger, Mélanie Simard, Caroline Genest, and Sophie Vachon for their technical help. This work was supported by the Canadian Institutes of Health Research. J.-P.J. holds a Canada Research Chair Tier 1 on Mechanisms of Neurodegeneration.

REFERENCES

Aggarwal SP, Zinman L, Simpson E, McKinley J, Jackson KE, Pinto H, Kaufman P, Conwit RA, Schoenfeld D, Shefner J, Cudkowicz M (2010) Safety and efficacy of lithium in combination with riluzole for treatment of amyotrophic lateral sclerosis: a randomised, double-blind, placebo-controlled trial. Lancet Neurol 9:481–488.

Almer G, Vukosavic S, Romero N, Przedborski S (1999) Inducible nitric oxide synthase up-regulation in a transgenic mouse model of familial amyotrophic lateral sclerosis. J Neurochem 72:2415–2425.

Anneser JM, Cookson MR, Ince PG, Shaw PJ, Borasio GD (2001) Glial cells of the spinal cord and subcortical white matter up-regulate neuronal nitric oxide synthase in sporadic amyotrophic lateral sclerosis. Exp Neurol 171:418–421.

Arai T, Hasegawa M, Akiyama H, Ikeda K, Nonaka T, Mori H, Mann D, Tsuchiya K, Yoshida M, Hashizume Y, Oda T (2006) TDP-43 is a component of ubiquitin-positive tau-negative inclusions in frontotemporal lobar degeneration and amyotrophic lateral sclerosis. Biochem Biophys Res Commun 351:602–611.

Atamna H, Kumar R (2010) Protective role of methylene blue in Alzheimer's disease via mitochondria and cytochrome c oxidase. J Alzheimers Dis 20 (Suppl 2):S439–S452.

Atamna H, Nguyen A, Schultz C, Boyle K, Newberry J, Kato H, Ames BN (2008) Methylene blue delays cellular senescence and enhances key mitochondrial biochemical pathways. FASEB J 22: 703–712.

Bahremand A, Nasrabady SE, Ziai P, Rahimian R, Hedayat T, Payandemehr B, Dehpour AR (2010) Involvement of nitric oxide-cGMP pathway in the anticonvulsant effects of lithium chloride on PTZ-induced seizure in mice. Epilepsy Res 89:295–302.

Barber SC, Shaw PJ (2010) Oxidative stress in ALS: key role in motor neuron injury and therapeutic target. Free Radic Biol Med 48: 629–641.

Baumer D, Ansorge O, Almeida M, Talbot K (2010) The role of RNA processing in the pathogenesis of motor neuron degeneration. Expert Rev Mol Med 12:e21.

Bogaert E, d'Ydewalle C, Van Den Bosch L (2010) Amyotrophic lateral sclerosis and excitotoxicity: from pathological mechanism to therapeutic target. CNS Neurol Disord Drug Targets 9:297–304.

Boillee S, Vande Velde C, Cleveland DW (2006) ALS: a disease of motor neurons and their nonneuronal neighbors. Neuron 52:39–59.

Bosco DA, Morfini G, Karabacak NM, Song Y, Gros-Louis F, Pasinelli P, Goolsby H, Fontaine BA, Lemay N, McKenna-Yasek D, Frosch MP, Agar JN, Julien JP, Brady ST, Brown RH Jr (2010) Wild-type and mutant SOD1 share an aberrant conformation and a common pathogenic pathway in ALS. Nat Neurosci 13:1396–1403.

Bruijn LI, Becher MW, Lee MK, Anderson KL, Jenkins NA, Copeland NG, Sisodia SS, Rothstein JD, Borchelt DR, Price DL, Cleveland DW (1997) ALS-linked SOD1 mutant G85R mediates damage to astrocytes and promotes rapidly progressive disease with SOD1-containing inclusions. Neuron 18:327–338.

Bruijn LI, Houseweart MK, Kato S, Anderson KL, Anderson SD, Ohama E, Reaume AG, Scott RW, Cleveland DW (1998) Aggregation and motor neuron toxicity of an ALS-linked SOD1 mutant independent from wild-type SOD1. Science 281:1851–1854.

Callaway NL, Riha PD, Bruchey AK, Munshi Z, Gonzalez-Lima F (2004) Methylene blue improves brain oxidative metabolism and memory retention in rats. Pharmacol Biochem Behav 77:175–181.

Cha CI, Kim JM, Shin DH, Kim YS, Kim J, Gurney ME, Lee KW (1998) Reactive astrocytes express nitric oxide synthase in the spinal cord of transgenic mice expressing a human Cu/Zn SOD mutation. Neuroreport 9:1503–1506.

Chattopadhyay M, Valentine JS (2009) Aggregation of copper-zinc superoxide dismutase in familial and sporadic ALS. Antioxid Redox Signal 11:1603–1614.

Chio A, Borghero G, Calvo A, Capasso M, Caponnetto C, Corbo M, Giannini F, Logroscino G, Mandrioli J, Marcello N, Mazzini L, Moglia C, Monsurrò MR, Mora G, Patti F, Perini M, Pietrini V, Pisano F, Pupillo E, Sabatelli M, Salvi F, Silani V, Simone IL, Sorarù G, Tola MR, Volanti P, Beghi E (2010) Lithium carbonate in amyotrophic lateral sclerosis: lack of efficacy in a dose-finding trial. Neurology 75:619–625.

Clifton J, Leikin JB (2003) Methylene blue. Am J of Ther 10:289–291.

Eroglu L, Caglayan B (1997) Anxiolytic and antidepressant properties of methylene blue in animal models. Pharmacol Res 36:381–385.

Feng HL, Leng Y, Ma CH, Zhang J, Ren M, Chuang DM (2008) Combined lithium and valproate treatment delays disease onset, reduces neurological deficits and prolongs survival in an amyotrophic lateral sclerosis mouse model. Neuroscience 155:567–572.

Fornai F, Longone P, Cafaro L, Kastsiuchenka O, Ferrucci M, Manca ML, Lazzeri G, Spalloni A, Bellio N, Lenzi P, Modugno N, Siciliano G, Isidoro C, Murri L, Ruggieri S, Paparelli A (2008) Lithium delays progression of amyotrophic lateral sclerosis. Proc Natl Acad Sci U S A 105:2052–2057.

Forsberg K, Jonsson PA, Andersen PM, Bergemalm D, Graffmo KS, Hultdin M, Jacobsson J, Rosquist R, Marklund SL, Brännström T (2010) Novel antibodies reveal inclusions containing non-native SOD1 in sporadic ALS patients. PLoS One 5:e11552.

Gill A, Kidd J, Vieira F, Thompson K, Perrin S (2009) No benefit from chronic lithium dosing in a sibling-matched, gender balanced, investigator-blinded trial using a standard mouse model of familial ALS. PLoS One 4:e6489.

Gros-Louis F, Soucy G, Larivière R, Julien JP (2010) Intracerebroventricular infusion of monoclonal antibody or its derived Fab fragment against misfolded forms of SOD1 mutant delays mortality in a mouse model of ALS. J Neurochem 113:1188–1199.

Gurney ME (1997) The use of transgenic mouse models of amyotrophic lateral sclerosis in preclinical drug studies. J Neurol Sci 152 (Suppl 1):S67–S73.

Gurney ME, Pu H, Chiu AY, Dal Canto MC, Polchow CY, Alexander DD, Caliendo J, Hentati A, Kwon YW, Deng HX, et al. (1994) Motor neuron degeneration in mice that express a human Cu,Zn superoxide dismutase mutation. Science 264:1772–1775.

Johnson BS, Snead D, Lee JJ, McCaffery JM, Shorter J, Gitler AD (2009) TDP-43 is intrinsically aggregation-prone, and amyotrophic lateral sclerosis-linked mutations accelerate aggregation and increase toxicity. J Biol Chem 284:20329–20339.

Lagier-Tourenne C, Polymenidou M, Cleveland DW (2010) TDP-43 and FUS/TLS: emerging roles in RNA processing and neurodegeneration. Hum Mol Genet 19:R46–R64.

Lougheed R, Turnbull J (2011) Lack of effect of methylene blue in the SOD1 G93A mouse model of amyotrophic lateral sclerosis. PLoS One 6:e23141.

McComas AJ, Upton AR, Sica RE (1973) Motoneurone disease and ageing. Lancet 2:1477–1480.

Medina DX, Caccamo A, Oddo S (2011) Methylene blue reduces abeta levels and rescues early cognitive deficit by increasing proteasome activity. Brain Pathol 21:140–149.

Miclescu A, Sharma HS, Martijn C, Wiklund L (2010) Methylene blue protects the cortical blood-brain barrier against ischemia/reperfusion-induced disruptions. Crit Care Med 38:2199–2206.

Miller RG, Mitchell JD, Lyon M, Moore DH (2007) Riluzole for amyotrophic lateral sclerosis (ALS)/motor neuron disease (MND). Cochrane Database Syst Rev:CD001447.

Narsapur SL, Naylor GJ (1983) Methylene blue. A possible treatment for manic depressive psychosis. J Affect Disord 5:155–161.

National Toxicology Program (2008) Toxicology and carcinogenesis studies of methylene blue trihydrate (cas no. 7220-79-3) in F344/N rats and B6C3F1 mice (gavage studies). Natl Toxicol Program Tech Rep Ser:1–224.

Naylor GJ, Dick DA, Johnston BB, Hopwood SE, Dick EG, Smith AH, Kay D (1981) Possible explanation for therapeutic action of lithium, and a possible substitute (methylene-blue). Lancet 2:1175–1176.

Neumann M, Sampathu DM, Kwong LK, Truax AC, Micsenyi MC, Chou TT, Bruce J, Schuck T, Grossman M, Clark CM, McCluskey LF, Miller BL, Masliah E, Mackenzie IR, Feldman H, Feiden W, Kretzschmar HA, Trojanowski JQ, Lee VM (2006) Ubiquitinated TDP-43 in frontotemporal lobar degeneration and amyotrophic lateral sclerosis. Science 314:130–133.

Orrell RW (2010) Motor neuron disease: systematic reviews of treatment for ALS and SMA. Br Med Bull 93:145–159.

Peter C, Hongwan D, Küpfer A, Lauterburg BH (2000) Pharmacokinetics and organ distribution of intravenous and oral methylene blue. Eur J Clin Pharmacol 56:247–250.

Pizzasegola C, Caron I, Daleno C, Ronchi A, Minoia C, Carrì MT, Bendotti C (2009) Treatment with lithium carbonate does not improve disease progression in two different strains of SOD1 mutant mice. Amyotroph Lateral Scler 10:221–228.

Pizzuti A, Petrucci S (2011) Mitochondrial disfunction as a cause of ALS. Arch Ital Biol 149:113–119.

Prudencio M, Hart PJ, Borchelt DR, Andersen PM (2009) Variation in aggregation propensities among ALS-associated variants of SOD1: correlation to human disease. Hum Mol Genet 18:3217–3226.

Riha PD, Rojas JC, Gonzalez-Lima F (2011) Beneficial network effects of methylene blue in an amnestic model. Neuroimage 54:2623–2634.

Sasaki S, Shibata N, Iwata M (2001) Neuronal nitric oxide synthase immunoreactivity in the spinal cord in amyotrophic lateral sclerosis. Acta Neuropathol 101:351–357.

Sasaki S, Warita H, Abe K, Iwata M (2002) Neuronal nitric oxide synthase (nNOS) immunoreactivity in the spinal cord of transgenic mice with G93A mutant SOD1 gene. Acta Neuropathol 103:421–427.

Schirmer RH, Adler H, Pickhardt M, Mandelkow E (2011) Lest we forget you—methylene blue. Neurobiol Aging 32(2325):e2327–2316.

Shin JH, Cho SI, Lim HR, Lee JK, Lee YA, Noh JS, Joo IS, Kim KW, Gwag BJ (2007) Concurrent administration of Neu2000 and lithium produces marked improvement of motor neuron survival, motor function, and mortality in a mouse model of amyotrophic lateral sclerosis. Mol Pharmacol 71:965–975.

Swarup V, Phaneuf D, Bareil C, Robertson J, Rouleau GA, Kriz J, Julien JP (2011) Pathological hallmarks of amyotrophic lateral sclerosis/frontotemporal lobar degeneration in transgenic mice produced with TDP-43 genomic fragments. Brain 134:2610–2626.

Taniguchi S, Suzuki N, Masuda M, Hisanaga S, Iwatsubo T, Goedert M, Hasegawa M (2005) Inhibition of heparin-induced tau filament formation by phenothiazines, polyphenols, and porphyrins. J Biol Chem 280:7614–7623.

Ticozzi N, Ratti A, Silani V (2010) Protein aggregation and defective RNA metabolism as mechanisms for motor neuron damage. CNS Neurol Disord Drug Targets 9:285–296.

Turner BJ, Talbot K (2008) Transgenics, toxicity and therapeutics in rodent models of mutant SOD1-mediated familial ALS. Prog Neurobiol 85:94–134.

Urushitani M, Sik A, Sakurai T, Nukina N, Takahashi R, Julien JP (2006) Chromogranin-mediated secretion of mutant superoxide dismutase proteins linked to amyotrophic lateral sclerosis. Nat Neurosci 9:108–118.

Wang J, Xu G, Li H, Gonzales V, Fromholt D, Karch C, Copeland NG, Jenkins NA, Borchelt DR (2005) Somatodendritic accumulation of misfolded SOD1-L126Z in motor neurons mediates degeneration: alphaB-crystallin modulates aggregation. Hum Mol Genet 14: 2335–2347.

Wen Y, Li W, Poteet EC, Xie L, Tan C, Yan LJ, Ju X, Liu R, Qian H, Marvin MA, Goldberg MS, She H, Mao Z, Simpkins JW, Yang SH (2011) Alternative mitochondrial electron transfer as a novel strategy for neuroprotection. J Biol Chem 286:16504–16515.

Wiklund L, Basu S, Miclescu A, Wiklund P, Ronquist G, Sharma HS (2007) Neuro- and cardioprotective effects of blockade of nitric oxide action by administration of methylene blue. Ann N Y Acad Sci 1122:231–244.

Wischik CM, Edwards PC, Lai RY, Roth M, Harrington CR (1996) Selective inhibition of Alzheimer disease-like tau aggregation by phenothiazines. Proc Natl Acad Sci U S A 93:11213–11218.

Wong PC, Pardo CA, Borchelt DR, Lee MK, Copeland NG, Jenkins NA, Sisodia SS, Cleveland DW, Price DL (1995) An adverse property of a familial ALS-linked SOD1 mutation causes motor neuron disease characterized by vacuolar degeneration of mitochondria. Neuron 14:1105–1116.

Yamashita M, Nonaka T, Arai T, Kametani F, Buchman VL, Ninkina N, Bachurin SO, Akiyama H, Goedert M, Hasegawa M (2009) Methylene blue and dimebon inhibit aggregation of TDP-43 in cellular models. FEBS Lett 583:2419–2424.

(Accepted 26 December 2011)
(Available online 3 January 2012)